Journal *of* Singularities
Volume 24 (2022), 1-78

received: 16 June 2019
in revised form: 3 October 2021
DOI: 10.5427/jsing.2022.24a

DYNAMICS OF SINGULAR COMPLEX ANALYTIC VECTOR FIELDS WITH ESSENTIAL SINGULARITIES II

ALVARO ALVAREZ–PARRILLA AND JESÚS MUCIÑO–RAYMUNDO

Abstract. Let X be a *singular complex analytic vector field* on the Riemann sphere described by two polynomials $P(z)$, $E(z)$ of degrees r and d respectively; in such way that X has poles at the roots of $P(z)$, an isolated essential singularity at infinity arising from the exponential of $E(z)$ and no zeros on the complex plane. These vector fields are transcendental of 1–order d. We study the families of the above singular complex analytic vector fields X. For each pair (r, d), with $r + d \geq 1$, the family of these vector fields is an open complex manifold of dimension $r + d + 1$. Our goal is the geometric description of the vector fields X, in particular the behaviour of its singularity at infinity. We first exploit that each vector field X has a canonical associated global singular analytic distinguished parameter (the function determined by the integral of the corresponding 1–form of time). Secondly, we develop in full detail the natural one to one correspondence between: vector fields, global singular analytic distinguished parameters and the Riemann surfaces of these distinguished parameters. These Riemann surfaces are biholomorphic to $\mathbb{C}$ and have d logarithmic branch points over infinity, d logarithmic branch points over finite asymptotic values and r finitely ramified branch points. As a valuable tool, we introduce (r, d)–*configuration trees*, which are weighted directed rooted trees. An (r, d)–configuration tree completely encodes the Riemann surface of a vector field X, including its associated singular flat metric.

Our main result states that the (r, d)–configuration trees provide local holomorphic parameters, for the corresponding family of vector fields. Explicit geometrical and dynamical information is supplied by (r, d)–configuration trees. In fact, given a vector field in the family, the phase portrait of the associated real vector field on the Riemann sphere is decomposed into real flow invariant regions, half planes and strips. The structural stability (under perturbation in the corresponding family) of the phase portrait of the real vector field, is characterized by using (r, d)–configuration trees. The number of (orientation preserving) topologically classes of real phase portraits is counted in terms of certain conditions of the discrete parameters (r, d). The germ of the isolated essential singularity of the vector field X is described as a combinatorial word consisting of hyperbolic, elliptic, parabolic and (suitable) *entire* angular sectors at infinity. Our work has its roots in the seminal study of R. Nevanlinna.

1. Introduction

Motivated by the nature of meromorphic and essential singularities of complex analytic vector fields on Riemann surfaces [36], [37], [25], [1], [2], we study the families

$$\mathscr{E}(r,d) = \left\{ X(z) = \frac{1}{P(z)} \mathrm{e}^{E(z)} \frac{\partial}{\partial z} \;\middle|\; \begin{array}{c} P, E \in \mathbb{C}[z],\ P \ \text{ monic}, \\ \deg P = r,\ \deg E = d,\ r+d \geq 1 \end{array} \right\}, \tag{1}$$

of vector fields on the Riemann sphere $\widehat{\mathbb{C}}$, having r poles on $\mathbb{C}$ and an isolated essential singularity at ∞, for $d \geq 1$. The appearance of poles is one of the main new features, respect to the previous work in [1].

2020 *Mathematics Subject Classification.* Primary: 32S65; Secondary: 37F75, 30F10, 30D20, 32M25.
Key words and phrases. Complex analytic vector fields and Riemann surfaces and Essential singularities.

Each $X \in \mathscr{E}(r,d)$ is provided with a global singular analytic distinguished parameter

$$\Psi_X(z) = \int^z P(\zeta)\mathrm{e}^{-E(\zeta)}d\zeta : \mathbb{C}_z \longrightarrow \widehat{\mathbb{C}}_t, \tag{2}$$

which in turn has an associated Riemann surface

$$\mathcal{R}_X = \{(z, \Psi_X(z))\}, \tag{3}$$

whose origin can be traced back to the seminal work of R. Nevanlinna [39], [40].
There is a bijective correspondence, induced by Ψ_X, between

$$X \in \mathscr{E}(r,d) \quad \longleftrightarrow \quad \left\{ \begin{array}{l} \text{branched coverings } \pi_2 : \mathcal{R}_X \longrightarrow \big(\widehat{\mathbb{C}}_t, \frac{\partial}{\partial t}\big) \text{ having} \\ d \text{ logarithmic branch points over } \infty, \\ d \text{ logarithmic branch points over } \{a_\sigma\} \subset \mathbb{C}_t, \\ 0 \leq n \leq r \text{ finitely ramified branch points over } \{\widetilde{p}_\iota\} \subset \mathbb{C}_t \end{array} \right\}, \tag{4}$$

where $\pi_2(z,t) = t$. Along this work, $(\widehat{\mathbb{C}}_z, X)$ denotes a pair, Riemann sphere and a singular complex analytic vector field; $\big((\mathbb{C}_z, z_0), X\big)$ denotes a germ of a singular analytic vector field X on $(\mathbb{C}_z, z_0)$. The work of M. Taniguchi [45], [46] is a keystone for understanding the right side of (4). Analogous correspondences have been previously used in [1], [2], [3]. The function Ψ_X is single valued and $(\Psi_X)_* X = \frac{\partial}{\partial t}$ provides a *global flow box* for X, see Lemma 2.4. There exists a biholomorphism $\mathbb{C}_z \cong \mathcal{R}_X$. The Riemann surface $\mathcal{R}_X$ is described by gluing half planes $\overline{\mathbb{H}}^2$ and finite height strips $\{0 \leq \mathfrak{Im}\,(t) \leq h\}$, see Lemma 5.9.

Three natural cases arise from the values (r,d):

- $X \in \mathscr{E}(r,0)$ has r poles on $\mathbb{C}_z$ and Ψ_X is a polynomial map. See W. M. Boothby [15], [16] for pioneering work and S. K. Lando *et al.* [30] chapters 1 and 5 for advances in the combinatorial direction.
- $X \in \mathscr{E}(0,d)$ has an isolated essential singularity at $\infty \in \widehat{\mathbb{C}}_z$, no zeros or poles. Ψ_X is an infinitely ramified covering map as in (4). See R. Nevanlinna [39] chapter XI, M. Taniguchi [45], [46]; and [1].
- $X \in \mathscr{E}(r,d)$, r, $d \geq 1$, has r poles on $\mathbb{C}_z$ and an isolated essential singularity at $\infty \in \widehat{\mathbb{C}}_z$. Ψ_X is an infinitely ramified covering map as in (4).

Obviously, $\mathscr{E}(r,d)$ is an open complex submanifold of $\mathbb{C}^{r+d+1}$, see [2]. However for the study of analytical, geometrical and topological aspects of X and Ψ_X, "geometrical parameters" that shed light on the description of the vector fields are desirable. Recall for instance the role of the critical value map $\{f(z)_c = z^2 + c\} \mapsto c$, as dynamical parameters for the Mandelbrot set of the quadratic family; our search is for parameters with analogous properties. In our case, even though the map

$$\big\{\text{coefficients of } P(z), E(z) \text{ from } X\big\} \longmapsto \left\{ \begin{array}{c} \text{critical and asymptotic values} \\ \{\widetilde{p}_\iota\} \cup \{a_\sigma\} \subset \mathbb{C}_t \text{ of } \Psi_X \end{array} \right\}$$

is holomorphic, *the critical and asymptotic values of* Ψ_X *are insufficient to completely describe the family* $\mathscr{E}(r,d)$. See Example 8.5, Figure 13 for an instance in $\mathscr{E}(0,3)$ and Corollary 14.1.

The classical notion of divisor for $X \in \mathscr{E}(r,0)$, as a meromorphic section of the tangent line bundle $T\widehat{\mathbb{C}}_z$, provides a finite collection of pairs; poles and zeros with their orders. The divisor characterizes the vector field up to multiplicative factor, see Lemma 4.2. However, for $d \geq 1$ the essential singularity of X at ∞ encodes the information related to the exponential. Following the idea of divisor, for the transcendental case $d \geq 1$, we introduce a non–Hausdorff compactification of $\mathbb{C}_z$ with $2d$ copies of ∞. This allows us to obtain a finite collection of triplets; branch points in (4) with their ramification index. The triplets play the role of the divisor for $X \in \mathscr{E}(r,d)$, see

§4.2 and Definition 5.1. An advantage is that the information contained in the triplets includes the poles of X, the critical and asymptotic values of Ψ_X.

Once again, the information contained in the triplets is not enough for a complete description of X. With this in mind, in Definition 7.7, we introduce (r, d)–*configuration trees* Λ_X which are weighted directed rooted trees that completely encode the branched Riemann surfaces $\mathcal{R}_X$, for $X \in \mathscr{E}(r, d)$. They provided explicit "geometrical parameters", which allows us to obtain a *complete global analytical and geometrical description* for X.

The *vertices* of Λ_X are the triplets associated to the branch points in $\mathcal{R}_X$, over $\mathbb{C}_t$ as in (4), including their ramification index.

The *weighted edges* of Λ_X provide us with the relative position of the branch points on $\mathcal{R}_X$, as follows.

1) Each *edge* specifies which pair of branch points share the same sheet of $\mathcal{R}_X$.

2) The *weight* of the edge tells us the relative number of sheets of $\mathcal{R}_X$, we must go "up or down" on the surface in order to find another sheet containing other branch points.

Letting

$$\mathscr{E}(r,d)^* \doteq \left\{ X \in \mathscr{E}(r,d) \;\middle|\; \begin{array}{l} \mathcal{R}_X \text{ has at least two branch points over different} \\ \text{critical and asymptotic values of } \Psi_X \end{array} \right\},$$

we have the following result.

Main Theorem ((r, d)–configuration trees as parameters for $\mathscr{E}(r, d)$)**.**
For each pair (r, d), $r + d \geq 2$, there is an isomorphism, as complex manifolds of dimension $r + d + 1$, between $\mathscr{E}(r, d)^*$ and equivalence classes of (r, d)–configuration trees with at least two vertices, i.e.

$$\mathscr{E}(r,d)^* \cong \left\{ \left[\Lambda_X\right] \;\middle|\; \Lambda_X \textit{ is a } (r,d)\textit{–configuration tree with at least two vertices} \right\}.$$

The vector fields avoided in $\mathscr{E}(r, d)^*$ are of two kinds; those in $\mathscr{E}(0, 1)$ and those in $\mathscr{E}(r, 0)$ with a unique pole. In §8 explicit examples of Λ_X can be found, while in §6 a digression on some of the difficulties encountered in the proof of the Main Theorem, are presented. Moreover, these difficulties require the consideration of classes $[\Lambda_X]$ of (r, d)–configuration trees. Roughly speaking, the description of the classes originates from a re–labelling of the vertices of Λ_X, see Definition 9.5. The proof is presented in §9, with the description of the equivalence relation and their classes $[\,\cdot\,]$ in §9.4. Our Main Theorem extends results of [1] §8.5 in the families $\mathscr{E}(0, d)$, to the families $\mathscr{E}(r, d)$ with $r + d \geq 1$.

We decode the information at ∞, that is we shall answer the following question:

How can we describe the essential singularity of $X \in \mathscr{E}(r, d)$ at $\infty \in \widehat{\mathbb{C}}_z$?

The classical idea is to look at the germ at infinity $\big((\widehat{\mathbb{C}}_z, \infty), X\big)$ and try to split into a finite union of hyperbolic H, elliptic E, parabolic P and entire $\mathscr{E}$ angular sectors, this last based upon $\mathrm{e}^z \frac{\partial}{\partial z}$ at infinity; see Equation (104) and Figure 21. Thus obtaining a cyclic word $\mathcal{W}_X$ associated to $\big((\widehat{\mathbb{C}}_z, \infty), X\big)$. Recall the work of I. Bendixon, A. A. Andronov and F. Dumortier *et al.* (see [4] p. 304, [5] p. 84 and theorem 5.1 in [1]).

For the essential singularity of X at ∞ the analytic/topological nature of the invariants of X is certainly a novel aspect, see §14. Recall the following properties:

• The germ at infinity $\big((\widehat{\mathbb{C}}_z, \infty), X\big)$ is a local analytic invariant of X under biholomorphism germs of $(\widehat{\mathbb{C}}_z, \infty)$, and also under complex affine transformations $Aut(\mathbb{C}) \subset PSL(2, \mathbb{C})$ of $\mathbb{C}_z$.

• The cyclic word $\mathcal{W}_X = W_1 W_2 \cdots W_k$ is a local topological invariant of the phase portrait of $\mathfrak{Re}\,(X)$ under local homeomorphisms of $(\widehat{\mathbb{C}}_z, \infty)$ preserving the orientation.

The following theorem answers the above posed question, as well as the dynamical description of X and its associated real vector field $\mathfrak{Re}\,(X)$.

Theorem (Dynamical applications)**.** *Let be $X \in \mathscr{E}(r,d)$.*
1) The cyclic word $\mathcal{W}_X$ associated to X at ∞ is recognized as

$$\big((\widehat{\mathbb{C}}_z,\infty),\mathfrak{Re}\,(X)\big) \longmapsto \mathcal{W}_X = W_1 W_2 \cdots W_k, \quad W_\iota \in \{H, E, P, \mathscr{E}\}, \tag{5}$$

with exactly $2d$ letters $W_\iota = \mathscr{E}$.
2) The cyclic word $\mathcal{W}_X$ is a topological invariant of the germ $\big((\widehat{\mathbb{C}}_z,\infty),\mathfrak{Re}\,(X)\big)$.
3) Let $\big((\widehat{\mathbb{C}}_z,\infty),Y\big)$ be a singular complex analytic vector field germ, the following are equivalent:
- *The germ $\big((\widehat{\mathbb{C}}_z,\infty),Y\big)$ is analytically equivalent to the restriction of a vector field X in $\mathscr{E}(r,d)$ for $d \geq 1$.*
- *The cyclic word $\mathcal{W}_Y$ of the germ $\big((\widehat{\mathbb{C}}_z,\infty),\mathfrak{Re}\,(Y)\big)$ satisfies that*
  i) the residue of the 1–form of time ω_Y of Y is $Res(\omega_Y,\infty) = 0$,
  ii) the Poincaré–Hopf index of Y is $PH(Y,0) = 2 + r$,
  iii) the word $\mathcal{W}_Y$ has exactly $2d \geq 2$ entire sectors $\mathscr{E}$.

4) The phase portrait of $\mathfrak{Re}\,(X)$ is structurally stable (under perturbations in $\mathscr{E}(r,d)$) if and only if
  i) X has only simple poles,
  ii) all edges of Λ_X have non–zero imaginary component.

5) The number of (orientation preserving) topologically classes of phase portraits

$$\{\mathfrak{Re}\,(X) \mid X \in \mathscr{E}(r,d)\} \quad \text{on} \quad \widehat{\mathbb{C}}_z$$

is infinite if and only if

$$(r,d) \in \big\{(r \geq 2, 1), (r \geq 1, 2), (r \geq 0, d \geq 3)\big\}.$$

For the accurate assertions and proofs, see Theorem 12.2, Theorem 11.2 and Theorem 11.3, respectively. A stronger version of the decomposition of the phase portrait into $\mathfrak{Re}\,(X)$–invariant components, can be found as Theorem 10.1.

Throughout this work, the objects previously described are related via the diagram

$$\begin{tikzcd} & X \in \mathscr{E}(r,d) \arrow[dl, leftrightarrow] \arrow[dr, leftrightarrow] & & & \\ {[\Lambda_X]} \arrow[rr, leftrightarrow] & & (r,d)\text{–soul} \arrow[r] & \underbrace{\big((\widehat{\mathbb{C}}_z,\infty),X\big)}_{\substack{\text{local analytic} \\ \text{invariant of } X \text{ at } \infty}} \arrow[r] & \underbrace{\mathcal{W}_X = W_1 W_2 \cdots W_k}_{\substack{\text{local topological} \\ \text{invariant of } \mathfrak{Re}\,(X) \text{ at } \infty}}. \end{tikzcd}$$

The *soul of* X, Definition 9.7, is the smallest flat Riemann surface inside $\mathcal{R}_X$ that encodes all the combinatorial information of X. The analogous idea appears in Riemannian geometry [18] as the soul, and in vector fields [37] §5.2 as the dynamical locus. Summing up, the Main Theorem provides the global analytic bijection, on $\widehat{\mathbb{C}}$, between

- a vector field $X \in \mathscr{E}(r,d)$,
- a class $[\Lambda_X]$ of (r,d)–configuration trees, and
- an (r,d)–soul.

Clearly, the germ $\big((\widehat{\mathbb{C}}_z,\infty),X\big)$, does not determine the class of X in $\mathscr{E}(r,d)/Aut(\mathbb{C})$, see Remark 12.1.

For $\mathscr{E}(r,d)$, the topological classification of functions Ψ_X is coarser than the topological classification of phase portraits of vector fields $\mathfrak{Re}\,(X)$, see Remark 11.4. In particular, the Riemann surface $\mathcal{R}_X$ admits an infinite number of half planes $\overline{\mathbb{H}}^2$ if and only if $d \geq 1$. However, following R. Nevanlinna, Example 13.2 provides a Riemann surface admitting a decomposition in an infinite number of half planes, where the corresponding vector field does not belong to any $\mathscr{E}(r,d)$.

The study of complex functions and vector fields under geometric tools, in our context combinatorial with complex weights, is possible due to the richness of their geometric structure. The roots of which goes back to H. A. Schwarz [42] and F. Klein [28]. Our Main Theorem provides a geometrical characterization of the vector fields X, functions Ψ_X and Riemann surfaces $\mathcal{R}_X$ originated from the families $\mathscr{E}(r,d)$. It enhances the work of A. Speiser [43], R. Nevanlinna [39], [40] p. 291 and G. Elfving [20] on the classification, via line complexes, of simply connected Riemann surfaces $\mathcal{R}_X$ related to meromorphic functions Ψ_X. M. Taniguchi [45], [46] and K. Biswas *et al.* [12], [13], [14] develop analytic aspects of the functions Ψ_X, for $d \geq 1$. More recently, the study of parameter spaces for complex analytic vector fields is a current subject of interest; *e.g.* J. Muciño–Raymundo *et al.* [37], [36] in the rational case; B. Branner *et al.* [17], M.–E. Frías–Armenta *et al.* [23], K. Dias *et al.* [19], M. Kilmeš *et al.* [27] in the polynomial case.

Some of the proofs presented are based upon technical results of [1]. The minimal previous results, evidence and examples are provided in this work for a self contained reading and understanding.

In the combinatorial framework recall the fruitful ideas of Belyĭ functions and dessin's d'enfants, promoted by A. Grothendieck; (r,d)–configuration trees follow this, see §13.4.1. The extension of these ideas to $\mathscr{E}(r,d)$ will appear elsewhere. A clear topological description of $\mathcal{R}_X$ as a ramified covering, see (4), is missing for the more general vector fields $Y(z) = (Q(z)/P(z))\mathrm{e}^{E(z)}\frac{\partial}{\partial z}$ having zeros, it remains for future projects. The possible construction of effective local parameters for $\mathscr{E}(r,d)$, avoiding the equivalence classes in $\{[\Lambda_X]\}$ are discussed in the Epilogue §14.

2. Different facets for singular analytic vector fields $X \in \mathscr{E}(r,d)$

2.1. **Vector fields, differential forms, orientable quadratic differentials, flat metrics, distinguished parameters, Riemann surfaces.** Let

$$X(z) = \frac{1}{P(z)}\,\mathrm{e}^{E(z)}\frac{\partial}{\partial z} \in \mathscr{E}(r,d), \quad \deg P = r,\ \deg E = d,\ r+d \geq 1, \tag{6}$$

be a singular complex analytic vector field in the family (1). The polynomials describing it can be expressed as

$$\begin{aligned} P(z) &= (z-p_1)\cdots(z-p_r) \doteq z^r + b_1 z^{r-1} + \cdots + b_r, \\ E(z) &= \mu\,(z-e_1)\cdots(z-e_d) \doteq \mu\left(z^d + c_1 z^{d-1} + \cdots + c_d\right), \quad \mu \in \mathbb{C}^*. \end{aligned} \tag{7}$$

Note that if $d=0$ then $P(z)$ is non-necessarily monic, so in this case, let

$$\lambda \doteq \mathrm{e}^{E(z)} = \mathrm{e}^{\mu c_0} \in \mathbb{C}^*. \tag{8}$$

We denote by

$$\mathcal{P} \doteq \{p_1, \ldots, p_\iota, \ldots, p_r\} \tag{9}$$

the set of *poles of* X, allowing repetitions.

A *trajectory of* X is a maximal $z(\tau) : (a,b) \subseteq \mathbb{R} \longrightarrow \widehat{\mathbb{C}}_z$, where $a, b \in \mathbb{R}\cup\{\pm\infty\}$, $a<b$, satisfying that $\frac{dz(\tau)}{d\tau} = \mathfrak{Re}\,(X(z(\tau)))$. Equivalently, $z(\tau)$ is a trajectory of the associated real vector field $\mathfrak{Re}\,(X)$.

The *associated singular analytic* differential 1–form,

$$\omega_X = P(z)\,\mathrm{e}^{-E(z)}dz, \tag{10}$$

is such that $\omega_X(X) \equiv 1$, also called the 1–form of time of X.

A *singular analytic quadratic differential* $\mathcal{Q}$ on $\widehat{\mathbb{C}}_z$ is *orientable* if it is globally given as $\mathcal{Q} = \omega \otimes \omega$, for some singular analytic differential form ω on $\widehat{\mathbb{C}}_z$. In our case we have the quadratic differential,

$$\mathcal{Q}_X = \omega_X \otimes \omega_X = P^2(z)\, \mathrm{e}^{-2E(z)} dz^2. \tag{11}$$

The singular *horizontal trajectories* of $\mathcal{Q}_X$ on $\mathbb{C}_z \backslash \mathcal{P}$ are equivalent to the trajectories of the real vector field $\mathfrak{Re}\,(X)$, see for instance equation (2.2) of [1].
Since ω_X is holomorphic on $\mathbb{C}_z$, the local notion of *distinguished parameter* can be extended as below (see [29], [44] for the local case).

Definition 2.1. Let $X \in \mathscr{E}(r, d)$, the map

$$\Psi_X(z) = \int_{z_0}^{z} P(\zeta)\, \mathrm{e}^{-E(\zeta)} d\zeta : \mathbb{C}_z \longrightarrow \widehat{\mathbb{C}}_t$$

is a *global distinguished parameter for* X (note the dependence on $z_0 \in \mathbb{C}_z$).

The *singular flat Riemannian metric* g_X *with singular set* $\mathcal{P} \subset \mathbb{C}_z$ on $\mathbb{C}_z \backslash \mathcal{P}$ is defined as the pullback under $\Psi_X : (\mathbb{C}_z \backslash \mathcal{P}, g_X) \to (\mathbb{C}_t, \delta)$, where δ is the usual flat Riemannian metric on $\mathbb{C}_t$. The singularities of g_X at $p_\iota \in \mathcal{P}$ are cone points with angle $(2\nu_\iota + 2)\pi$, where $-\nu_\iota \leq -1$ is the order of the pole p_ι of X. The trajectories of $\mathfrak{Re}\,(X)$ and $\mathfrak{Im}\,(X)$ are unitary geodesics in $(\mathbb{C}_z \backslash \mathcal{P}, g_X)$.
The graph of Ψ_X

$$\mathcal{R}_X = \{(z, t) \mid t = \Psi_X(z)\} \subset \mathbb{C}_z \times \widehat{\mathbb{C}}_t$$

is a Riemann surface. Let π_1 and π_2 be the projections from $\mathcal{R}_X$ to $\mathbb{C}_z$ and $\widehat{\mathbb{C}}_t$, respectively. The flat metric on $\big(\mathcal{R}_X, \pi_2^*(\frac{\partial}{\partial t})\big)$ is induced by the usual metric on $\big(\widehat{\mathbb{C}}, \delta\big)$, equivalently $\big(\widehat{\mathbb{C}}_t, \frac{\partial}{\partial t}\big)$, via the projection of π_2. Since π_1, as in Diagram 12, is an isometry.

Lemma 2.2. *The following diagram commutes*

$$\begin{tikzcd}
\big(\widehat{\mathbb{C}}_z, X\big) \arrow[drr, "\Psi_X"'] & & \big(\mathcal{R}_X, \pi_2^*(\frac{\partial}{\partial t})\big) \arrow[ll, "\pi_1"'] \arrow[d, "\pi_2"] \\
& & \big(\widehat{\mathbb{C}}_t, \frac{\partial}{\partial t}\big).
\end{tikzcd} \tag{12}$$

Moreover, Ψ_X *is single valued, by removing* $\infty \in \widehat{\mathbb{C}}_z$*. The projection* π_1 *is a biholomorphism between*

$$\big(\mathcal{R}_X, \pi_2^*(\tfrac{\partial}{\partial t})\big) \quad \textit{and} \quad (\mathbb{C}_z, X).$$

□

In what follows, we shall use the abbreviated form $\mathcal{R}_X$ instead of the more cumbersome

$$\left(\mathcal{R}_X, \pi_2^*\left(\frac{\partial}{\partial t}\right)\right),$$

see Figures 7, 8, 11 and 14.
In Diagram 12 we abuse notation slightly by saying that the domain of Ψ_X is $\widehat{\mathbb{C}}_z$. This is a delicate issue.

Remark 2.3. By integrating along asymptotic paths associated to asymptotic values of Ψ_X at the essential singularity $\infty \in \widehat{\mathbb{C}}_z$, the choice of initial z_0 and end points z for the integral defining Ψ_X can be relaxed to include $\infty \in \widehat{\mathbb{C}}_z$ as end point, see Definition 3.4 and Figure 2.

Lemma 2.4. *1. The map* Ψ_X *is a global flow box of* X*,* i.e.

$$(\Psi_X)_* X = \frac{\partial}{\partial t} \qquad \textit{on the whole } \mathbb{C}_z.$$

2. For fixed initial condition $z_0 \in \mathbb{C}_z \backslash \mathcal{P}$, the maximal (under analytic continuation) time domain of the complex flow φ of X is provided by $\mathcal{R}_X$, that is

$$\varphi(z_0, \cdot\,) : \mathcal{R}_X \backslash \cup_{p_\iota \in \mathcal{P}} \left\{(p_\iota, \widetilde{p}_\iota)\right\} \longrightarrow \mathbb{C}_z \backslash \mathcal{P},$$

is a maximal complex trajectory solution.

Proof. For assertion 2, note that the punctured $\mathcal{R}_X \backslash \cup_{p_\iota \in \mathcal{P}} \left\{(p_\iota, \widetilde{p}_\iota)\right\}$ is a translation Riemann surface, following [48] §3.3 and [35]. Moreover, $\mathcal{R}_X$ is provided with singular horizontal and vertical foliations $\mathfrak{Re}\left(\pi_2^*(\frac{\partial}{\partial t})\right)$, $\mathfrak{Im}\left(\pi_2^*(\frac{\partial}{\partial t})\right)$, of real and imaginary time. In the spirit of Riemann surface theory, the complex trajectory $\varphi(z_0, \cdot\,) \doteq \pi_1(\cdot\,)$ is holomorphic and single valued function of the variable in this punctured Riemann surface. □

2.2. The singular complex analytic dictionary.

Proposition 2.5 (Dictionary between the singular analytic objects originating from $X \in \mathscr{E}(r, d)$, [1] p. 137)**.** *The following diagram describes a canonical bijective correspondence between its objects*

$$\begin{tikzcd}[column sep=small]
 & X(z) = \frac{1}{P(z)}\,\mathrm{e}^{E(z)}\frac{\partial}{\partial z} \arrow[dl, leftrightarrow] \arrow[dr, leftrightarrow] & \\
\omega_X(z) = P(z)\,\mathrm{e}^{-E(z)}dz \arrow[d, leftrightarrow] & & \Psi_X(z) = \int^z P(\zeta)\,\mathrm{e}^{-E(\zeta)}d\zeta \arrow[d, leftrightarrow] \\
\mathcal{Q}_X = P^2(z)\,\mathrm{e}^{-2E(z)}dz^2 \arrow[dr, leftrightarrow] & & \left(\mathcal{R}_X, \pi_2^*(\frac{\partial}{\partial t})\right) \arrow[dl, leftrightarrow] \\
 & \left((\mathbb{C}, g_X), \mathfrak{Re}\,(X)\right) &
\end{tikzcd} \quad . \tag{13}$$

□

Remark 2.6. The correspondence (13) must be understood up to choice of initial point z_0 for the integral defining the global distinguished parameter. Thus, Ψ_X and $\Psi_X + \mathtt{t}_0$ are considered the same object.

3. Analytic characteristics of $X \in \mathscr{E}(r, d)$

3.1. Order of growth at a singular point of X.

In the classic literature, the *order of growth or growth order at* ∞ is defined for entire functions, these invariants extend for vector fields, see [1] §4.1 and references therein. In the present work, we only require the use of the *1–order*.

Let $\psi : (\mathbb{C}\backslash\{0\}, 0) \to \mathbb{C}$ be a germ of a complex analytic function with an isolated singularity at $z = 0$; *i.e.* ψ has a pole or an isolated essential singularity at the origin. For $\varepsilon > 0$, let

$$M_\varepsilon(\psi) = \max_{|z|=\varepsilon}\{\log|\psi(z)|\}.$$

When the number $\rho \in \mathbb{R}$ determined by

$$\rho(\psi) = \limsup_{\varepsilon\to 0} \frac{\log(M_\varepsilon(\psi))}{-\log(\varepsilon)}$$

exists, it is called the *1–order of growth of* ψ *at* 0.

Definition 3.1. Let $\left((\mathbb{C}, 0), X(z) = f(z)\frac{\partial}{\partial z}\right)$ be a germ of a singular analytic vector field, with 0 an isolated singularity of X. The *1–order of* X *at* 0 is the corresponding 1–order of f, *i.e.* $\rho(X) := \rho(f)$. Analogously, if $\omega(z) = dz/f(z)$ is a germ of a differential form with an isolated singularity at 0, then ω inherits the *1–order* from that of the function $1/f$.

Lemma 3.2 ([1] p. 144)**.** *If* $X = \frac{1}{P(z)}\,\mathrm{e}^{E(z)}\frac{\partial}{\partial z} \in \mathscr{E}(r, d)$, *then at* $z = \infty$,

$$X \text{ has 1–order } \rho(X) = deg(E(z)) = d.$$

In this case the 1–order of ω *and* Ψ_X *agree and is the negative of the 1–order of* X. □

3.2. **Asymptotic values of Ψ_X.** Asymptotic values for meromorphic functions in the classical setting appear in many instances, see [26] p. 66, [39] pp. 298–303. We follow W. Bergweiler *et al.* [10], essentially verbatim from Definition 3.3 to Definition 3.6, below.

Let $\Psi : \mathbb{C}_z \longrightarrow \widehat{\mathbb{C}}_t$ be a meromorphic function, a priori not related to some vector field. The inverse function Ψ^{-1} can be defined on a Riemann surface which is conformally equivalent to $\mathbb{C}$ via Ψ^{-1}. We want to study the singularities of Ψ^{-1}. This can be done by adding to $\mathbb{C}_z$ some ideal points and defining neighborhoods of these points.

Definition 3.3. Take $a \in \widehat{\mathbb{C}}_t$ and denote by $D(a,\rho)$ the disk of radius $\rho > 0$ (in the spherical metric) centred at a. For every $\rho > 0$, choose a component $U(\rho)$ of $\Psi^{-1}(D(a,\rho))$ in such a way that $\rho_1 < \rho_2$ implies $U(\rho_1) \subset U(\rho_2)$. Note that the function $U : \rho \to U(\rho)$ is completely determined by its germ at 0.
Two possibilities can occur for the germ of U:
1) $\cap_{\rho>0} U(\rho) = \{z_0\}$, $z_0 \in \mathbb{C}_z$. In this case $a = \Psi(z_0)$.
   Moreover, if $a \in \mathbb{C}_t$ and $\Psi'(z_0) \neq 0$, or $a = \infty$ and z_0 is a simple pole of Ψ, then z_0 is called an *ordinary point*.
   On the other hand, if $a \in \mathbb{C}_t$ and $\Psi'(z_0) = 0$, or if $a = \infty$ and z_0 is a multiple pole of Ψ, then z_0 is called a *critical point* and a is called a *critical value*. We also say that the critical point z_0 *lies over* a.
2) $\cap_{\rho>0} U(\rho) = \varnothing$. Then we say that our choice $\rho \to U(\rho)$ defines a *transcendental singularity of* Ψ^{-1}, and that the transcendental singularity U *lies over* a.
   For every $\rho > 0$, the open set $U(\rho) \subset \mathbb{C}_z$ is called a *neighborhood of the transcendental singularity* U. So for $z_k \in \mathbb{C}_z$, we say that $z_k \to U$ if for every $\rho > 0$ there exists k_0 such that $z_k \in U(\rho)$ for $k \geq k_0$.

Definition 3.4. If U is a transcendental singularity of Ψ^{-1} then a is an *asymptotic value of* Ψ, which means that there exists an *asymptotic path* $\alpha(\tau) : (0,\infty) \longrightarrow \mathbb{C}_z$ tending to ∞ such that $\lim_{\tau\to\infty} \Psi(\alpha(\tau)) = a$.

In particular, it follows that every neighborhood $U(\rho)$ of a transcendental singularity U is unbounded.
If a is an asymptotic value of Ψ, then there is at least one transcendental singularity over a. Certainly there can be many different transcendental singularities as well as critical and ordinary points over the same point a.

Definition 3.5. A transcendental singularity U over a is called *direct* if there exists $\rho > 0$ such that $\Psi(z) \neq a$ for $z \in U(\rho)$, this is also true for all smaller values of ρ.
Moreover, U is called *indirect* if it is not direct, *i.e.* for every $\rho > 0$ the function Ψ takes the value a in $U(\rho)$, in which case the function Ψ takes the value a infinitely often in $U(\rho)$.

Definition 3.6. The transcendental singularity U is a *logarithmic branch point of* Ψ^{-1} *over* a, if $\Psi : U(\rho) \longrightarrow D(a,\rho)\backslash\{a\}$ is a universal covering for some $\rho > 0$. The (unbounded) neighborhoods $U(\rho)$ are called *exponential tracts*.

The simplest case of a direct singularity is a logarithmic branch point, see Example 4.1.

3.3. **Poles and zeros of X.** When we apply the above definitions to germs of the distinguished parameter Ψ_X, centered at the isolated singularities $\{p_1, \ldots, p_r, \infty\}$ of $X \in \mathscr{E}(r,d)$, three cases appear; poles, zeros and essential singularities. The local analytic normal forms of poles and zeros of X are well known. Figure 1 shows their real phase portraits, for further details see [36], [1] p. 133 and examples 4, 5 and 6 in [3].

Remark 3.7. *Analytic normal form for poles.* Let $p_\iota \in \mathcal{P}$ be a pole of X, having order[1] $-\nu_\iota \leq -1$. This corresponds to a critical point of Ψ_X, thus a *finite covering*

$$\Psi_X : U(\rho) \longrightarrow D(\widetilde{p}_\iota, \rho) \backslash \{\widetilde{p}_\iota\},$$

where

$$\widetilde{p}_\iota = \Psi(p_\iota) \text{ is the critical value.}$$

Furthermore, because of the local analytic normal forms, up to local biholomorphism

$$X(z) = \frac{1}{(z - p_\iota)^{\nu_\iota}} \frac{\partial}{\partial z} \quad \text{and} \quad \Psi_X(z) = \frac{(z - p_\iota)^{\nu_\iota + 1}}{\nu_\iota + 1} \quad \text{on } (\mathbb{C}, p_\iota). \tag{14}$$

The local phase portrait of $\mathfrak{Re}\,(X)$ at p_ι has $2(\nu_\iota + 1)$ hyperbolic sectors. See Figure 1.

Remark 3.8. *Analytic normal form for zeros.* The point $\infty \in \widehat{\mathbb{C}}_z$ is a zero for $X \in \mathscr{E}(r, d)$ if and only if $r \geq 1$ and $d = 0$. In this case ∞ is the unique zero of X and has order $s \doteq r + 2 \geq 3$. Ψ_X is a polynomial and ∞ is a pole of it. Using $\{w\}$ as a local chart at ∞, the local analytic normal forms of X and Ψ_X on $(\mathbb{C}_w, 0)$ are

$$X(z) = w^s \frac{\partial}{\partial w} \quad \text{and} \quad \Psi_X(z) = \frac{w^{1-s}}{(1-s)}, \quad s \geq 3. \tag{15}$$

The local phase portrait of $\mathfrak{Re}\,(X)$ at ∞ has $2(s - 1)$ elliptic sectors. See Figure 1.

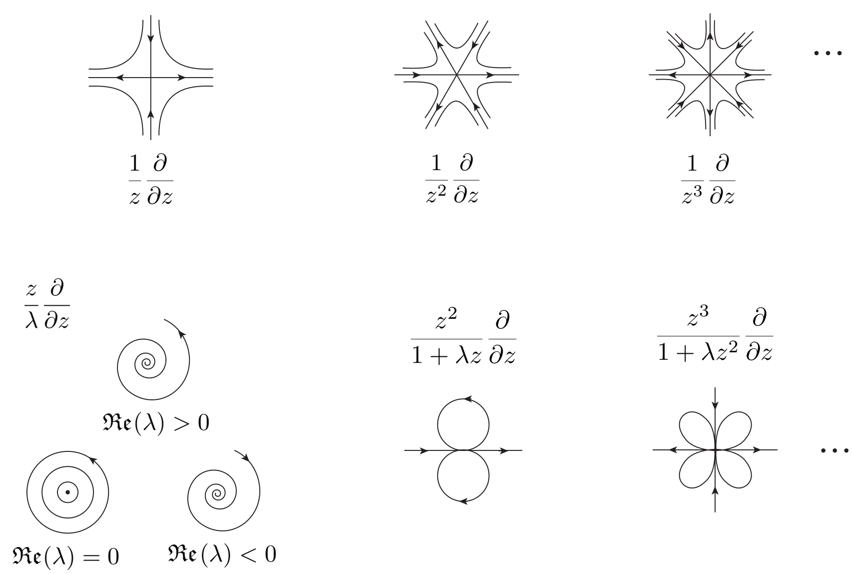

FIGURE 1. Normal forms of X and phase portraits of $\mathfrak{Re}\,(X)$ at poles or zeros in $z = 0$. Top row: for a pole of order $-\nu_\iota \leq -1$, the phase portrait has $2(\nu_\iota + 1)$ separatrices arriving or leaving the pole and $2(\nu_\iota + 1)$ hyperbolic sectors. Bottom row: simple zeros and zeros of order $s \geq 2$, here $\lambda = Res(\omega_X, 0)$. For simple zeros, the phase portrait is the pullback via $\Psi_X(z) = \lambda \log z$ of the constant vector field $Y(t) = \frac{\partial}{\partial t}$. For $s \geq 2$ the trajectories of $\mathfrak{Re}\,(X)$ form a flower with $2(s - 1)$ elliptic sectors. In our case $X \in \mathscr{E}(r, 0)$, note that $\lambda = 0$ and $s \geq 3$.

[1] We convene that the order $-\nu_\iota$ of a pole p_ι is to be negative.

Recalling (8) and summing up, we get the following.

Proposition 3.9 (Topological properties of $X \in \mathscr{E}(r,0)$)**.** *Let*

$$X(z) = \frac{\lambda}{P(z)}\frac{\partial}{\partial z} \in \mathscr{E}(r,0), \quad \deg P = r \geq 1,\ \lambda \in \mathbb{C}^*,$$

be a rational vector field, the following properties hold.

1) X has a zero of order $r+2 \geq 3$ at $\infty \in \widehat{\mathbb{C}}_z$.

2) The local phase portrait of $\mathfrak{Re}\,(X)$ at ∞ has $2(r+1)$ elliptic sectors.

3) X has a pole of order $-\nu_\iota$ at p_ι (a zero of $P(z)$ of order ν_ι).

4) The local phase portrait of $\mathfrak{Re}\,(X)$ at p_ι has $2(\nu_\iota+1)$ hyperbolic sectors.

5) The global phase portrait of X has a decomposition into

- *$2(r+1)$ half planes $(\overline{\mathbb{H}}^2_\pm, \frac{\partial}{\partial t})$ and*
- *M finite height horizontal strips of the form $\big(\{0 \leq \mathfrak{Im}\,(t) \leq h\}, \frac{\partial}{\partial t}\big)$, where $0 \leq M \leq r-1$ and each $h > 0$.*

Proof. Assertion (5) follows by a topological description of the separatrices of $\mathfrak{Re}\,(X)$ from the saddle points p_ι; see Figure 10 for examples of the assertions (4)–(5), in the case of three simple poles. More detail about the decomposition in (5), will be provided in Lemma 5.9. □

A simple example that will be used throughout follows.

Example 3.1. Consider the vector field

$$X(z) = \frac{\lambda}{(z-p_1)^r}\frac{\partial}{\partial z} \in \mathscr{E}(r,0), \quad r \geq 1, \tag{16}$$

and its distinguished parameter

$$\Psi_X(z) = \frac{1}{\lambda}\int_{z_0}^{z} (\zeta - p_1)^r d\zeta = \frac{1}{\lambda(r+1)}\big((z-p_1)^{r+1} - (z_0-p_1)^{r+1}\big). \tag{17}$$

the pole p_1 of X is the critical point of Ψ_X and its critical value is

$$\widetilde{p}_1 = \Psi_X(p_1) = -\frac{1}{\lambda(r+1)}(z_0-p_1)^{r+1}. \tag{18}$$

See also Example 8.2. The vector field in Equation (16) is such that, $\mathcal{R}_X$ has only one branch point. Whence, the subfamily of these vector fields is in $\mathscr{E}(r,d)\backslash\mathscr{E}^*(r,d)$, which are forbidden in the Main Theorem.

4. Branch points of $\mathcal{R}_X$

4.1. **Local ramification data for $\mathcal{R}_X$.** For $d \geq 1$, the point $\infty \in \widehat{\mathbb{C}}_z$ is an isolated essential singularity of

$$X(z) = \frac{1}{P(z)}\,\mathrm{e}^{E(z)}\frac{\partial}{\partial z},$$

and the distinguished parameter Ψ_X, belongs to the family

$$SF_{r,d} = \left\{ \Psi_X(z) = \int_{z_0}^{z} P(\zeta)\,\mathrm{e}^{-E(\zeta)}d\zeta \;\middle|\; P, E \in \mathbb{C}[z],\ \deg P = r,\ \deg E = d \right\}, \tag{19}$$

of *structurally finite entire functions of type* (r,d), see [45]. We recall the simplest object.

Example 4.1. Consider the vector field

$$X(z) = \mathrm{e}^{\mu(z+c_1)} \frac{\partial}{\partial z} \in \mathscr{E}(0,1) \tag{20}$$

and its corresponding distinguished parameter

$$\Psi_X(z) = \frac{1}{\mu} \int_{z_0}^{z} \mathrm{e}^{-\mu(\zeta+c_1)} d\zeta = \frac{1}{\mu}\big(\mathrm{e}^{-\mu(z_0+c_1)} - \mathrm{e}^{-\mu(z+c_1)}\big), \tag{21}$$

with $\mu \in \mathbb{C}^*$, $c_1 \in \mathbb{C}$ as in (7). Of course $\infty \in \widehat{\mathbb{C}}_z$ is an isolated essential singularity of both. Moreover, Ψ_X has two asymptotic values

$$a_1 = \frac{1}{\mu}\mathrm{e}^{-\mu(z_0+c_1)} \in \mathbb{C}_t \quad \text{and} \quad a_2 = \infty \in \widehat{\mathbb{C}}_t \tag{22}$$

with exponential tracts the half planes

$$U_1(\rho) = \{z \in \mathbb{C}_z \mid \mathfrak{Re}\,(\mu z) > \rho\} \;\; \text{and} \;\; U_2(\rho) = \{z \in \mathbb{C}_z \mid \mathfrak{Re}\,(\mu z) < -\rho\},$$

respectively. The multivalued function

$$\Psi_X^{-1}(t) = \frac{1}{\mu} \log\left(- \frac{\mathrm{e}^{\mu(z_0+c_1)}}{t\,\mu\,\mathrm{e}^{\mu(z_0+c_1)} - 1} \right) - c_1$$

has two logarithmic branch points: one over the finite asymptotic value a_1 and the other over the asymptotic value $a_2 = \infty$. Note that Equation (20) defines a forbidden stratum in the whole family $\mathscr{E}(r,d)$ of the Main Theorem.

In order to determine the Riemann surface $\mathcal{R}_X$ precisely, one needs the knowledge of the branch points under π_2

$$\{(z_{\mathfrak{a}}, t_{\mathfrak{a}})\} \subset \mathcal{R}_X, \quad z_{\mathfrak{a}} \in \{p_1, p_2, \ldots, p_n, \infty\}, \quad t_{\mathfrak{a}} \doteq \Psi_X(z_{\mathfrak{a}}), \quad 0 \le n \le r. \tag{23}$$

The subindex $\mathfrak{a}$ will be very useful in several constructions. The next result clearly explains the singularities of Ψ_X^{-1}.

Lemma 4.1 (The existence of finitely ramified and logarithmic branch points)**.** *Let*

$$\Psi_X : \mathbb{C}_z \to \widehat{\mathbb{C}}_t$$

be a structurally finite entire function of type (r,d). Then

1) Ψ_X has r critical values $\{\widetilde{p}_\iota\} \subset \mathbb{C}_t$ (counted with multiplicity),

2) Ψ_X^{-1} has d direct singularities corresponding to d logarithmic branch points over d finite asymptotic values $\{a_\sigma\} \subset \mathbb{C}_t$ of Ψ_X, and

3) Ψ_X^{-1} has d direct singularities corresponding to d logarithmic branch points over $\infty \in \widehat{\mathbb{C}}_t$.

Furthermore, Ψ_X^{-1} has no indirect singularities.

Proof. Case (r,d) with $d \ge 1$ can be found as lemma 8.4 in [1] with a proof that relies heavily on the work of M. Taniguchi [45], [46]. □

4.2. **Branch point enumeration.** As motivation, let $T\widehat{\mathbb{C}}_z$ be the holomorphic tangent bundle of $\widehat{\mathbb{C}}_z$. For $X \in \mathscr{E}(r,0)$, the *divisor of the meromorphic section* $X : \widehat{\mathbb{C}}_z \longrightarrow T\widehat{\mathbb{C}}_z$ is the assignment[2]

$$X \;\longmapsto\; (\infty, r+2) \cup \big\{(p_\iota, -\nu_\iota)\big\}_{\iota=1}^{n}, \tag{24}$$

where $\sum_{\iota=1}^{n} \nu_\iota = r$ and $n \le r$, the equality holds if and only if all the poles of X are simple.

The fact that zeros and poles determine a meromorphic vector field on $\mathbb{C}_z$ up to scalar factor is a very useful result for meromorphic vector fields on $\widehat{\mathbb{C}}_z$. It is a result from the Brill–Noether theory in algebraic geometry, or the Poincaré–Hopf theory in differential equations.

[2]A formal sum of pairs (p,ν) denoting a point in $\widehat{\mathbb{C}}_z$ and its order in $\mathbb{Z}^*$, positive for a zero of the vector field, negative for a pole.

Lemma 4.2. *Let ν_j, $\nu_\iota \in \mathbb{N}$, a divisor*
$$\big\{(q_j,\nu_j)\big\}_{j=1}^{s} \cup \big\{(p_\iota,-\nu_\iota)\big\}_{\iota=1}^{n} \subset \widehat{\mathbb{C}}_z \times \mathbb{Z}^*$$
determines a non-empty family of meromorphic vector fields $\{\lambda Y \mid \lambda \in \mathbb{C}^*\}$ on $\widehat{\mathbb{C}}_z$ if and only if
$$\sum_{j=1}^{s} \nu_j - \sum_{\iota=1}^{n} \nu_\iota = s - r = 2.$$
□

We would like to extend Lemma 4.2 to the case of $X \in \mathscr{E}(r,d)$, $d \geq 1$. Of course the divisor (24) is not well defined since X is not meromorphic on $\widehat{\mathbb{C}}_z$.
In order to accomplish this, an accurate enumeration of the branch points $\{(z_{\mathfrak{a}}, t_{\mathfrak{a}})\} \subset \mathcal{R}_X$ in (23) is required. In what follows, the reader might find it helpful to follow along with Figures 7–8, 11–17 in §8.

For $r \geq 1$, the point $z_{\mathfrak{a}}$ is a **pole** $p_\iota \in \mathbb{C}_z$ of X having order $-\nu_\iota \leq -1$ if and only if its image $\widetilde{p}_\iota = \Psi_X(p_\iota) \in \mathbb{C}_t$ is a critical value of Ψ_X. Moreover $(p_\iota, \widetilde{p}_\iota) \in \mathcal{R}_X$ is a finitely ramified branch point (under π_2) with ramification index $\nu_\iota + 1 \geq 2$. Recall (14).
Enlarging the pairs in the divisor, we enumerate the corresponding finitely ramified branch points using *triplets*

$$\big\{ \textcircled{\iota} \doteq (p_\iota, \widetilde{p}_\iota, -\nu_\iota)\big\}_{\iota=1}^{n} \subset \mathcal{R}_X, \ \text{with order } -\nu_\iota \leq -1 \text{ and } \sum_{\iota=1}^{n} \nu_\iota = r. \tag{25}$$

Abusing notation, we say that the triplets are in $\mathcal{R}_X$.

For $d \geq 1$, after enumerating the poles as above, we also need to consider the logarithmic branch points of Ψ_X^{-1} in $\mathcal{R}_X \subset \mathbb{C}_z \times \mathbb{C}_t$. We shall use two compactifications: the usual one for $\mathbb{C}_t$, namely the Riemann sphere $\widehat{\mathbb{C}}_t$, and a non–Hausdorff one for $\mathbb{C}_z$ as follows.

Definition 4.3. The *non–Hausdorff closure*
$$\overline{\mathbb{C}}_z \doteq \Big(\big(\widehat{\mathbb{C}} \times \{1\}\big) \sqcup \big(\widehat{\mathbb{C}} \times \{2\}\big) \sqcup \cdots \sqcup \big(\widehat{\mathbb{C}} \times \{2d\}\big) \Big) \Big/ \sim \tag{26}$$
is the sphere with $2d \geq 2$ infinities, that is the disjoint union of $2d$ copies of the Riemann sphere $\widehat{\mathbb{C}}$ with the equivalence relation $(z,\sigma) \sim (z,\eta)$ for all $\sigma, \eta \in \{1,\ldots,2d\}$ when $z \neq \infty$.

The point $\infty \in \widehat{\mathbb{C}}_z$ is an **isolated essential singularity of** X. Hence, we will denote the $2d$ different infinities, referred to in (26) and Lemma 4.1, by
$$\{\infty_\sigma \doteq (\infty, \sigma)\}_{\sigma=1}^{2d} \subset \overline{\mathbb{C}}_z. \tag{27}$$
In order to include the logarithmic branch points, $\mathcal{R}_X$ extends to $\overline{\mathcal{R}}_X \subset \overline{\mathbb{C}}_z \times \widehat{\mathbb{C}}_t$. By simplicity, we shall use the same notation $\mathcal{R}_X$ for this extension. Lemma 4.1 allows us to accurately denote the distinct asymptotic values of Ψ_X by
$$\begin{aligned} &\{a_j\}_{j=1}^{m} \subset \mathbb{C}_t && \text{with multiplicities } \{\mathtt{m}_j \geq 1\}_{j=1}^{m},\ \textstyle\sum_{j=1}^{m} \mathtt{m}_j = d \text{ and} \\ &a_{m+1} = \infty \in \widehat{\mathbb{C}}_t && \text{with multiplicity } d. \end{aligned} \tag{28}$$
Thus, $\pi_2^{-1}(a_j)$ contains $\mathtt{m}_j$ (resp. d) logarithmic branch points for each exponential tract $U_\sigma(\rho)$ associated to the asymptotic value a_j, $j = 1,\ldots,m$ (resp. $j = m+1$).
Recalling the multiplicities, the correspondence between indices is given by
$$\begin{array}{rl} \sigma \in & \underbrace{1,\ \ldots\ ,\mathtt{m}_1},\ \underbrace{\mathtt{m}_1+1\ ,\ \ldots\ ,\mathtt{m}_1+\mathtt{m}_2},\ \ldots\ ,\ \underbrace{d-\mathtt{m}_m+1,\ \ldots\ ,d},\ \underbrace{d+1,\ \ldots\ ,2d}, \\ j = j(\sigma) \in & \qquad 1 \qquad\quad ,\qquad\qquad 2 \qquad\qquad\ ,\ \ldots\ ,\qquad\quad m \qquad\quad\ ,\qquad m+1 \qquad , \end{array} \tag{29}$$
where σ enumerates the logarithmic branch points, while $j = j(\sigma)$ enumerates the distinct asymptotic values $a_j \in \widehat{\mathbb{C}}_t$, in accordance with (28).

Remark 4.4. 1. The asymptotic paths $\alpha_\sigma(\tau)$ lie in the non–Hausdorff closure $\overline{\mathbb{C}}_z$. If $\alpha_\sigma(\tau) : (0,\infty) \longrightarrow \overline{\mathbb{C}}_z$ is an asymptotic path approaching $\infty_\sigma \in \overline{\mathbb{C}}_z$ associated to the asymptotic value $a_{j(\sigma)}$, then we may assume that $\alpha_\sigma(\tau)$ is restricted to one exponential tract (the one containing $\infty_\sigma \in \overline{\mathbb{C}}_z$). The actual choice of $\alpha_\sigma(\tau)$ inside the exponential tract $U_\sigma(\rho)$ will be made explicit in Proposition 4.8.4 and Remark 4.9.2.
2. Each asymptotic path $\alpha_\sigma(\tau)$ together with the distinguished parameter Ψ_X gives rise to the asymptotic value

$$a_{j(\sigma)} = \lim_{\substack{z\to\infty_\sigma \\ z\in\alpha_\sigma}} \Psi_X(z) = \lim_{\tau\to\infty} \int_{z_0}^{\alpha_\sigma(\tau)} P(\zeta)\mathrm{e}^{-E(\zeta)}d\zeta \in \widehat{\mathbb{C}}_t. \tag{30}$$

3. Because of the multiplicity of $a_{j(\sigma)}$, when $1 \le j(\sigma) \le m$ there are exactly $\mathtt{m}_j$ asymptotic paths $\alpha_\sigma(\tau)$ and $\mathtt{m}_j$ exponential tracts for each of the m distinct finite asymptotic values $a_{j(\sigma)} \in \mathbb{C}_t$, see Figure 2. Moreover, there are d asymptotic paths and d exponential tracts for the asymptotic value $a_{m+1} = \infty \in \widehat{\mathbb{C}}_t$.

Recalling that logarithmic branch points are infinitely ramified and using the notation provided by Equation (27), we will denote the logarithmic branch points of Ψ_X^{-1} over the asymptotic values $a_{j(\sigma)} \in \mathbb{C}_t$ of Ψ_X, as *triplets*

$$n{+}\sigma \doteq (\infty_\sigma, a_{j(\sigma)}, -\infty) \in \mathcal{R}_X, \quad \text{for } \sigma \in \{1,\dots,2d\}. \tag{31}$$

Abusing notation, we say that the triplets are in $\mathcal{R}_X$.

The above discussion proves the following.

Lemma 4.5. *For $X \in \mathscr{E}(r,d)$, there is a bijective correspondence between:*
· *the $2d$ logarithmic branch points of Ψ_X^{-1}, $n{+}\sigma$ in $\mathcal{R}_X$,*
· *the $2d$ asymptotic values a_σ of Ψ_X (counted with multiplicities) in $\widehat{\mathbb{C}}_t$,*
· *the $2d$ exponential tracts $U_\sigma(\rho)$ in $\widehat{\mathbb{C}}_z$ and*
· *the $2d$ asymptotic paths $\alpha_\sigma(\tau)$ in $\overline{\mathbb{C}}_z$.* □

Remark 4.6. 1. An immediate advantage of the correspondence in Lemma 4.5 is that the index σ simultaneously enumerates all of the objects in question. In particular, from now on we agree that

$$a_\sigma \text{ is referring to } a_{j(\sigma)} \in \widehat{\mathbb{C}}_t, \text{ as in (29).}$$

For example the set $\{a_{j(\sigma)}\}$ corresponds to one point in $\mathbb{C}_t$ for $\sigma = \mathtt{m}_1+1,\dots,\mathtt{m}_1+\mathtt{m}_2$.
2. In $\widehat{\mathbb{C}}_z$, each exponential tract is an angular sector about ∞. Hence the exponential tracts have a natural counterclockwise ordering about $\infty \in \widehat{\mathbb{C}}_z$ arising from $S^1 = \{\mathrm{e}^{i\theta}\}$. The ordering will be made explicit in Proposition 4.8.3; see also Figure 2 and the last row in Figure 3.

We have the following *ad hoc* notion, that expands the concept of divisor of X as a meromorphic section, Equation (24).

Definition 4.7. Let $X \in \mathscr{E}(r,d)$, $d \ge 1$, the assignment

$$X \longmapsto \underbrace{\Big\{ \iota = \big(p_\iota, \widetilde{p}_\iota, -\nu_\iota\big)\Big\}_{\iota=1}^{n}}_{\text{pole vertices}} \cup \underbrace{\Big\{ n{+}\sigma = \big(\infty_\sigma, a_\sigma, -\infty\big)\Big\}_{\sigma=1}^{d}}_{\text{essential vertices}}$$
$$\cup \underbrace{\Big\{ n{+}\sigma = \big(\infty_\sigma, \infty, -\infty\big)\Big\}_{\sigma=d+1}^{2d}}_{\text{vertices over } \infty} \tag{32}$$

is the *divisor of* X.

The notation in Equation (32) will be useful at several stages of the proof of the main result. The following section explains the equidistribution of the exponential tracts and thus provides a natural ordering/enumeration for the asymptotic values.

4.3. **Approximation of $X \in \mathscr{E}(r,d)$, $d \geq 1$, via rational vector fields $X_{\mathtt{n}}$.** The vector fields $X \in \mathscr{E}(r,d)$ for $d \geq 1$ can be approximated by rational vector fields of the form $X_{\mathtt{n}}(z) = \frac{1}{\mathtt{P}_{\mathtt{n}}(z)}\frac{\partial}{\partial z}$. Analogous ideas for other differential equations are applied in [34]. Moreover, as will be shown, the construction behaves nicely providing insight into de combinatorial/geometrical structure of X, Ψ_X and $\mathcal{R}_X$.

Let X be as in (6) and recall Euler's formula

$$\mathrm{e}^{-E(z)} = \lim_{\mathtt{n}\to\infty}\Big(1 - \frac{E(z)}{\mathtt{n}}\Big)^{\mathtt{n}}. \tag{33}$$

Thus

$$X_{\mathtt{n}}(z) = \frac{1}{P(z)\big(1 - \frac{E(z)}{\mathtt{n}}\big)^{\mathtt{n}}}\frac{\partial}{\partial z} \quad \text{and} \quad \Psi_{\mathtt{n}}(z) = \int_{z_0}^{z} P(\zeta)\Big(1 - \frac{E(\zeta)}{\mathtt{n}}\Big)^{\mathtt{n}} d\zeta \tag{34}$$

converge to

$$X(z) = \frac{1}{P(z)}\mathrm{e}^{E(z)}\frac{\partial}{\partial z} \quad \text{and} \quad \Psi_X(z) = \int_{z_0}^{z} P(\zeta)\mathrm{e}^{-E(\zeta)}d\zeta \tag{35}$$

uniformly on compact sets of $\mathbb{C}_z$. Furthermore,

$$\mathcal{R}_{X_{\mathtt{n}}} = \{(z, \Psi_{\mathtt{n}}(z)) \mid z \in \mathbb{C}_z\}$$

converges to $\mathcal{R}_X$, in the Caratheodory topology; see K. Biswas *et al.* [12], [13] for details on Caratheodory convergence.

Because of the Dictionary Proposition 2.5 (see also Remarks 3.7 and 3.8), as $\mathtt{n} \to \infty$, the successions $\{X_{\mathtt{n}}\}$, $\{\Psi_{\mathtt{n}}\}$ and $\{\mathcal{R}_{X_{\mathtt{n}}}\}$ enjoy the following features.

Each $X_{\mathtt{n}}$ has:

- n poles at the roots $\{p_\iota\}_{\iota=1}^{n}$ of $P(z)$ with orders $\{-\nu_\iota\}$, where $r = \sum_{\iota=1}^{n}\nu_\iota$,
- d poles at the roots $\{\widehat{e}_\sigma = \widehat{e}_\sigma(\mathtt{n})\}_{\sigma=1}^{d}$ of $\mathtt{n} - E(z)$, each of order $-\mathtt{n}$ and
- a zero of order $r + d\mathtt{n} + 2$ at $\infty \in \widehat{\mathbb{C}}_z$.

In consequence, each $\Psi_{\mathtt{n}}$ has:

- n critical points $\{p_\iota\}_{\iota=1}^{n}$ at the roots of $P(z)$, with n critical values $\{\widetilde{p}_\iota(\mathtt{n}) \doteq \Psi_{\mathtt{n}}(p_\iota)\}_{\iota=1}^{n}$, where $r = \sum_{\iota=1}^{n}\nu_\iota$,
- d critical points $\{\widehat{e}_\sigma = \widehat{e}_\sigma(\mathtt{n})\}_{\sigma=1}^{d}$ at the roots of $\mathtt{n} - E(z)$ with critical values $\{\widetilde{e}_\sigma(\mathtt{n}) \doteq \Psi_{\mathtt{n}}(\widehat{e}_\sigma)\}_{\sigma=1}^{d}$ and
- a pole of order $-(r + d\mathtt{n} + 2)$ at $\infty \in \widehat{\mathbb{C}}_z$.

Each $\mathcal{R}_{X_{\mathtt{n}}}$ has:

- n finitely ramified branch points $\{(p_\iota, \widetilde{p}_\iota(\mathtt{n}), -\nu_\iota)\}_{\iota=1}^{n}$ with ramification index corresponding to $\nu_\iota + 1$ where $-\nu_\iota$ is the order of the pole p_ι, where $r = \sum_{\iota=1}^{n}\nu_\iota$,
- d finite ramification points $\{(\widehat{e}_\sigma(\mathtt{n}), \widetilde{e}_\sigma(\mathtt{n}), -\mathtt{n})\}_{\iota=1}^{d}$ with ramification index $\mathtt{n} + 1$ and
- a finite ramification point $(\infty, \infty, r + \mathtt{n}d + 2)$ with ramification index $r + \mathtt{n}d + 3$.

Clearly the critical points p_ι do not change as $\mathtt{n} \to \infty$; however the critical values $\widetilde{p}_\iota(\mathtt{n}) \in \mathbb{C}_t$ do, but remain finite without changing their ramification index, thus each finitely ramified branch point $(p_\iota, \widetilde{p}_\iota(\mathtt{n}), -\nu_\iota)$ converges to the finitely ramified branch point

$$(p_\iota, \widetilde{p}_\iota, -\nu_\iota) = (p_\iota, \Psi_X(p_\iota), -\nu_\iota).$$

As the critical points $\{\widehat{e}_\sigma(\mathtt{n})\}$ approach $\infty \in \widehat{\mathbb{C}}_z$, the corresponding critical values $\{\widetilde{e}_\sigma(\mathtt{n})\}$ converge to the finite asymptotic values $\{a_\sigma\}$ of Ψ_X, as follows.
In $\widehat{\mathbb{C}}_z$, arguments (directions) and angular sectors at ∞ are well defined. The succession $\widehat{e}_\sigma(\mathtt{n})$ converges to a ray with constant argument θ_σ starting at $\infty \in \mathbb{C}_z$. Moreover, the rays θ_σ and $\theta_{\sigma+1}$ are exactly $2\pi/d$ radians apart.

The careful examination of the phase portraits of the rational vector fields $\mathfrak{Re}\,(X_{\mathtt{n}})$ shows the following features:
i) the zero at ∞ of $X_{\mathtt{n}}$ determines $2r+2\mathtt{n}d+2$ elliptic sectors, and the same number of separatrices,
ii) the d poles at $\widehat{e}_\sigma$ of $X_{\mathtt{n}}$ determine $2\mathtt{n}+2$ hyperbolic sectors, and the same number of separatrices.

The above is summarized in the following.

Proposition 4.8. *Let $d \geq 1$ and $X \in \mathscr{E}(r,d)$. Then, the sequence of polynomial distinguished parameters $\Psi_{X_{\mathtt{n}}}$ given by (34), converges to Ψ_X. Furthermore:*
1) Each of the r sequences of finitely ramified branch points $(p_\iota, \widetilde{p}_\iota(\mathtt{n}), -\nu_\iota) \in \mathcal{R}_{X_{\mathtt{n}}}$ converges to the finitely ramified branch point $(p_\iota, \widetilde{p}_\iota, -\nu_\iota) \in \mathcal{R}_X$.
2) Each of the d sequences of finitely ramified branch points $(\widehat{e}_\sigma(\mathtt{n}), \widetilde{e}_\sigma(\mathtt{n}), -\mathtt{n}) \in \mathcal{R}_{X_{\mathtt{n}}}$ converges to the logarithmic branch point of Ψ_X^{-1}, $(\infty_\sigma, a_\sigma, -\infty) \in \mathcal{R}_X$.
3) The $2d$ exponential tracts of Ψ_X are angular sectors of angle π/d about $\infty \in \widehat{\mathbb{C}}_z$ and they alternate so that each exponential tract corresponding to a finite asymptotic value is in between two exponential tracts corresponding to the asymptotic value $\infty \in \widehat{\mathbb{C}}_t$.
4) There exist $2d$ asymptotic paths $\alpha_\sigma(\tau)$ associated to the asymptotic values $\{a_\sigma\}_{\sigma=1}^{2d}$ of Ψ_X which are angularly equidistributed about $\infty \in \widehat{\mathbb{C}}_z$. □

Remark 4.9. 1. Figure 2 shows the angular equidistribution of the exponential tracts around ∞ for $X \in \mathscr{E}(r,d)$.
2. By recalling that

$$E(z) = \mu\left(z^d + c_1 z^{d-1} + \cdots + c_d\right) \text{ in (33)},$$

a simple calculation shows that:
a) For the finite asymptotic values $a_\sigma \in \mathbb{C}_t$ of Ψ_X, without loss of generality we can choose asymptotic paths $\alpha_\sigma(\tau)$ arriving at $\infty \in \widehat{\mathbb{C}}_z$ with angle $\theta_\sigma = \operatorname{Arg}\left(\mu^{1/d}\right) + \frac{2\pi}{d}\sigma$ for $\sigma = 1, \ldots, d$.
b) Likewise, the asymptotic paths $\alpha_\sigma(\tau)$ corresponding to the asymptotic value $\infty \in \widehat{\mathbb{C}}_t$ arrive at $\infty \in \widehat{\mathbb{C}}_z$ with angle $\theta_\sigma = \operatorname{Arg}\left(\mu^{1/d}\right) + \frac{2\pi}{d}(\sigma - d) + \frac{\pi}{d}$ for $\sigma = d+1, \ldots, 2d$.

Example 4.2. Let

$$X(z) = \frac{\mathrm{e}^{z^d}}{z^r}\frac{\partial}{\partial z} \in \mathscr{E}(r,d), \qquad \text{for } d \geq 1.$$

Euler's formula provides the approximation of X by the vector fields

$$X_{\mathtt{n}}(z) = \frac{1}{z^r\left(1 - \frac{z^d}{\mathtt{n}}\right)^{\mathtt{n}}}\frac{\partial}{\partial z}, \qquad \text{for } \mathtt{n} \geq 1,$$

so

$$\Psi_{\mathtt{n}}(z) = \int_0^z \zeta^r\left(1 - \frac{\zeta^d}{\mathtt{n}}\right)^{\mathtt{n}} d\zeta = \frac{z^{r+1}\,{}_2F_1\left(-\mathtt{n}, \frac{r+1}{d}; \frac{r+1}{d} + 1; \frac{z^d}{\mathtt{n}}\right)}{r+1},$$

where ${}_2F_1$ is the classical Gauss's hypergeometric function, see for instance [41] ch. 15.
The poles of $X_{\mathtt{n}}$ are 0, of order $-r$, and $\{\widehat{e}_\sigma(\mathtt{n}) \doteq e^{\frac{2i\pi\sigma}{d}}\mathtt{n}^{1/d}\}_{\sigma=1}^{d}$, of order $-\mathtt{n}$. Of course the poles of $X_{\mathtt{n}}$ are the critical points of $\Psi_{\mathtt{n}}$,

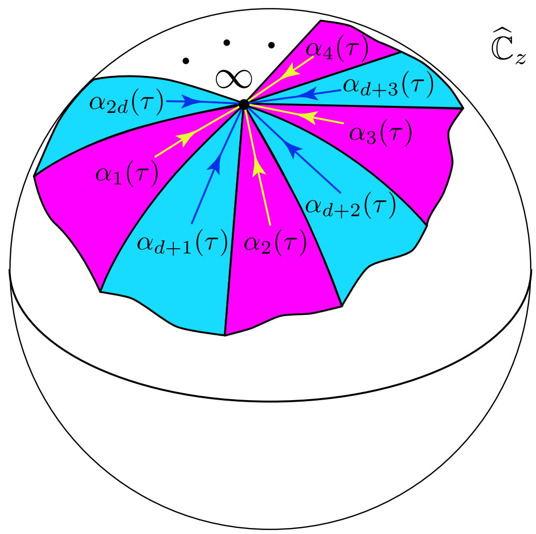

FIGURE 2. Angular equidistribution of the $2d$ exponential tracts about $\infty \in \widehat{\mathbb{C}}_z$, corresponding to the asymptotic values of $\Psi_X(z)$ for $X \in \mathscr{E}(r,d)$, $d \geq 1$. Purple angular sectors represent exponential tracts corresponding to finite asymptotic values $a_\sigma \in \mathbb{C}_t$, in yellow their asymptotic paths $\alpha_\sigma(\tau)$, for $\sigma = 1, \ldots, d$. Blue angular sectors represent exponential tracts corresponding to the asymptotic value $\infty \in \widehat{\mathbb{C}}_t$, in dark blue their asymptotic paths, $\alpha_\sigma(\tau)$, for $\sigma = d+1, \ldots, 2d$. Once again, the $2d$ asymptotic paths are equally distributed about $\infty \in \widehat{\mathbb{C}}_z$. Note that for the family $\mathscr{E}(r,d)$ this equidistribution property is independent of r.

On the other hand, the critical values of $\Psi_{\mathtt{n}}$ are given by $\Psi_{\mathtt{n}}(0) = 0$ and

$$\widetilde{e}_\sigma(\mathtt{n}) \doteq \Psi_{\mathtt{n}}(e^{\frac{2i\pi\sigma}{d}} \mathtt{n}^{1/d}) = e^{2i\pi\sigma \frac{(r+1)}{d}} \frac{\Gamma\left(\frac{r+1}{d}+1\right)}{(r+1)} \frac{\mathtt{n}^{(r+1)/d}\,\Gamma(\mathtt{n}+1)}{\Gamma\left(\mathtt{n}+\frac{r+1}{d}+1\right)}, \tag{36}$$

for $\sigma = 1, \ldots, d$.
Furthermore $X_{\mathtt{n}}$ has a unique zero at $\infty \in \widehat{\mathbb{C}}_z$ of order $r + \mathtt{n}d + 2$.
Hence each Riemann surface

$$\mathcal{R}_{X_{\mathtt{n}}} = \{(z, \Psi_{\mathtt{n}}(z)) \mid z \in \mathbb{C}_z\}$$

has $(0,0,-r) \in \mathcal{R}_X$ as a branch point with ramification index $r+1$ and d branch points

$$(\widehat{e}_\sigma(\mathtt{n}), \widetilde{e}_\sigma(\mathtt{n}, -\mathtt{n})) \in \mathcal{R}_X, \qquad \text{for } \sigma = 1, \ldots, d,$$

with ramification index $\mathtt{n}+1$.

Letting $\mathtt{n} \to \infty$ and since

$$\lim_{\mathtt{n}\to\infty} \frac{\Gamma(\mathtt{n}+1)\,\mathtt{n}^{\frac{r+1}{d}}}{\Gamma\left(\mathtt{n}+\frac{r+1}{d}+1\right)} = 1,$$

we conclude that the critical values $\widetilde{e}_\sigma(\mathtt{n})$ converge, along the asymptotic paths $\alpha_\sigma(\tau) = \tau e^{2i\pi\sigma/d}$ suggested by the sequence of critical points $\{\widehat{e}_\sigma(\mathtt{n})\}_{\mathtt{n}=1}^{\infty}$, to the finite asymptotic values a_σ of

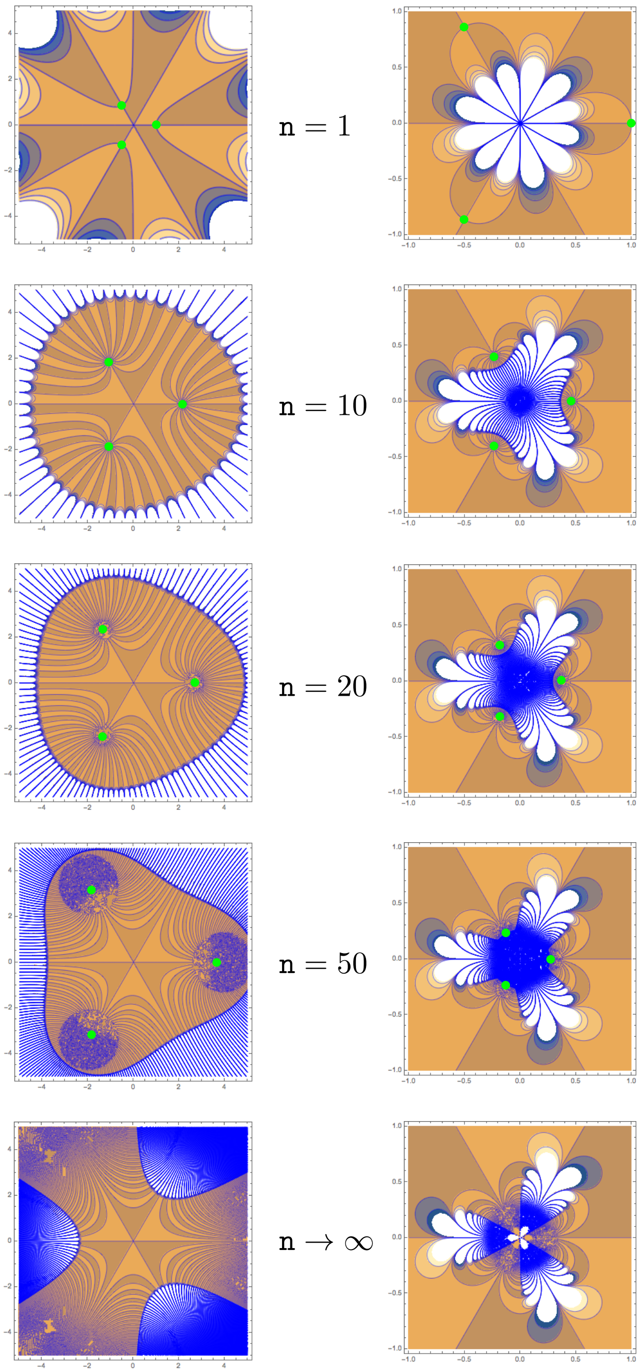

FIGURE 3. Phase portraits of $\mathfrak{Re}\,(X_{\mathtt{n}})$ for $\mathtt{n} = 1, 10, 20, 50$ converging to $\mathfrak{Re}\,(X)$ with $X \in \mathscr{E}(2,3)$ as in Example 4.2. Left hand side portrays a neighborhood of the origin, and the right hand side a neighborhood of $\infty \in \widehat{\mathbb{C}}_z$. Note that by approaching $\infty \in \widehat{\mathbb{C}}_z$ along paths that avoid the poles $\{e^{\frac{2i\pi\sigma}{d}}\mathtt{n}^{1/d}\}_{\sigma=1}^{d}$ (green dots), the value of $\Psi_{\mathtt{n}}(z)$ converges to $\infty \in \widehat{\mathbb{C}}_t$.

$\Psi_X(z) = \int_0^z \zeta^r \mathrm{e}^{-\zeta^d} d\zeta$, given by

$$a_\sigma = e^{2i\pi\sigma\frac{(r+1)}{d}} \frac{\Gamma\left(\frac{r+1}{d}+1\right)}{(r+1)} \in \mathbb{C}_t, \qquad \text{for } \sigma = 1, \dots, d. \tag{37}$$

Furthermore, traveling along the asymptotic paths $\alpha_\sigma(\tau) = \tau \mathrm{e}^{2i\pi(\sigma-d)/d}\mathrm{e}^{i\pi/d}$, that arrive at $\infty \in \widehat{\mathbb{C}}_z$ with angle $\frac{2\pi}{d}(\sigma - d) + \frac{\pi}{d}$, for $\sigma = d+1, \dots, 2d$, we see that $\Psi_{\mathtt{n}}(z)$ converges to $\infty \in \widehat{\mathbb{C}}_t$. Thus there are d (classes of) asymptotic paths that give rise to the asymptotic value $\infty \in \widehat{\mathbb{C}}_t$. Using the techniques presented in [3], for $r = 2$, $d = 3$, we visualize the phase portraits of $\mathfrak{Re}\,(X_{\mathtt{n}})$ and $\mathfrak{Re}\,(X)$. The poles $\{e^{\frac{2i\pi\sigma}{d}} \mathtt{n}^{1/d}\}_{\sigma=1}^d$ are portrayed as green dots. Note that at $\infty \in \widehat{\mathbb{C}}_z$ there is a zero of $X_{\mathtt{n}}$ of order exactly $r + d\mathtt{n} + 2 = 3\mathtt{n} + 4$. See Figure 3.

5. The geometry of the Riemann surface $\mathcal{R}_X$; setup for the proof of Main Theorem

The goals of this section are: to understand the geometry of the Riemann surface $\mathcal{R}_X$ for $X \in \mathscr{E}(r,d)$ and to set up the geometrical/combinatorial elements in order to define vertices, edges and weights of the (r,d)–configuration trees.

5.1. Branch points of $\mathcal{R}_X$ as vertices.

Since the branch points of $\mathcal{R}_X$ over $\infty \in \widehat{\mathbb{C}}_t$ are independent of $X \in \mathscr{E}(r,d)$, they will not enter the proof of the Main Theorem, thus the following concept is natural.

Definition 5.1. For $d \geq 1$, the *reduced divisor of* $X \in \mathscr{E}(r,d)$ is

$$X \longmapsto \underbrace{\left\{\iota = (p_\iota, \widetilde{p}_\iota, -\nu_\iota)\right\}_{\iota=1}^n}_{\text{pole vertices}} \cup \underbrace{\left\{ n+\sigma = (\infty_\sigma, a_\sigma, -\infty)\right\}_{\sigma=1}^d}_{\text{essential vertices}} \tag{38}$$
$$= \left\{ \mathfrak{a} = (z_{\mathfrak{a}}, t_{\mathfrak{a}}, -\nu_{\mathfrak{a}})\right\}_{\mathfrak{a}=1}^{n+d}.$$

Remark 5.2. The corresponding critical points of Ψ_X and transcendental singularities of Ψ_X^{-1} are

$$z_{\mathfrak{a}} \in \{p_1, \dots, p_\iota, \dots p_n, \infty_1, \dots, \infty_\sigma \dots \infty_d\} \subset \overline{\mathbb{C}}_z \tag{39}$$

once again $n \leq r$, with equality if and only if all the poles of X are simple. Recalling Remark 4.6.2, the $n+m$ critical and finite asymptotic values of Ψ_X are

$$t_{\mathfrak{a}} \in \{\widetilde{p}_1, \dots, \widetilde{p}_\iota, \dots, \widetilde{p}_n, a_1, \dots, a_{j(\sigma)}, \dots, a_m\} \subset \mathbb{C}_t, \tag{40}$$

where $m \leq d$, with equality if and only if all the finite asymptotic values of Ψ_X are of multiplicity one.
The main features of $\mathfrak{a}$ are summarized in Table 1.

5.2. The families of surfaces $\mathcal{R}_X$ having only one vertex.

We describe the families of vector fields avoided in the Main Theorem, *i.e.* those having exactly one branch point over $\mathbb{C}_t$.

TABLE 1. Branch points of $\mathcal{R}_X$.

Branch point $(z_{\mathfrak{a}}, t_{\mathfrak{a}}) \in \mathcal{R}_X$	Vertex ⓐ $= (z_{\mathfrak{a}}, t_{\mathfrak{a}}, -\nu_{\mathfrak{a}})$	Notation in (r,d)–configuration trees; meaning
$(p_\iota, \widetilde{p}_\iota)$ (25)	$\iota = (p_\iota, \widetilde{p}_\iota, -\nu_\iota)$	Pole vertices when $r \geq 1$; $\widetilde{p}_\iota = \Psi_X(p_\iota)$ is a critical value of Ψ_X, p_ι is a pole of X having order $-\nu_\iota \leq -1$, hence $(p_\iota, \widetilde{p}_\iota)$ is a branch point with ramification index $\nu_\iota + 1 \geq 2$.
(∞, ∞)	(∞, ∞, s)	Zero vertex when $d = 0$, $r \geq 1$ in which case $s = 2 + r$; $\infty \in \widehat{\mathbb{C}}_z$ is a zero of X having order s.
$(\infty_\sigma, a_\sigma)$ (31)	$n{+}\sigma = (\infty_\sigma, a_\sigma, -\infty)$	Essential vertices when $d \geq 1$; $\infty \in \widehat{\mathbb{C}}_z$ is an essential singularity of X, $a_\sigma \in \mathbb{C}_t$ being a finite asymptotic value of Ψ_X, with exponential tract $U_\sigma(\rho)$, so $(\infty_\sigma, a_\sigma, -\infty)$ is a logarithmic branch point of Ψ_X^{-1} in $\mathcal{R}_X \subset \overline{\mathbb{C}}_z \times \widehat{\mathbb{C}}_t$.

Lemma 5.3. *Let $X \in \mathscr{E}(r,d)$. The distinguished parameter Ψ_X has exactly one finite critical or asymptotic value $t_1 \in \mathbb{C}_t$ if and only if*

$$(r,d) = \begin{cases} (r \geq 1, 0) & X \textit{ has a unique pole of order } -r, \\ & \textit{in which case } t_1 \textit{ is the finite critical value,} \\ (0,1) & X \textit{ has an isolated essential singularity at } \infty \in \widehat{\mathbb{C}}_z, \\ & \textit{in which case } t_1 \textit{ is the finite asymptotic value.} \end{cases}$$

Proof. ($\Leftarrow$) The case X has a unique pole of order $-r$, is obvious: the distinguished parameter is given by Equation (17) and the unique finite critical value is given by Equation (18).
When $(r,d) = (0,1)$, the distinguished parameter is given by Equation (21) and the unique finite asymptotic value is given by Equation (22).
($\Rightarrow$) By Lemma 4.1, Ψ_X^{-1} has d logarithmic branch points over d finite asymptotic values of Ψ_X, d logarithmic branch points over $\infty \in \widehat{\mathbb{C}}_t$ and r critical values (counted with multiplicity).
Let $\{(z_{\mathfrak{a}}, t_1)\} \subset \pi_2^{-1}(t_1) \subset \mathcal{R}_X$ be all the branch points over t_1. The set $\{(z_{\mathfrak{a}}, t_1)\}$ consists of
• exactly d logarithmic branch points over t_1 and
• n $(\leq r)$ finitely ramified branch points (p_ι, t_1) of ramification indices $\nu_\iota + 1$ with $r = \sum_{\iota=1}^{n \leq r} \nu_\iota$.
Note that there are $d + n \geq 1$ *distinct* branch points of $\mathcal{R}_X$.

Moreover, $\mathcal{R}_X$ is a connected Riemann surface (it is the graph of Ψ_X). The restriction of the second projection over the punctured plane

$$\pi_2 : \mathcal{R}_X \backslash \{\pi_2^{-1}(t_1)\} \longrightarrow \mathbb{C} \backslash \{t_1\}$$

is a holomorphic cover without ramification. The subgroups G of $\pi_1(\mathbb{C} \backslash \{t_1\}) \cong \mathbb{Z}$ classify topologically these covers.
For $G = \mathbb{Z}_{r+1}$ with $r \geq 1$, the cover is finite cyclic and we can recognize that $\Psi_X(z)$ is as in (17), using Riemann's removable singularity theorem. This implies $X \in \mathscr{E}(r,0)$ has a unique pole as in the first assertion.

While for $G = \mathbb{Z}$, using Lemma 4.1 assertion 3 we can recognize $\Psi_X(z)$ as in (21), which in turn provides the corresponding $X \in \mathscr{E}(0,1)$.
The case $G = id$, gives $\Psi_X(z) = \frac{1}{\lambda}(z - p_1)$ and the constant vector field $X(z) = \lambda \frac{\partial}{\partial z}$, that does not belong to $\mathscr{E}(r, d)$. $\square$

5.3. **Diagonals of $\mathcal{R}_X$ as edges.** According to Lemma 5.3 from now on, we assume that there are two or more finite critical or asymptotic values $t_\mathfrak{a} \in \mathbb{C}_t$ of Ψ_X.

In order to completely describe $\mathcal{R}_X$, we also require information of the relative position of the branch points of the surface, recall Diagram 12. Let $\{ⓐ = (z_\mathfrak{a}, t_\mathfrak{a}, -\nu_\mathfrak{a})\}_{\mathfrak{a}=1}^{n+d}$ as in Equation (38).

Consider the oriented straight line segment $\overline{t_\mathfrak{a} t_\mathfrak{r}} \subset \mathbb{C}_t$. The inverse image
$$\pi_2^{-1}(\overline{t_\mathfrak{a} t_\mathfrak{r}}) = \{\Delta_{\vartheta\mathfrak{a}\mathfrak{r}}\} \subset \mathcal{R}_X$$
is a set consisting of a finite ($d = 0$) or an infinite ($d \geq 1$) number of copies of $\overline{t_\mathfrak{a} t_\mathfrak{r}}$. A priori, for each segment $\Delta_{\vartheta\mathfrak{a}\mathfrak{r}}$, the projection $\pi_1(\Delta_{\vartheta\mathfrak{a}\mathfrak{r}}) \subset \overline{\mathbb{C}}_z$ can have regular points at its end points.

Definition 5.4. 1. A segment $\Delta_{\vartheta\mathfrak{a}\mathfrak{r}}$ *is a diagonal of* $\mathcal{R}_X$ when the interior of $\pi_1(\Delta_{\vartheta\mathfrak{a}\mathfrak{r}})$ is in $\mathbb{C}_z$ and the endpoints of $\pi_1(\Delta_{\vartheta\mathfrak{a}\mathfrak{r}})$ are $z_\mathfrak{a}, z_\mathfrak{r} \in \{p_1, \ldots, p_n, \infty_1, \ldots, \infty_d\} \subset \overline{\mathbb{C}}_z$; critical points of Ψ_X or transcendental singularities of Ψ_X^{-1}.
2. A given diagonal
$$\Delta_{\vartheta\mathfrak{a}\mathfrak{r}} \textit{ starts at } ⓐ = (z_\mathfrak{a}, t_\mathfrak{a}, -\nu_\mathfrak{a}) \textit{ and ends at } ⓡ = (z_\mathfrak{r}, t_\mathfrak{r}, -\nu_\mathfrak{r}).$$
We shall say that the branch points of π_2, ⓐ and ⓡ, *share the same sheet*
$$\mathbb{C}_{\Delta_{\vartheta\mathfrak{a}\mathfrak{r}}} \backslash \{\text{suitable branch cuts}\}$$
in $\mathcal{R}_X$.

Remark 5.5. 1. By notational simplicity, if we drop the index ϑ from $\Delta_{\vartheta\mathfrak{a}\mathfrak{r}}$, then we are specifying the unique diagonal $\Delta_{\mathfrak{a}\mathfrak{r}}$. The following identification will be useful in the proof of the Main Theorem
$$\underbrace{\Delta_{\mathfrak{a}\mathfrak{r}} \subset \mathcal{R}_X \text{ with endpoints ⓐ, ⓡ}}_{\text{diagonal}} \longleftrightarrow \underbrace{\Delta_{\mathfrak{a}\mathfrak{r}}}_{\substack{\text{oriented}\\ \text{edge}}}. \tag{41}$$

2. Note that since Ψ_X is a single valued function, there can not be homoclinic trajectories of $\mathfrak{Re}(X)$ from a pole p to itself; *i.e.* there does not exist a diagonal $\Delta_{\iota\kappa}$ whose endpoints are the finitely ramified branch points $(p_\iota, \widetilde{p}_\iota, -\nu_\iota)$ and $(p_\kappa, \widetilde{p}_\kappa, -\nu_\kappa)$, with $\pi_1(p_\iota) = \pi_1(p_\kappa) = p$.
3. The diagonals $\Delta_{\mathfrak{a}\mathfrak{r}}$ can have endpoints as follows:
1) $\Delta_{\iota\kappa}$ has as endpoints $(p_\iota, \widetilde{p}_\iota, -\nu_\iota)$ and $(p_\kappa, \widetilde{p}_\kappa, -\nu_\kappa)$, $\iota \neq \kappa$, *i.e.* two finitely ramified branch points corresponding to pole vertices. For an example see Figure 8 in §8.
2) $\Delta_{\iota\sigma}$ has as endpoints $(p_\iota, \widetilde{p}_\iota, -\nu_\iota)$ and $(\infty_\sigma, a_\sigma, -\infty)$, *i.e.* a finitely ramified branch point and a logarithmic branch pointof Ψ_X^{-1}, corresponding to a pole and an essential vertex or viceversa. For an example see Figure 14 in §8.
3) $\Delta_{\sigma\rho}$ has as endpoints $(\infty_\sigma, a_\sigma, -\infty)$ and $(\infty_\rho, a_\rho, -\infty)$, $\sigma \neq \rho$, where the subscripts are as in (29), *i.e.* two logarithmic branch points of Ψ_X^{-1}, corresponding to essential vertices, with finite asymptotic values a_σ, a_ρ and exponential tracts α_σ, α_ρ. For an example see Figure 13 in §8.

Following the notation in [23], for $\Delta_{\mathfrak{a}\mathfrak{r}}$ a diagonal the associated *semi–residue* is
$$S(\omega_X, z_\mathfrak{a}, z_\mathfrak{r}) \doteq \int_{z_\mathfrak{a}}^{z_\mathfrak{r}} P(\zeta) \mathrm{e}^{-E(\zeta)} d\zeta = t_\mathfrak{r} - t_\mathfrak{a}. \tag{42}$$

Lemma 5.6 (Existence of diagonals in $\mathcal{R}_X$). *Suppose that there are at least two branch points $\left\{ⓐ = (z_\mathfrak{a}, t_\mathfrak{a}, -\nu_\mathfrak{a})\right\}_{\mathfrak{a}=1}^{n+d} \subset \mathcal{R}_X$. Then every branch point ⓐ is an endpoint of at least two diagonals, an incoming diagonal and an outgoing diagonal.*

Proof. Consider any branch point $ⓐ = (z_\mathfrak{a}, t_\mathfrak{a}, -\nu_\mathfrak{a}) \in \pi_2^{-1}(t_\mathfrak{a})$, with $t_\mathfrak{a}$ as in Equation (40). Suppose that there is no diagonal $\Delta_{\mathfrak{a}\mathfrak{r}}$ with endpoint ⓐ. This implies that ⓐ does not share a sheet, $\mathbb{C}_t\backslash\{\text{suitable branch cuts}\}$, with any other branch point $ⓡ = (z_\mathfrak{r}, t_\mathfrak{r}, -\nu_\mathfrak{r}) \in \pi_2^{-1}(t_\mathfrak{r})$, for some finite asymptotic or critical value $t_\mathfrak{r} \neq t_\mathfrak{a}$ (note that the existence of $t_\mathfrak{r}$ is guaranteed by Lemma 5.3). In other words the only sheets, $\mathbb{C}_t\backslash\{\text{suitable branch cuts}\}$, of $\mathcal{R}_X$ containing the branch point ⓐ are of the form $\mathbb{C}_t\backslash\{L_\mathfrak{a}\}$, for $L_\mathfrak{a} = [t_\mathfrak{a}, \infty)$. Hence by the same arguments as in Lemma 5.3, the Riemann surface $\mathcal{R}_X$ will have at least 2 connected components (one containing ⓐ and the other containing ⓡ), leading to a contradiction. □

5.4. **Geometrical building blocks and the weights of edges.** Our elementary building blocks are pairs, Riemann surface and complex analytic vector fields, as follows.

Definition 5.7. The pair $\left(\overline{\mathbb{H}}^2_\pm, \frac{\partial}{\partial t}\right)$ will be called a *(closed) half plane*; the closure of $\overline{\mathbb{H}}^2_\pm$ is considered in $\mathbb{C}$, hence its boundary is $\mathbb{R}$.
Likewise, $\left(\{0 \leq \mathfrak{Im}\,(t) \leq h\}, \frac{\partial}{\partial t}\right)$ will be called a *(closed) finite height horizontal strip*, where $h \geq 0$ is a parameter.

In the flat surface category, surgery tools are widely used, *v.g.* [44] p. 56 "welding of surfaces", [36], or [48] §3.2.–3.3 for general discussion.

Corollary 5.8 (Isometric glueing). *Let (M^0, g_X), (N^0, g_Y) be two flat surfaces arising from two singular complex analytic vector fields X and Y. Assume that both spaces M^0, N^0 have as geodesic boundary components of the same length: the trajectories $\sigma_1(\tau)$, $\sigma_2(\tau)$ of $\mathfrak{Re}\,(X)$ and $\mathfrak{Re}\,(Y)$, $\tau \in I \subset \mathbb{R}$. The isometric glueing of them along these geodesic boundary, is well defined, and provides a new flat surface on $M^0 \cup N^0$ arising from a new complex analytic vector field.* □

Lemma 5.9. *Let $X \in \mathscr{E}(r, d)$.*
1) The Riemann surface $\mathcal{R}_X$ can be constructed by isometric glueing of
- *half planes $(\overline{\mathbb{H}}^2_\pm, \frac{\partial}{\partial t})$ and*
- *finite height horizontal strips $\left(\{0 \leq \mathfrak{Im}\,(t) \leq h\}, \frac{\partial}{\partial t}\right)$, where $h \geq 0$.*

2) There exists a one–to–one correspondence

$$\left\{ \begin{array}{c} \textit{finite height horizontal strips} \\ \left(\{0 \leq \mathfrak{Im}\,(z) \leq h\}, \frac{\partial}{\partial t}\right) \end{array} \right\} \longleftrightarrow \left\{ \begin{array}{c} \textit{diagonals } \Delta_{\mathfrak{a}\mathfrak{r}} \textit{ with} \\ \left|\mathfrak{Im}\left(\int_{z_\mathfrak{a}}^{z_\mathfrak{r}} \omega_X\right)\right| = h \geq 0 \end{array} \right\},$$

here $ⓐ = (z_\mathfrak{a}, t_\mathfrak{a}, -\nu_\mathfrak{a})$ and $ⓡ = (z_\mathfrak{r}, t_\mathfrak{r}, -\nu_\mathfrak{r})$.

3) The case when $\mathfrak{Im}\left(\int_{z_\mathfrak{a}}^{z_\mathfrak{r}} \omega_X\right) = 0$ corresponds to the finite height horizontal strip degenerating into a segment of trajectory of $\mathfrak{Re}\,(X)$ between the branch points ⓐ and ⓡ, i.e. a horizontal diagonal $\Delta_{\mathfrak{a}\mathfrak{r}}$.

Proof. Assertion (1) follows by first recalling that π_2, as in Lemma 2.2, is a branch cover over $\widehat{\mathbb{C}}_t$. Lemma 4.1 tell us which critical or asymptotic values provide a first decomposition of $\mathcal{R}_X$ into half planes or finite height horizontal strips. Finally the pullback under π_2 of the vector field $\frac{\partial}{\partial t}$ to $\mathcal{R}_X$ determines the decomposition (the details are left to the reader).
Assertion (2) and (3) follow directly from Definition 5.4. □

Definitions 5.10, 5.12 below apply for singular flat Riemann surfaces (not necessarily of type $\mathcal{R}_X$).

Definition 5.10. Let $\{t_{\mathtt{k}}\}_{\mathtt{k}=1}^{\mathtt{r}} \subset \mathbb{C}_t$ be a finite set of distinct points. A *sheet* is a copy of $\mathbb{C}_t$ with $\mathtt{r} \geq 1$ branch cuts $L_{\mathtt{k}}$; *i.e.* $\mathbb{C}_t$ is cut along horizontal right segments $L_{\mathtt{k}} = [t_{\mathtt{k}}, \infty)$, remaining connected. Explicitly,

$$\mathbb{C}_t \backslash \{L_{\mathtt{k}}\}_{\mathtt{k}=1}^{\mathtt{r}} \doteq \left[\mathbb{C}_t \backslash \big(\cup_{\mathtt{k}=1}^{\mathtt{r}} [t_{\mathtt{k}}, \infty)\big)\right] \cup_{\mathtt{k}=1}^{\mathtt{r}} \{[t_{\mathtt{k}}, \infty)_+, [t_{\mathtt{k}}, \infty)_-\}, \tag{43}$$

having $2\mathtt{r}$ horizontal boundaries $[t_{\mathtt{k}}, \infty)_{\pm}$, where the subscripts $\pm$ refer to the obvious upper or lower boundary using $\mathfrak{Im}\,(t)$.

See Figure 4 for examples of sheets.

Remark 5.11. Note that branch cuts (and the corresponding boundaries) need not be to the right, they could be more general simple paths, however for notational simplicity and ease of the proofs we shall only use right cuts $[t_{\mathtt{k}}, \infty)_{\pm}$ as in (43).

Definition 5.12. A *diagonal of the sheet* $\mathbb{C}_t \backslash \{L_{\mathtt{k}}\}_{\mathtt{k}=1}^{\mathtt{r}}$ is an oriented straight line segment

$$\Delta_{\mathfrak{a}\mathfrak{r}} = \overline{t_{\mathfrak{a}} t_{\mathfrak{r}}} \subset \mathbb{C}_t \backslash \{L_{\mathtt{k}}\}_{\mathtt{k}=1}^{\mathtt{r}}, \tag{44}$$

starting at $t_{\mathfrak{a}}$ and ending at $t_{\mathfrak{r}}$, here $\mathfrak{r}, \mathfrak{a}$ are as in Equation (40).

The abuse of notation in Equations (41), (42), and (44), will be cleared in the proof of the main Theorem. See Figures 4.b, 4.c and Figure 8 for examples of diagonals of sheets.

We introduce four non-elementary building blocks, pictured in Figure 4, their Definitions 5.13, 5.15, 5.17 include geometrical and combinatorial frameworks.

Recalling Example 4.1, we propose the following.

Definition 5.13. A *semi–infinite helicoid* is the Riemann surface of

$$\int_{z_0}^{z} \mathrm{e}^{-\mu(\zeta+c_1)} d\zeta - a_\sigma = -\frac{1}{\mu} \mathrm{e}^{-\mu(z+c_1)} : \overline{\mathbb{H}}^2_{\pm} \subset \mathbb{C}_z \longrightarrow \mathbb{C}_t$$

having a horizontal boundary $[a_\sigma, \infty)_{\pm}$, geometrically it is an infinite succession of half–planes

$$\Big((\overline{\mathbb{H}}^2_{\pm} \cup \overline{\mathbb{H}}^2_{\mp} \cup \dots), \tfrac{\partial}{\partial t} \Big).$$

glued in the usual way, Corollary 5.8. See Figure 4.a.

Remark 5.14. In the combinatorial framework, for $X \in \mathscr{E}(r, d)$, each essential vertex $(n{+}\sigma) = (\infty_\sigma, a_\sigma, -\infty)$ has associated two semi–infinite helicoids, up and down, respectively. Pictorically, we will represent each one by a small coil in our figures. However, the semi–infinite helicoids and their coils do not appear in the (r, d)–configuration trees.

Geometric characteristics: a semi–infinite helicoid
- lies over the finite asymptotic value $a_\sigma \in \mathbb{C}_t$,
- has an infinite number of sheets,
- its horizontal boundary is coloured in orange,
- is up or down (resp. the domain of the integral in Definition 5.13 is $\overline{\mathbb{H}}^2_+$ or $\overline{\mathbb{H}}^2_-$).

Recalling Example 4.1, we have the following.

Definition 5.15. For $K \in \mathbb{Z}$, a $|K|$*–helicoid* is the Riemann surface of

$$\int_{z_0}^{z} \mathrm{e}^{-\mu(\zeta+c_1)} d\zeta - a_\sigma = -\frac{1}{\mu} \mathrm{e}^{-\mu(z+c_1)} : \mathcal{D} \subset \mathbb{C}_z \longrightarrow \mathbb{C}_t$$

where

$$\mathcal{D} = \begin{cases} \{0 \leq \mathfrak{Im}\,(\mu z) \leq 2\pi(K+1)\}, & K \geq 0 \\ \{2\pi K \leq \mathfrak{Im}\,(\mu z) \leq 2\pi\}, & K < 0, \end{cases}$$

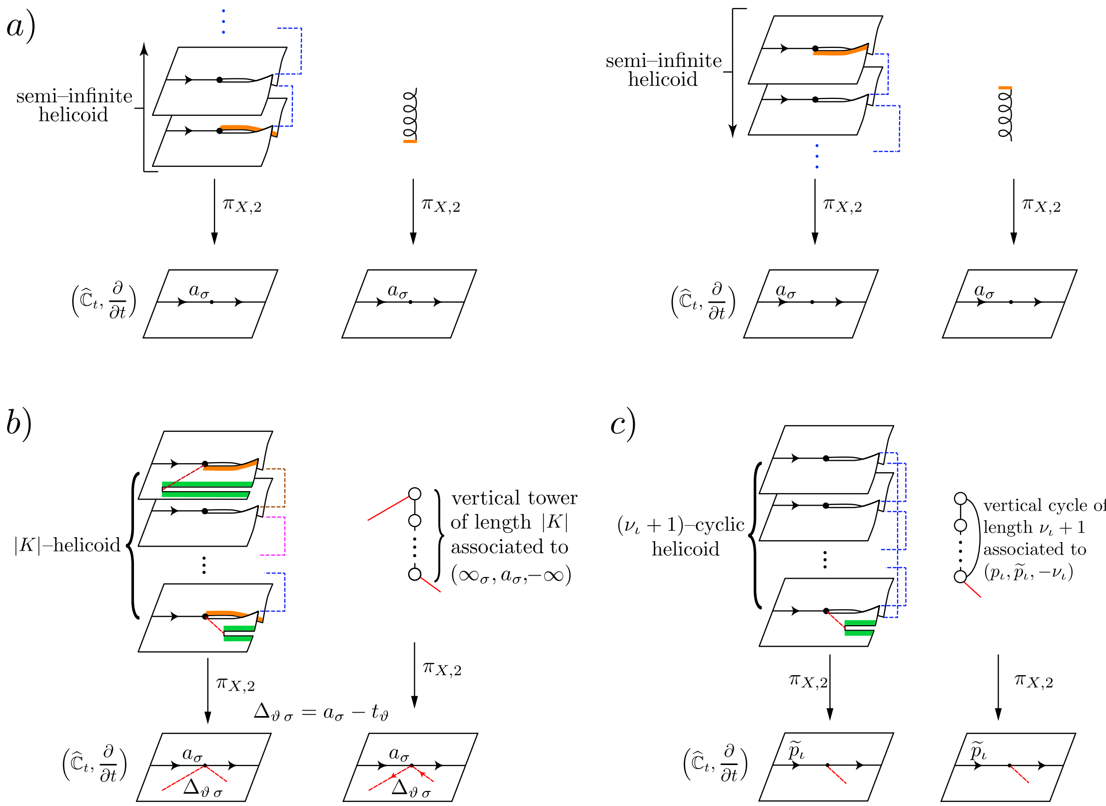

FIGURE 4. non-elementary building blocks as sheets with branch cuts glued appropriately in $\mathcal{R}_X$, and combinatorially as a graph. (a) The semi–infinite (up and down) helicoids. (b) A $|K|$–helicoid. (c) An $(\nu_\iota + 1)$–cyclic helicoid, for $(\nu_\iota + 1) \geq 2$. In cases (b) and (c) the red segments are diagonals.

having a finite number $\ell \geq 2$ of branch cuts $\{L_{\mathtt{k}}\}_{\mathtt{k}=2}^{\ell}$. Geometrically it is a succession of $2(|K|+1)$ half–planes

$$\Big((\overline{\mathbb{H}}^2_{\pm} \cup \overline{\mathbb{H}}^2_{\mp} \cup \ldots \cup \overline{\mathbb{H}}^2_{\mp}), \frac{\partial}{\partial t} \Big)$$

glued in the usual way, with 2ℓ horizontal boundaries.
In the combinatorial framework, for $X \in \mathscr{E}(r, d)$, the following objects are equivalent:
a $|K|$–helicoid,
a *vertical tower of length* $|K|$.
See Figure 4.b.

Remark 5.16. Each essential vertex $(n+\sigma) = (\infty_\sigma, a_\sigma, -\infty)$ determines at least one $|K(\sigma)|$–helicoid.

Geometric characteristics: a $|K|$–helicoid
• lies over the finite asymptotic value $a_\sigma \in \mathbb{C}_t$,
• has $|K| + 1$ sheets and there are three sub cases.
If $K > 0$ or $K < 0$, the $|K|$–helicoid:

• goes up or down depending on the sign of $K \neq 0$,
• has $\ell \geq 2$ diagonals with common extreme points over $a_\sigma \in \mathbb{C}_t$,
• in particular, there are always 2 diagonals present: one on the image of the strip

$$\{0 \leq \mathfrak{Im}\,(z) \leq 2\pi\},$$

and the other on the image of the strip

$$\{2\pi K \leq \mathfrak{Im}\,(z) \leq 2\pi(K+1)\}$$

K sheets above/below,
• has $2\ell \geq 4$ horizontal boundaries (arising from diagonals, coloured green) and 2 horizontal boundaries (orange).
If $K = 0$, the $|K|$–helicoid:
• has $\ell \geq 0$ diagonals having common extreme points over $a_\sigma \in \mathbb{C}_t$,
• has $2\ell \geq 0$ horizontal boundaries from diagonals (green) and 2 horizontal boundaries (orange).

Recalling the case of a pole, Example 3.1, we have the following.

Definition 5.17. A $(\nu_\iota + 1)$–*cyclic helicoid* is the Riemann surface of

$$\frac{1}{\lambda}\int_{z_0}^{z}(\zeta - p_\iota)^{\nu_\iota}\, d\zeta + \widetilde{p}_\iota = \frac{1}{\lambda}\frac{(z-p_\iota)^{\nu_\iota+1}}{\nu_\iota+1} : \mathbb{C}_z \longrightarrow \mathbb{C}_t$$

having a finite number $\{L_{\mathfrak{k}}\}_{\mathfrak{k}=0}^{\ell}$, $\ell \in \mathbb{N}\cup\{0\}$, of branch cuts. Geometrically it is a finite succession of $2\nu_\iota + 2$ half–planes

$$\Big(\big(\overline{\mathbb{H}}^2_\pm \cup \overline{\mathbb{H}}^2_\mp \cup \ldots \cup \overline{\mathbb{H}}^2_\mp\big), \tfrac{\partial}{\partial t}\Big)$$

glued in the usual way, with $2\ell \geq 0$ horizontal boundaries.
In the combinatorial framework for $X \in \mathscr{E}(r,d)$, the following three objects are equivalent:
a $(\nu_\iota + 1)$–cyclic helicoid,
a *vertical cycle of length* $\nu_\iota + 1$,
a pole vertex $\iota = (p_\iota, \widetilde{p}_\iota, -\nu_\iota)$.
See Figure 4.c.

Geometric characteristics: a $(\nu_\iota + 1)$–cyclic helicoid
• lies over the finite critical value $\widetilde{p}_\iota \in \mathbb{C}_t$,
• has $\nu_\iota + 1$ sheets,
• has $\ell \geq 0$ diagonals with common extreme points over $\widetilde{p}_\iota$.

Remark 5.18 (Cut and paste of the different geometric pieces for $X \in \mathscr{E}(r,d)$)**.** The paste of a semi–infinite helicoid and a cyclic helicoid is forbidden. The paste of two semi–infinite helicoids will appear essentially only for $X \in \mathscr{E}(0,1)$, as in Example 4.1.
Semi–infinite helicoids and $|K|$–helicoids are glued along their orange horizontal boundaries, see Figure 4.

Remark 5.19 (The weights of the edges)**.** 1. In order to construct the surface $\mathcal{R}_X$ by glueing the geometric pieces described in Lemma 5.9, we shall need to specify not only the branch points $\big\{\mathfrak{a} = (z_{\mathfrak{a}}, t_{\mathfrak{a}}, -\nu_{\mathfrak{a}})\big\}_{\mathfrak{a}=1}^{n+d}$ and the corresponding diagonals $\{\Delta_{\mathfrak{a}\mathfrak{r}}\}$ of the sheets, but also how many sheets each geometric piece has.
2. In what follows, the term "vertical" refers to the z–direction in $\overline{\mathbb{C}}_z \times \mathbb{C}_t$. Let $(z_{\mathfrak{a}}, t_{\mathfrak{a}}, -\nu_{\mathfrak{a}}) \in \mathcal{R}_X$ be a fixed branch point, we consider the usual lifting

$$\beta(\theta) = \pi_2^{-1}\big(t_{\mathfrak{a}} + \rho\, \mathrm{e}^{i2\pi\theta}\big) \subset \mathcal{R}_X \quad \text{where} \quad \theta \in [\theta_{min}, \theta_{max}] \subset \mathbb{R},$$

for appropriate θ_{min}, θ_{max} and small enough $\rho > 0$. Three cases appear:
i) Going around a branch point $t_{\mathfrak{a}}$ counterclockwise corresponds to going *up* on the ramified surface $\mathcal{R}_X$ and hence the number that separates the sheets is positive.
ii) Similarly going around the branch point clockwise corresponds to going *down*.

iii) Furthermore, going K times around a finitely ramified branch point of $\mathcal{R}_X$ of ramification index ν is equivalent to going around it $K \pmod{\nu}$ times.
3. Whenever there are two (or more) diagonals sharing the same branch point, the number of sheets that separate the diagonals in question can be counted on the Riemann surface $\mathcal{R}_X$ as number of planes traversed by a small enough circular path $\beta(\theta)$ around the common branch point. In this way, by choosing a *local zero level sheet* for each branch point of $\mathcal{R}_X$, we will be able to assign a weight to each edge/diagonal attached to the branch point (relative to the local zero level sheet).

6. Why is the geometrical description of $\mathscr{E}(r,d)$ difficult?

In order to get an accurate combinatorial description of $\mathcal{R}_X$ for the family $\mathscr{E}(r,d)$, we shall need to specify two basic sets:
i) The vertices or branch points

$$\left\{ \iota = (p_\iota, \widetilde{p}_\iota, -\nu_\iota)\right\}_{\iota=1}^{n} \cup \left\{ n{+}\sigma = (\infty_\sigma, a_\sigma, -\infty)\right\}_{\sigma=1}^{d} = \left\{ \mathfrak{a} = (z_\mathfrak{a}, t_\mathfrak{a}, -\nu_\mathfrak{a})\right\}_{\mathfrak{a}=1}^{n+d}$$

of $\mathcal{R}_X$, *i.e.* the reduced divisor of X, Definition 5.1.
ii) A subset of the diagonals $\{\Delta_{\mathfrak{a}\mathfrak{r}}\}$, Equation (41), connecting the branch points (in particular it will be useful to know which branch points share specific sheets of $\mathcal{R}_X$).

The implicit combinatorial obstacles are:

D.1 No canonical choice for the initial integration point of $\Psi_X(z) = \int_{z_0}^{z} \omega_X$ can be given.

D.2 There is no preferred/canonical *global zero level* of $\mathcal{R}_X$, denoted (GZL),
$$\mathbb{C}_{\Delta_{\mathfrak{a}\mathfrak{r}}} \backslash \{\text{suitable branch cuts}\} \quad \subset \quad \mathcal{R}_X,$$
that is to be chosen to start the description of $\mathcal{R}_X$ as a combinatorial object.

D.3 No canonical order can be given to the branch points $\left\{ \mathfrak{a} = (z_\mathfrak{a}, t_\mathfrak{a}, -\nu_\mathfrak{a})\right\}_{\mathfrak{a}=1}^{n+d}$ of $\mathcal{R}_X$.

D.4 A priori, the choice of a minimal subset of the diagonals required to describe $\mathcal{R}_X$ is non-canonical.

In particular, note that difficulty D.1 will have a repercussion on the labeling of the vertices in Definition 7.7, while difficulties D.2 and D.3 are associated to the choice of a suitable root vertex 1 in the reduced divisor. Difficulty D.4 will require a certain ordering of the subset of the diagonals on each sheet of $\mathcal{R}_X$, as will appear in Definition 7.6.

The resolution of these choices/conventions motivates the notion of equivalence classes $[\Lambda_X]$ as in our Main Theorem, see §9.4.

There are also analytical obstructions/obstacles:

D.5 Not all the collections of vertices $\left\{ \iota = (p_\iota, \widetilde{p}_\iota, -\nu_\iota)\right\}_{\iota=1}^{n} \cup \left\{ n{+}\sigma = (\infty_\sigma, a_\sigma, -\infty)\right\}_{\sigma=1}^{d}$ are possible as branch points for $\mathcal{R}_X$, only those that are a solution to the system of transcendental equations

$$\begin{cases} \Psi_X(p_\iota) = \widetilde{p}_\iota & \\ \Psi_X^{(\ell)}(p_\iota) = 0 & 1 \le \ell \le \nu_\iota, \quad \iota = 1, \dots, n, \\ \lim\limits_{\tau\to\infty} \alpha_\sigma(\tau) = \infty_\sigma & \\ \lim\limits_{\tau\to\infty} \Psi_X\big(\alpha_\sigma(\tau)\big) = a_\sigma & \sigma = 1, \dots, d. \end{cases} \tag{45}$$

The last two equalities are analytical expressions of the geometrical structure of Figure 2.

Difficulty D.5 motivates the following concept.

Definition 6.1. An abstract collection of $n + d$ vertices

$$\left\{ \textcircled{\iota} = (p_\iota, \widetilde{p}_\iota, -\nu_\iota) \right\}_{\iota=1}^{n} \cup \left\{ \textcircled{n+\sigma} = (\infty_\sigma, a_\sigma, -\infty) \right\}_{\sigma=1}^{d}$$

is *realizable* if it is a solution of (45), for some Ψ_X, for $X \in \mathscr{E}(r,d)$.

7. Combinatorial objects: (r,d)–configuration trees

In order to make precise the choices required to resolve the issues D.1–5, we introduce the following auxiliary concepts: weighted directed zero–rooted trees and (r,d)–configuration trees. These can be understood as associated to some $\mathcal{R}_X$, even though they are abstract graphs, a priori not necessarily associated to the Riemann surface $\mathcal{R}_X$.
To accomplish the above, we shall use some basic notions of graph theory, namely trees, oriented or not, with and without roots and weights, see [30] pp. 46, 379 for standard concepts. It is natural to use the branch points of $\mathcal{R}_X$, described by the reduced divisor, Definition 5.1,

$$\left\{ \textcircled{\mathfrak{a}} = (z_\mathfrak{a}, t_\mathfrak{a}, -\nu_\mathfrak{a}) \right\}_{\mathfrak{a}=1}^{n+d} \quad \text{with} \quad z_\mathfrak{a} \in \overline{\mathbb{C}}_z,\ t_\mathfrak{a} \in \mathbb{C}_t \text{ and } \nu_\mathfrak{a} \in \mathbb{N} \cup \{\infty\},$$

as vertices of our graphs, **with a possible re–labelling when needed**.

To resolve issue D.1, we introduce *directed rooted trees* which have one vertex designated as the *root* $\textcircled{\textcircled{\varrho}}$ and oriented edges

$$\Lambda = \Big\{ \underbrace{\textcircled{1}, \ldots, \textcircled{\mathfrak{r}}, \ldots, \textcircled{\mathfrak{a}}, \ldots, \textcircled{\mathfrak{m}}}_{\text{vertices}};\ \underbrace{\textcircled{\textcircled{\varrho}}}_{\text{root}};\ \underbrace{\Delta_{\mathfrak{a}\mathfrak{r}}, \ldots}_{\substack{\mathfrak{m}-1 \\ \text{oriented edges}}} \Big\}, \tag{46}$$

where $\mathfrak{m} \leq n + d$. Note that not all vertices in Definition 5.1 are necessarily used. We shall consider directed rooted trees that have an orientation away from the root and convene that $\Delta_{\mathfrak{a}\mathfrak{r}}$ denotes the edge starting at $\textcircled{\mathfrak{a}}$ and ending at $\textcircled{\mathfrak{r}}$. The *tree–order* is the partial ordering on the vertices of (46) such that, $\textcircled{\iota} < \textcircled{\mathfrak{r}}$ if and only if the unique path from the root $\textcircled{\textcircled{\varrho}}$ to $\textcircled{\mathfrak{r}}$ passes through $\textcircled{\iota}$. The *depth* of the vertex $\textcircled{\mathfrak{r}}$ is the length of the path (number of edges) from the root.

As noted in Remark 5.19, the building blocks provide weights for the edges of the directed rooted trees.

Definition 7.1. Given a directed rooted tree as in (46), by assigning a weight $K(\mathfrak{a},\mathfrak{r}) \in \mathbb{Z}$ to each edge $\Delta_{\mathfrak{a}\mathfrak{r}}$, we obtain a *weighted directed rooted tree*

$$\Big\{ \underbrace{\textcircled{1}, \ldots, \textcircled{\mathfrak{m}}}_{\text{vertices}};\ \underbrace{\textcircled{\textcircled{\varrho}}}_{\text{root}};\ \underbrace{(\Delta_{\mathfrak{r}\mathfrak{a}}, K(\mathfrak{r},\mathfrak{a})), \ldots}_{\substack{\mathfrak{m}-1 \\ \text{weighted edges}}} \Big\}.$$

A *zero parent of a vertex* $\textcircled{\mathfrak{a}} \neq \textcircled{\textcircled{\varrho}}$ is the unique vertex $\textcircled{\mathfrak{r}}$ connected to $\textcircled{\mathfrak{a}}$ on the path to the root, whose edge $(\Delta_{\mathfrak{r}\mathfrak{a}}, K(\mathfrak{r},\mathfrak{a}))$ has in addition $K(\mathfrak{r},\mathfrak{a}) = 0$.

For some weighted directed rooted trees the root is not a zero parent.

Example 7.1. For the weighted directed rooted tree with all its weights equal to 1, namely

$$\Big\{ \textcircled{1}, \ldots, \textcircled{\mathfrak{m}};\ \textcircled{\textcircled{\varrho}};\ (\Delta_{1\,2}, 1), \ldots, (\Delta_{\mathfrak{m}-1\,\mathfrak{m}}, 1) \Big\},$$

none of the vertices are zero parents.

Definition 7.2. A weighted directed rooted tree

$$\Lambda_{\textcircled{\varrho}} = \Big\{ \underbrace{\textcircled{1}, \ldots, \textcircled{\mathfrak{m}}}_{\text{vertices}};\ \underbrace{\textcircled{\textcircled{\varrho}}}_{\text{root}};\ \underbrace{(\Delta_{\mathfrak{r}\mathfrak{a}}, K(\mathfrak{r},\mathfrak{a})), \ldots}_{\substack{\mathfrak{m}-1 \\ \text{weighted edges}}} \Big\}, \tag{47}$$

whose root $\circledcirc{\varrho}$ is a zero parent is a *weighted directed zero–rooted tree.*

Definition 7.3. A *zero child of a vertex* $\textcircled{\mathfrak{r}}$ is a vertex $\textcircled{\mathfrak{a}}$ of which $\textcircled{\mathfrak{r}}$ is the zero parent. A *zero descendant of a vertex* $\textcircled{\mathfrak{r}}$ is any vertex which is either the zero child of $\textcircled{\mathfrak{r}}$ or is (recursively) the zero descendant of any of the zero children of $\textcircled{\mathfrak{r}}$.

From the above definitions, we immediately obtain the following.

Lemma 7.4. *Let* $\Lambda_{\textcircled{\varrho}}$ *be a weighted directed zero–rooted tree.*
1. The zero descendants of the root $\circledcirc{\varrho}$ *form the* horizontal rooted subtree of the root*, denoted by* $\Lambda_{H(\varrho)}$*. Note that the root of* $\Lambda_{H(\varrho)}$ *is once again* $\circledcirc{\varrho}$*.*
2. Each weighted edge $(\Delta_{\mathfrak{r}\mathfrak{a}}, K(\mathfrak{r},\mathfrak{a}))$ *with* $K(\mathfrak{r},\mathfrak{a}) \neq 0$*, defines a* horizontal rooted subtree $\Lambda_{H(\mathfrak{r},\mathfrak{a})}$*, with root* $\circledcirc{\mathfrak{r}}$*, of the* incoming edge $(\Delta_{\mathfrak{r}\mathfrak{a}}, K(\mathfrak{r},\mathfrak{a}))$*, vertices*

$$V_{H(\mathfrak{r},\mathfrak{a})} = \{\textcircled{\mathfrak{r}}, \textcircled{\mathfrak{a}}\} \cup \{\textcircled{\iota} \mid \textcircled{\iota} \text{ is a zero descendant of } \textcircled{\mathfrak{a}}\}$$

and edges

$$E_{H(\mathfrak{r},\mathfrak{a})} = \{(\Delta_{\mathfrak{r}\mathfrak{a}}, K(\mathfrak{r},\mathfrak{a}))\} \cup \{\text{edges that end on the zero descendants of } \textcircled{\mathfrak{a}}\}.$$

□

Note that, on each horizontal rooted subtree, the incoming edges are the only edges with non–zero weight.

Example 7.2. Consider the weighted directed zero–rooted tree

$$\begin{aligned}(48)\quad \Lambda_{\textcircled{1}} = \Big\{ &\textcircled{1}, \ldots, \textcircled{12}; \circledcirc{1};\\ &(\Delta_{1\,2}, 0), (\Delta_{2\,4}, 0), (\Delta_{4\,7}, -3), (\Delta_{7\,12}, 0), (\Delta_{7\,11}, 4),\\ &(\Delta_{1\,3}, 1), (\Delta_{3\,5}, 0), (\Delta_{3\,6}, 0), (\Delta_{6\,9}, 0), (\Delta_{6\,10}, 0), (\Delta_{5\,8}, 1)\Big\}.\end{aligned}$$

The root is $\circledcirc{1}$, and the incoming edges are $\Delta_{1\,3}$, $\Delta_{4\,7}$, $\Delta_{7\,11}$ and $\Delta_{5\,8}$. Then

$$\Lambda_{\textcircled{1}} = \Lambda_{H(1)} \cup \Lambda_{H(1,3)} \cup \Lambda_{H(4,7)} \cup \Lambda_{H(7,11)} \cup \Lambda_{H(5,8)},$$

provides the decomposition into horizontal rooted subtrees as in Lemma 7.4.
In Figure 5, the horizontal rooted subtree of the root is coloured red; the horizontal rooted subtrees, corresponding to the incoming edges, are coloured orange, blue, green, purple respectively. Note that the weight of each of the incoming edges could be any non–zero integer. The vertices $\textcircled{1}$, $\textcircled{4}$, $\textcircled{5}$ and $\textcircled{7}$ belong to more than one horizontal subtree.

Remark 7.5. The decomposition of $\Lambda_{\textcircled{\varrho}}$, given by Lemma 7.4, provides a disjoint partition on the set of edges. This relates to the fact that on $\mathcal{R}_X$, the diagonals between branch points are partitioned into disjoint sets according to the sheet they share.

In order to overcome difficulty D.4, we shall need one more concept. Consider the linear (weighted) directed tree

$$G = \{\mathcal{V}; \mathfrak{E}\},$$

with $\mathfrak{m}$ vertices

$$\mathcal{V} = \{\textcircled{\mathfrak{a}} \doteq (z_\mathfrak{a}, t_\mathfrak{a}, -\nu_\mathfrak{a})\}_{\mathfrak{a}=1}^{\mathfrak{m}}, \quad z_\mathfrak{a} \in \overline{\mathbb{C}}_z,\ t_\mathfrak{a} \in \mathbb{C}_t,\ \nu_\mathfrak{a} \in \mathbb{N} \cup \{\infty\},$$

where $\{t_\mathfrak{a}\}$ are different points, labelled so that

$$\mathfrak{Im}\,(t_\mathfrak{a}) \geq \mathfrak{Im}\,(t_{\mathfrak{a}+1}), \quad \mathfrak{Re}\,(t_\mathfrak{a}) \leq \mathfrak{Re}\,(t_{\mathfrak{a}+1});$$

and $\mathfrak{m}-1$ oriented weighted edges

$$\mathfrak{E} = \left\{\left(\Delta_{(\mathfrak{a}-1)\,\mathfrak{a}}, K(\mathfrak{a}-1,\mathfrak{a})\right)\right\}_{\mathfrak{a}=2}^{\mathfrak{m}},$$

where $\Delta_{(\mathfrak{a}-1)\,\mathfrak{a}} \doteq (t_\mathfrak{a} - t_{\mathfrak{a}-1})$, and $K(\mathfrak{a}-1,\mathfrak{a}) \in \mathbb{Z}$.

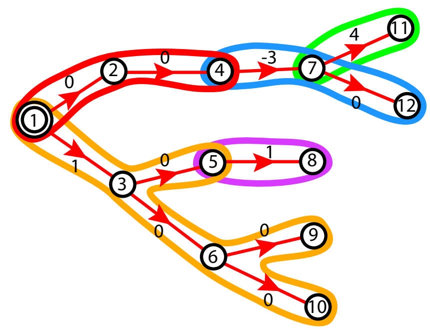

FIGURE 5. The decomposition into horizontal rooted subtrees of the weighted directed rooted tree of Example 7.2. The weights are placed beside the corresponding edges. The rooted subtree colored red is by definition the *global zero level subtree.*

In particular, G can be understood as embedded in $\overline{\mathbb{C}}_z \times \mathbb{C}_t$.
Note that the vertices are connected from left to right and top to bottom; starting with the top–&–left–most vertex and ending at the bottom–&–right–most vertex.

Definition 7.6. 1. The G constructed as above, is the *left–right–top–bottom linear (weighted) directed tree of the vertices* $\mathcal{V}$. The underlying undirected linear graph will be called the *undirected left–right–top–bottom linear (weighted) tree of the vertices* $\mathcal{V}$.
2. Moreover, for any choice of $\textcircled{\mathfrak{r}} \in \mathcal{V}$, the rooted tree

$$G_{\textcircled{\mathfrak{r}}} = \left\{ \mathcal{V}; \textcircled{\textcircled{\mathfrak{r}}}; \widehat{\mathfrak{E}} \right\}$$

where

$$\widehat{\mathfrak{E}} = \{\Delta_{\mathfrak{r}\,\mathfrak{r}+1}, \Delta_{\mathfrak{r}+1\,\mathfrak{r}+2}, \dots, \Delta_{\mathfrak{m}-1\,\mathfrak{m}}, \Delta_{\mathfrak{r}\,\mathfrak{r}-1}, \Delta_{\mathfrak{r}-1\,\mathfrak{r}-2}, \dots, \Delta_{2\,1}\},$$

is called a *linear (weighted) directed rooted tree with incoming vertex* $\textcircled{\mathfrak{r}}$.

Note that G and $G_{\textcircled{\mathfrak{r}}}$ have the same vertices, however different oriented edges $\mathfrak{E}$ and $\widehat{\mathfrak{E}}$. Figure 6 provides an example with seven vertices.

Recalling Table 1, we are now ready to to introduce the particular weighted directed zero–rooted trees that will encode the information needed to specify the Riemann surfaces $\mathcal{R}_X$. Issue D.5 will be dealt with by condition (1) of the following definition.

Definition 7.7. For $r + d \geq 1$, a (r, d)*–configuration tree* is a weighted directed zero–rooted tree

$$\Lambda = \left\{ V; \textcircled{\textcircled{\varrho}}; E \right\}$$

with:
• $n + d$ *vertices*

$$V = \left\{ \textcircled{\mathfrak{a}} = (z_{\mathfrak{a}}, t_{\mathfrak{a}}, -\nu_{\mathfrak{a}}) \right\}_{\mathfrak{a}=1}^{n+d}, \qquad z_{\mathfrak{a}} \in \overline{\mathbb{C}}_z,\ t_{\mathfrak{a}} \in \mathbb{C}_t \text{ and } \nu_{\mathfrak{a}} \in \mathbb{N} \cup \{\infty\},$$

where $\sum\limits_{-\nu_{\mathfrak{a}} \neq -\infty} \nu_{\mathfrak{a}} = r$;
• $n + d - 1$ *weighted oriented edges*

$$E = \left\{ (\Delta_{\mathfrak{a}\mathfrak{r}}, K(\mathfrak{a}, \mathfrak{r})) \mid \Delta_{\mathfrak{a}\mathfrak{r}} \text{ starts at } \textcircled{\mathfrak{a}} \text{ and ends at } \textcircled{\mathfrak{r}},\ K(\mathfrak{a}, \mathfrak{r}) \in \mathbb{Z} \right\},$$

with the orientation of the edges being away from the root.
In addition, the following conditions must be satisfied:

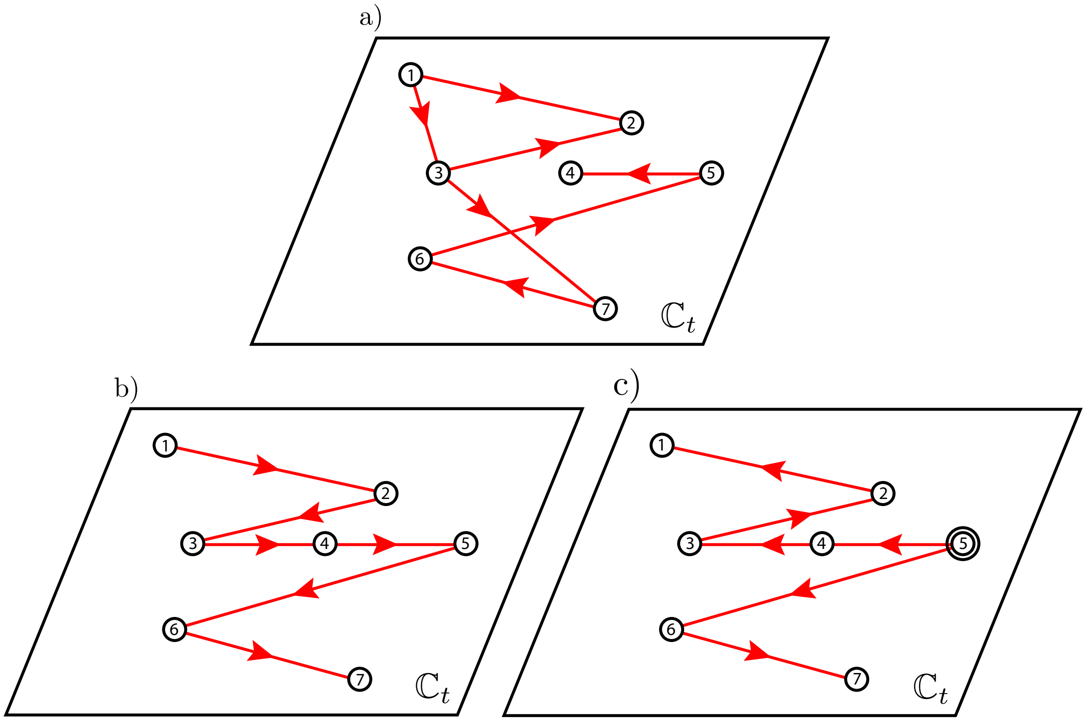

FIGURE 6. In (a), we have a directed graph with seven vertices $\mathcal{V} = \{①, \ldots, ⑦\}$. In (b) we have eliminated and added some edges to obtain a left–right–top–bottom linear directed tree G of vertices $\mathcal{V}$ with edges $\mathfrak{E} = \{\Delta_{1\,2}, \Delta_{2\,3}, \Delta_{3\,4}, \Delta_{4\,5}, \Delta_{5\,6}, \Delta_{6\,7}\}$. In (c) we have the linear directed rooted tree $G_{⑤}$ where ⑤ is both the incoming vertex and the root, having edges $\widehat{\mathfrak{E}} = \{\Delta_{5\,6}, \Delta_{6\,7}, \Delta_{5\,4}, \Delta_{4\,3}, \Delta_{3\,2}, \Delta_{2\,1}\}$, note the change of directions of the edges.

1) The set of vertices $\big\{ \textcircled{\mathfrak{a}} = (z_{\mathfrak{a}}, t_{\mathfrak{a}}, -\nu_{\mathfrak{a}}) \big\}_{\mathfrak{a}=1}^{n+d}$ must be realizable, *i.e.* they must satisfy the system of equations (45).
2) *Types of vertices.* Concerning the position of the vertices in $\overline{\mathbb{C}}_z$; $z_{\mathfrak{a}} \in \mathbb{C}_z$ if and only if $\nu_{\mathfrak{a}} \in \mathbb{N}$. Thus, the vertices are classified in two types

$$\textcircled{\iota} = \underbrace{\big(p_\iota, \widetilde{p}_\iota, -\nu_\iota\big)}_{\text{pole vertex}} \in \mathbb{C}_z \quad \text{and} \quad \textcircled{n+\sigma} = \underbrace{\big(\infty_\sigma, a_\sigma, -\infty\big)}_{\text{essential vertex}}.$$

3) If Λ consists of only one vertex, then

    the $(r, 0)$–configuration trees are $\Big\{ ① = \big(p_1, \widetilde{p}_1, -r\big); ①; \varnothing \Big\}$,

    the $(0, 1)$–configuration trees are $\Big\{ ① = \big(\infty_1, a_1, -\infty\big); ①; \varnothing \Big\}$.
4) *Root condition.* If $r = 0$, then the root ① is the essential vertex $① = \big(\infty_1, a_1, -\infty\big)$.

If $r \neq 0$, then the root ϱ is the pole vertex $\big(p_\varrho, \widetilde{p}_\varrho, -\nu_\varrho\big)$, whose z–coordinate is top and left most: *i.e.* $\mathfrak{Im}\,(\widetilde{p}_\varrho) \geq \mathfrak{Im}\,(\widetilde{p}_\iota)$ and when equality is achieved it is required that $\mathfrak{Re}\,(\widetilde{p}_\varrho) < \mathfrak{Re}\,(\widetilde{p}_\iota)$ for $1 < \iota \leq n$.

5) *Equality of vertices.* Given $\mathfrak{a} = (z_\mathfrak{a}, t_\mathfrak{a}, -\nu_\mathfrak{a})$ and $\mathfrak{r} = (z_\mathfrak{r}, t_\mathfrak{r}, -\nu_\mathfrak{r})$, if $z_\mathfrak{a} = z_\mathfrak{r}$ then $t_\mathfrak{a} = t_\mathfrak{r}$ and $\nu_\mathfrak{a} = \nu_\mathfrak{r}$, *i.e.* necessarily $\mathfrak{a} = \mathfrak{r}$ in Λ.
6) *Existence of edges.* There is no edge between the vertices $\mathfrak{a} = \big(z_\mathfrak{a}, t_\mathfrak{a}, -\nu_\mathfrak{a}\big)$ and $\mathfrak{r} = \big(z_\mathfrak{r}, t_\mathfrak{r}, -\nu_\mathfrak{r}\big)$ when $t_\mathfrak{a} = t_\mathfrak{r}$.
7) *Horizontal subtree structure.* We require that each of the horizontal rooted subtrees of Λ, be a linear (weighted) directed rooted subtree $G_{\mathfrak{r}}$ with incoming vertex $\mathfrak{r}$, as in Definition 7.6.

Remark 7.8. Comments on Definition 7.7.
1. The root condition (4) allows us to make a canonical choice of the root vertex; see Remark 4.6.2.
2. Condition (5) is equivalent to saying that $t_\mathfrak{a}$ and $\nu_\mathfrak{a}$ are functions of $z_\mathfrak{a}$. For instance in Examples 8.7 and 8.8, even though the finite asymptotic values of Ψ_X have multiplicity 3, we can use $z_\mathfrak{a} \in \overline{\mathbb{C}}_z$ to label the vertices of Λ_X.
3. As will be seen in the proof of the Main Theorem, condition (7) provides, for each sheet of $\mathcal{R}_X$, a choice of the diagonals that connect the branch points that share the same sheet. This choice will enable us to define appropriately the class $[\Lambda_X]$ of (r,d)–configuration trees.
4. In case that there is only one horizontal rooted subtree for Λ, Lemma 7.4 ensures that the only horizontal rooted subtree is $\Lambda_{H(\rho)}$.
5. When $r = 0$, Definition 7.7 reduces to the definition of a d–configuration tree presented in [1] §8.3. The equivalence becomes explicit by observing that the essential vertices $\sigma = \big(\infty_\sigma, a_\sigma, -\infty\big)$ of $(0,d)$–configuration trees correspond to the vertices $(\infty_\sigma, a_\sigma)$, pairs in [1], of d–configuration trees.

8. Low degree significative examples, from X to Λ_X

We provide examples of the correspondence from vector fields to Riemann surfaces and configuration trees

$$X \longmapsto \mathcal{R}_X \longmapsto \Lambda_X,$$

using the basic geometric/combinatorial pieces described in Figure 4.

About the meaning of the different data of Λ_X.

1) The vertices of Λ_X are in bijection with the reduced divisor of X (recall Definition 5.1, Table 1), and with the branch points of $\mathcal{R}_X$ with respect to π_2, restricted over $\mathbb{C}_t$, recall Diagram 12.
2) The edges correspond to a subset of the diagonals, connecting the branch points, necessary to describe completely the Riemann surface $\mathcal{R}_X$, recall Definition 5.4.1.
3) The root vertex $\varrho \doteq (z_\varrho, t_\varrho, -\nu_\varrho)$, as usual in graph theory, means the initial vertex in order to construct a tree, as in (46). From the analytic and geometric point of view, the root determines the initial point of $\Psi_X(z) = \int_{z_1}^{z} \omega_X$.
4) The weights $K(\mathfrak{a}, \mathfrak{r}) \in \mathbb{Z}$ in Definition 7.7: If we can describe all the branch points of $\mathcal{R}_X$ using only one sheet (Definition 5.10), then $K(\mathfrak{a}, \mathfrak{r}) = 0$. If several sheets are required, the weight of the edge $K(\mathfrak{a}, \mathfrak{r}) \in \mathbb{Z}\backslash\{0\}$ tells us the relative number of sheets of $\mathcal{R}_X$, we must go "up or down" on the surface in order to find another sheet containing other branch points. Vector fields having $K(\mathfrak{a}, \mathfrak{r}) \neq 0$ appear in Example 8.7 and §8.1.1.
In particular, if there are only two branch points, then there is no need to go up or down at the starting branch point, so the weight of the only edge is 0.

5) The *global zero level sheet* denoted *GZL* (which is in general non-canonical), indicates a subset of the branch points that share the same sheet as the root ①.

Remark 8.1. The notion of *skeleton* associated to Λ_X will be described in Definition 9.5 and the notion of (r,d)–*soul* in Definition 9.7. They play an active role in the proof of the Main Theorem.

• For $X \in \mathscr{E}(r,d)$, $d \geq 1$, the (r,d)–soul is necessarily a flat Riemann surface with boundary, and is obtained from $\mathcal{R}_X$ by removing its semi–infinite helicoids.

• In the case $X \in \mathscr{E}(r,0)$, the (r,d)–soul coincides with $\mathcal{R}_X$.

8.1. **The vector field $X \in \mathscr{E}(r,0)$ has $r \geq 1$ poles on $\mathbb{C}_z$ and Ψ_X is a polynomial map.**

Example 8.1. Consider the vector field of Example 3.1,

$$X(z) = \frac{\lambda}{(z-p_1)^r}\frac{\partial}{\partial z}$$

and recall the notion of $(\nu_\iota + 1)$–cyclic helicoid Definition 5.17. The $(r,0)$–configuration tree consists of one pole vertex and no edges

$$\Lambda_X = \Big\{ ① = (p_1, \widetilde{p}_1, -r); ①; \varnothing \Big\},$$

where $\widetilde{p}_1$ as in (18) is the critical value. In Figure 7 the case $r=2$ is pictured: On the left hand side the phase portrait of X is shown. Clearly there are 6 hyperbolic sectors, each corresponding to a half plane. On the second column the Riemann surface is shown. On the rightmost column the combinatorial objects are portrayed. For the general case $-r \leq -1$ see Figure 4.c.

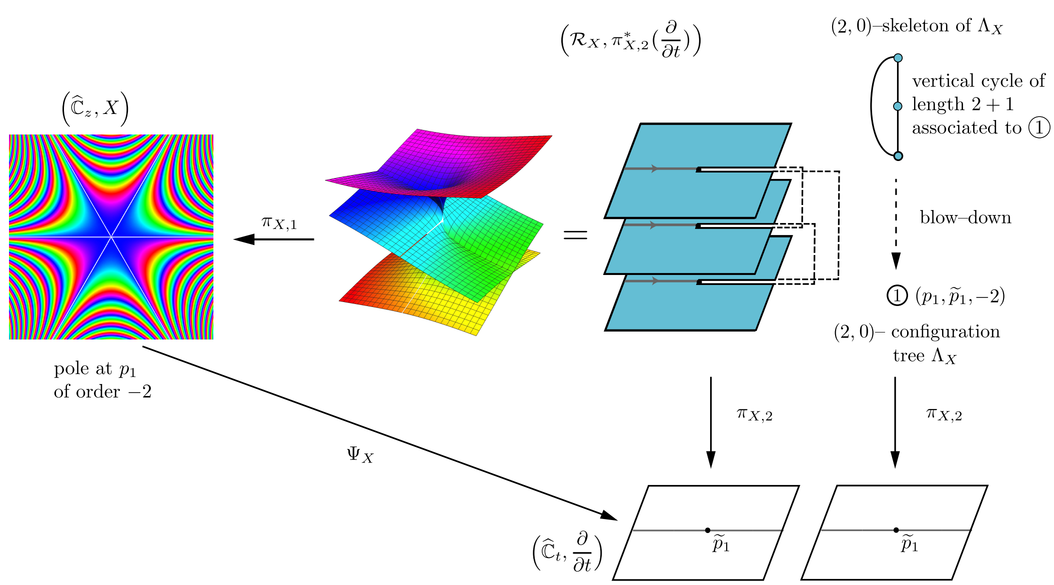

FIGURE 7. **Vector field $X(z) = \dfrac{1}{(z-p_1)^2}\dfrac{\partial}{\partial z}$ with a pole of order -2 at $p_1 \in \mathbb{C}_z$.** The surface $\mathcal{R}_X$ consists of three sheets with a branch cut, glued together to form a $(2+1)$–cyclic helicoid. On the right column, the $(2,0)$–configuration tree consisting of one vertex, and its corresponding $(2,0)$–skeleton are portrayed; see §9.2 and Definition 9.5.

In the next examples, we shall consider (r, d)–configuration trees with two or more vertices, hence weighted edges appear.

Example 8.2. Consider the vector field

$$X(z) = \frac{\lambda}{(z-p_1)^{\nu_1}(z-p_2)^{\nu_2}} \frac{\partial}{\partial z} \in \mathscr{E}(r, 0), \quad \nu_1 + \nu_2 = r, \ \nu_1, \nu_2 \geq 1, \tag{49}$$

and its distinguished parameter

$$\Psi_X(z) = \tfrac{1}{\lambda} \int_{z_0}^{z} (\zeta - p_1)^{\nu_1} (\zeta - p_2)^{\nu_2} d\zeta.$$

Without loss of generality, we assume that the critical values $\widetilde{p}_j = \Psi_X(p_j)$, $j = 1, 2$, satisfy $\mathfrak{Im}(\widetilde{p}_1) \geq \mathfrak{Im}(\widetilde{p}_2)$. The $(r, 0)$–configuration tree has two pole vertices and one edge

$$\Lambda_X = \Big\{ ① = (p_1, \widetilde{p}_1, -\nu_1), ② = (p_2, \widetilde{p}_2, -\nu_2); ①; (\Delta_{1\,2}, 0) \Big\},$$

where the edge $\Delta_{1\,2}$ is the semi–residue $S(\omega_X, p_1, p_2, \gamma) = \widetilde{p}_2 - \widetilde{p}_1$, which according to (42) is equivalent to the diagonal with the same notation. The weight of the edge is 0, since $\Delta_{1\,2}$ is in the global zero level sheet. See Figure 8 and 4.c.

If $\mathfrak{Im}(\widetilde{p}_1) > \mathfrak{Im}(\widetilde{p}_2)$, then the semi–residue $\Delta_{1\,2} = S(\omega_X, p_1, p_2, \gamma) = \widetilde{p}_2 - \widetilde{p}_1 \in \mathbb{C} \backslash \mathbb{R}$, giving origin to a finite height horizontal strip, see left drawing in Figure 8.

If $\mathfrak{Im}(\widetilde{p}_1) = \mathfrak{Im}(\widetilde{p}_2)$, then the diagonal $\Delta_{1\,2}$ up to orientation coincides with a saddle connection of the real vector field $\mathfrak{Re}(X)$.

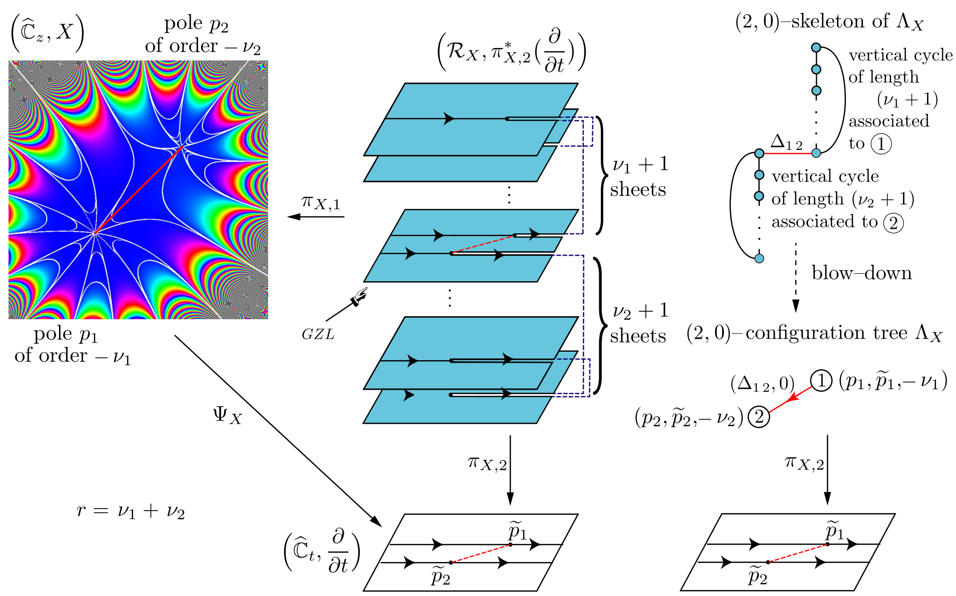

FIGURE 8. **Vector field** $X(z) = \frac{\lambda}{(z-p_1)^{\nu_1}(z-p_2)^{\nu_2}} \frac{\partial}{\partial z}$ **with two poles** p_ι **of order** $-\nu_\iota$**.** The diagonal $\Delta_{1\,2} \subset \mathcal{R}_X$ associated to the finitely ramified branch points and its projections via π_1 and π_2 are coloured red. The two branch points are the endpoints of the diagonal $\Delta_{1\,2} \subset \mathcal{R}_X$ on the global zero level sheet. The phase portrait (left drawing) is the case with poles of orders $-3 = -\nu_2$ and $-5 = -\nu_1$. See Example 8.2, and §9.2 for the drawing on the right.

8.1.1. *Vector fields in $\mathscr{E}(3,0)$ with three simple poles.* Consider $X \in \mathscr{E}(3,0)$ with simple poles,
• we fix two finite ramification values $\widetilde{p}_1 = 0$, $\widetilde{p}_2 = 1$, and
• leave free the third $\widetilde{p}_3$ in the twice punctured plane $\mathbb{C}\backslash\{0,1\}$.
This gives origin to a suitable family of vector fields $\mathfrak{F}$. There is a strong analytical and combinatorial dependence on the choice of the ramification values of the distinguished parameters Ψ_X.

Proposition 8.2. *Let $\mathfrak{F}$ be the family of vector fields defined by the map*

$$\begin{aligned} X(p_3, z) : (\mathbb{C}\backslash\{0, 1/2, 1\}) \times \mathbb{C} &\longrightarrow \mathscr{E}(3,0) \\ (p_3, z) &\longmapsto \frac{2p_3 - 1}{12z(z-1)(z-p_3)}\frac{\partial}{\partial z}. \end{aligned} \tag{50}$$

1) The corresponding distinguished parameters are the polynomials

$$\Psi(p_3, z) = \frac{12}{2p_3 - 1}\Big(\frac{1}{4}z^4 + \frac{-p_3 - 1}{3}z^3 + \frac{p_3}{2}z^2\Big) \in \mathbb{C}[z]. \tag{51}$$

2) The corresponding reduced divisors are

$$X(p_3, z) \quad \longmapsto \quad (0,0,-1) + (1,1,-1) + \Big(p_3, \widetilde{p}_3 = \frac{p_3^3(2-p_3)}{2p_3 - 1}, -1\Big). \tag{52}$$

3) The $(3,0)$–configuration trees $\Lambda_{X(p_3,z)}$ for $X(p_3,z)$ are given by Equations (58)–(76).

In simple words, each $\Lambda_{X(p_3,z)}$ describes the relative position of the branch points

$$1 = (0,0,-1), \quad 2 = (1,1,-1), \quad 3 = (p_3, \widetilde{p}_3, -1)$$

on the Riemann surface $\mathcal{R}_{X(p_3,z)}$.

Remark 8.3. Motivation for the family $\mathfrak{F}$. Let $X \in \mathscr{E}(r,d)$ be a vector field with at least two different poles p_1, p_2. The choice of

$$(p_1, \widetilde{p}_1) = (0,0),\ (p_2, \widetilde{p}_2) = (1,1) \in \mathbb{C}^2$$

as in (49) and (52) can be justified as follows.
1. We consider the complex analytic action

$$\mathcal{A} : Aut(\mathbb{C}) \times \mathscr{E}(r,d) \longrightarrow \mathscr{E}(r,d), \quad (T, X) \longmapsto T^*X, \tag{53}$$

of the affine transformation group $Aut(\mathbb{C})$ corresponding to those $T \in Aut(\widehat{\mathbb{C}}) = PSL(2,\mathbb{C})$ that fix ∞, see [2] for general theory. Using suitable T, we obtain $p_1 = 0$ and $p_2 = 1$. Note that the affine group $Aut(\mathbb{C})$ is the largest complex automorphism group that acts on $\mathscr{E}(r,d)$.
2. If $\Psi_X(z) = \int_{p_1=0}^{z} \omega_X$, then $\Psi_X(0) = 0 = \widetilde{p}_1$.
3. Considering $\{\lambda X \mid \lambda \in \mathbb{C}^*\}$ as a projective class, we normalize by a suitable λ_0, thus

$$\int_0^1 \tfrac{1}{\lambda_0}\omega_X = 1 = \widetilde{p}_2.$$

In the particular case $\mathscr{E}(3,0)$, we get Equation (50).

Proof. First step. A suitable tessellation for p_3. The degree four rational map

$$\mathbb{C}_{p_3} \longrightarrow \mathbb{C}_{\widetilde{p}_3}, \quad p_3 \longmapsto \widetilde{p}_3 = \frac{p_3^3(2-p_3)}{2p_3 - 1} \tag{54}$$

determines the behaviour of the third branch point $(p_3, \widetilde{p}_3, -1) \in \mathcal{R}_{X(p_3,z)}$. The rational map (54) has critical points $\{0, 1, 1/2\}$, with critical values $\{0, 1, \infty\}$. The inverse image $\widetilde{p}_3^{-1}(\mathbb{R})$ is drawn in Figure 9 using black, blue and orange segments to represent the inverse images of $(-\infty, 0)$, $[0,1]$ and $(1,\infty)$, respectively. There are eight open connected components

$$\{U_j\}_{j=1}^{8} = \mathbb{C}_{p_3}\backslash\widetilde{p}_3^{-1}(\mathbb{R})$$

determining a tessellation of $\mathbb{C}_{p_3}$. The regions U_j with even index are coloured white and those with odd index are coloured gray. They are the inverse image of the lower half plane $\mathbb{H}^2_-$ and the upper half plane $\mathbb{H}^2_+$, respectively.

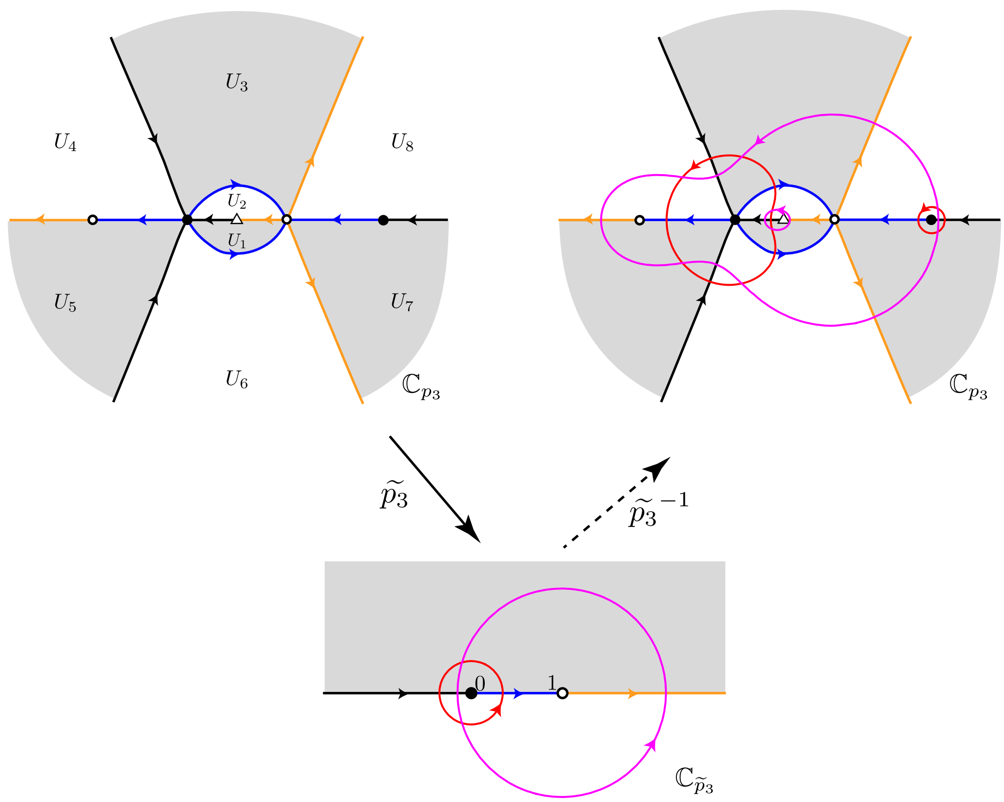

Figure 9. The degree four rational map $p_3 \longmapsto \widetilde{p}_3$ gives origin to eight open regions U_j, forming a tessellation of $\mathbb{C}_{p_3}$, see upper left figure. The points $0,\ 1,\ 1/2 \in \mathbb{C}_{p_3}$, coloured black, white, triangle vertices, correspond to the preimages of $0, 1, \infty \in \mathbb{C}_{\widetilde{p}_3}$, respectively. The upper right figure provides a description of the lift of the red α and magenta β circles under $\widetilde{p}_3^{-1}$. The blue tree $\widetilde{p}_3^{-1}\big([0,1]\big)$ is the *dessin d'enfant* of the map $\widetilde{p}_3$.

To understand the suitability of the tessellation in $\mathbb{C}_{p_3}$ we need the behaviour of $\widetilde{p}_3^{-1}$ along topological loops α and β enclosing the other two critical values 0 and 1. The loops will be chosen so that they are generators of the fundamental group $\pi_1(\mathbb{C}_{\widetilde{p}_3}\backslash\{0,1\})$.

1) The red circle $\alpha \subset \mathbb{C}_{\widetilde{p}_3}$ represents loops in $\mathbb{C}_{\widetilde{p}_3}$, enclosing the critical value 0 but not 1.

2) The magenta circle $\beta \subset \mathbb{C}_{\widetilde{p}_3}$ represents loops in $\mathbb{C}_{\widetilde{p}_3}$ enclosing both 0 and 1.

The lifts of the circles α, β are described in Figure 9.

In order to proceed with the proof, the idea is as follows. If we determine the $(3,0)$–configuration trees of $X(p_3,z)$ at one point $p_3 \in U_j$, then by a continuity argument the analogous configuration tree remains valid for all $p_3 \in U_j$.

Second step. Computation of the $(3,0)$*–configuration trees.*

We shall need to consider the boundaries between the regions U_j, $j = 1, \dots, 8$. Let U_i and U_j denote two adjacent regions with common boundary (as open segments)

$$\partial U_{i,j} \doteq (\overline{U_i} \cap \overline{U}_j) \backslash \{ \widetilde{p_3}^{-1}(\{0,1,\infty\}) \}.$$

Moreover, we assign colors to the vertices and edges in Figure 10, as follows

$$\begin{gathered}
① = (0,0,-1) \text{ in red, } ② = (1,1,-1) \text{ in green, } ③ = (p_3,\widetilde{p}_3,-1) \text{ in blue,}\\
\Delta_{1\,2} = \overline{(0,0,-1),(1,1,-1)},\ \Delta_{2\,1} = \overline{(1,1,-1),(0,0,-1)} \text{ in dashed black line,}\\
\Delta_{1\,3} = \overline{(0,0,-1),(p_3,\widetilde{p}_3,-1)},\ \Delta_{3\,1} = \overline{(p_3,\widetilde{p}_3,-1),(0,0,-1)} \text{ in red,}\\
\Delta_{2\,3} = \overline{(1,1,-1),(p_3,\widetilde{p}_3,-1)},\ \Delta_{3\,2} = \overline{(p_3,\widetilde{p}_3,-1),(1,1,-1)} \text{ in green.}
\end{gathered}$$

Because of Definition 7.7.4 there are two possible cases for the root.
1) If $\widetilde{p}_3 \in \mathbb{H}^2_+ \cup (-\infty, 0)$ then the vertex ③ is the root, by Equation (54), this is equivalent to

$$p_3 \in U_1 \cup U_3 \cup U_5 \cup U_7 \cup \partial U_{3,4} \cup \partial U_{5,6} \cup \big(\partial U_{1,2} \cap (0,1/2)\big) \cup \big(\partial U_{7,8} \cap (2,\infty)\big). \tag{55}$$

2) If $\widetilde{p}_3 \notin \mathbb{H}^2_+ \cup (-\infty, 0)$ then the vertex ① is the root, once again by (54)

$$\begin{multlined} p_3 \in U_2 \cup U_4 \cup U_6 \cup U_8 \\ \cup \partial U_{2,3} \cup \partial U_{1,6} \cup \partial U_{4,5} \cup \partial U_{3,8} \cup \partial U_{6,7} \\ \cup \big(\partial U_{1,2} \cap (1/2,1)\big) \cup \big(\partial U_{7,8} \cap (1,2)\big). \end{multlined} \tag{56}$$

In either case, the diagonals/edges satisfy

$$\begin{gathered} \Delta_{i\,j} = -\Delta_{j\,i}, \quad i,j \in \{1,2,3\},\ i \neq j, \\ \Delta_{1\,2} + \Delta_{2\,3} + \Delta_{3\,1} = 0. \end{gathered} \tag{57}$$

The $(3,0)$–configuration trees can be deduced upon careful consideration of the phase portraits portrayed in Figure 10.

Case (1), the root is ③ *and colored blue.* From Equation (55), when

- $p_3 \in U_1$, the $(3,0)$–configuration tree is

$$\Lambda_{X(p_3,z)} = \Big\{①,②,③;③;(\Delta_{3\,2},0),\ (\Delta_{3\,1},1)\Big\},\ \text{with } \Delta_{3\,2}, \Delta_{3\,1} \in \mathbb{H}^2_-; \tag{58}$$

- $p_3 \in U_3$, the $(3,0)$–configuration tree is

$$\Lambda_{X(p_3,z)} = \Big\{①,②,③;③;(\Delta_{3\,1},0),\ (\Delta_{1\,2},0)\Big\},\ \text{with } \Delta_{1\,2} = 1 \text{ and } \Delta_{3\,1} \in \mathbb{H}^2_-; \tag{59}$$

- $p_3 \in U_5$, the $(3,0)$–configuration tree is

$$\Lambda_{X(p_3,z)} = \Big\{①,②,③;③;(\Delta_{3\,1},0),\ (\Delta_{1\,2},1)\Big\},\ \text{with } \Delta_{1\,2} = 1 \text{ and } \Delta_{3\,1} \in \mathbb{H}^2_-; \tag{60}$$

- $p_3 \in U_7$, the $(3,0)$–configuration tree is

$$\Lambda_{X(p_3,z)} = \Big\{①,②,③;③;(\Delta_{3\,2},0),\ (\Delta_{2\,1},1)\Big\},\ \text{with } \Delta_{2\,1} = -1 \text{ and } \Delta_{3\,2} \in \mathbb{H}^2_-; \tag{61}$$

- $p_3 \in \partial U_{1,2} \cap (0,1/2)$, the $(3,0)$–configuration tree is

$$\Lambda_{X(p_3,z)} = \Big\{①,②,③;③;(\Delta_{3\,1},0),\ (\Delta_{3\,2},1)\Big\},\ \text{with } \Delta_{3\,2} > 0 \text{ and } \Delta_{3\,2} > 1; \tag{62}$$

- $p_3 \in \partial U_{7,8} \cap (2,\infty)$, the $(3,0)$–configuration tree is

$$\Lambda_{X(p_3,z)} = \Big\{①,②,③;③;(\Delta_{3\,2},0),\ (\Delta_{2\,1},1)\Big\},\ \text{with } \Delta_{2\,1} = -1 \text{ and } \Delta_{3\,2} > 1; \tag{63}$$

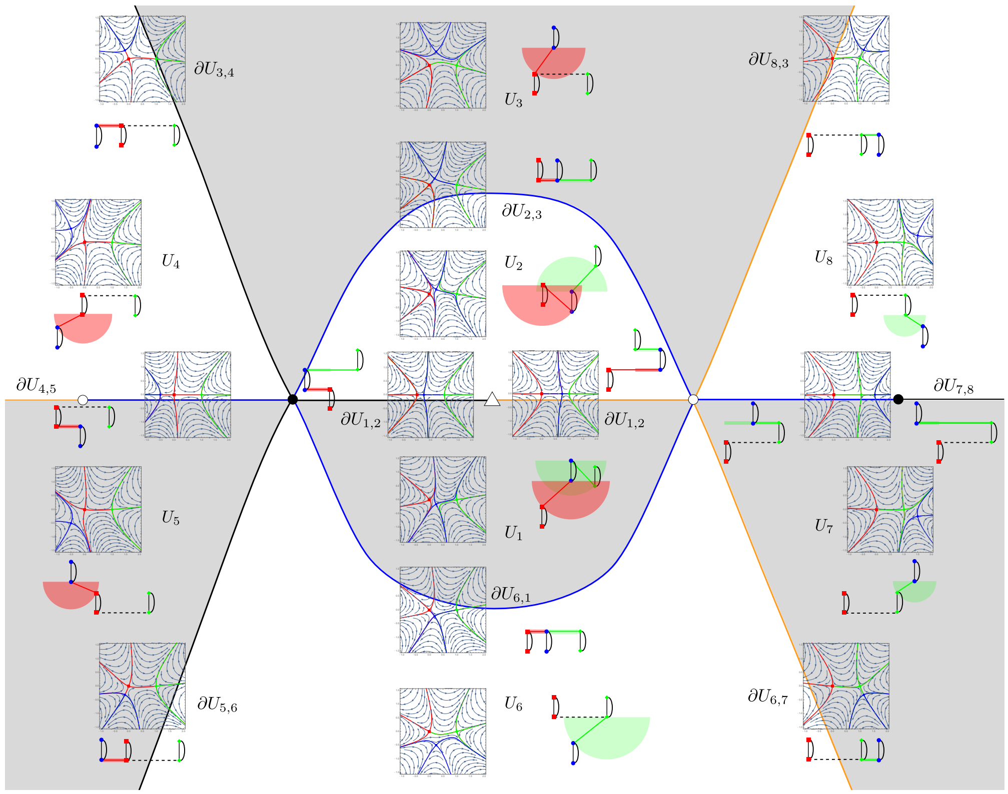

FIGURE 10. The plane $\mathbb{C}_{p_3}$ as vector field atlas of $X(p_3, z)$ and their corresponding $(3,0)$–skeletons of $\Lambda_{X(p_3,z)}$. This provides a bifurcation diagram for the phase portraits, there appear 12 (orientation preserving) topological classes of phase portraits of $\mathfrak{Re}\,(X(p_3, z))$. The shaded red and green areas represent the half planes or segments where the diagonal corresponding to $\widetilde{p}_3$ can move, its total winding number is 4 coinciding with the degree of the map $\widetilde{p}_3$ in (54).

- $p_3 \in \partial U_{3,4}$, the $(3,0)$–configuration tree is

$$\Lambda_{X(p_3,z)} = \Big\{1, 2, 3; 3; (\Delta_{3\,1}, 0),\ (\Delta_{1\,2}, 0)\Big\}, \text{ with } \Delta_{1\,2} = 1 \text{ and } \Delta_{3\,1} > 0; \tag{64}$$

- $p_3 \in \partial U_{5,6}$, the $(3,0)$–configuration tree is

$$\Lambda_{X(p_3,z)} = \Big\{1, 2, 3; 3; (\Delta_{3\,1}, 0),\ (\Delta_{1\,2}, 0)\Big\}, \text{ with } \Delta_{1\,2} = 1 \text{ and } \Delta_{3\,1} > 0. \tag{65}$$

Case (2), the root is 1 *and colored red.* From Equation (56), when

- $p_3 \in U_2$, the $(3,0)$–configuration tree is

$$\Lambda_{X(p_3,z)} = \Big\{1, 2, 3; 1; (\Delta_{1\,3}, 0),\ (\Delta_{3\,2}, 1)\Big\}, \text{ with } \Delta_{1\,3}, \Delta_{3\,2} \in \mathbb{H}^2_-; \tag{66}$$

- $p_3 \in U_4$, the $(3,0)$–configuration tree is

$$\Lambda_{X(p_3,z)} = \Big\{1, 2, 3; 1; (\Delta_{1\,2}, 0),\ (\Delta_{1\,3}, 1)\Big\}, \text{ with } \Delta_{1\,3} \in \mathbb{H}^2_-, \Delta_{3\,2} \in \mathbb{H}^2_+; \tag{67}$$

- $p_3 \in U_6$, the $(3,0)$–configuration tree is

$$\Lambda_{X(p_3,z)} = \Big\{ ①, ②, ③; ⓵; (\Delta_{1\,2}, 0),\ (\Delta_{2\,3}, 0) \Big\}, \text{ with } \Delta_{1\,2} = 1 \text{ and } \Delta_{2\,3} \in \mathbb{H}^2_-; \tag{68}$$

- $p_3 \in U_8$, the $(3,0)$–configuration tree is

$$\Lambda_{X(p_3,z)} = \Big\{ ①, ②, ③; ⓵; (\Delta_{1\,2}, 0),\ (\Delta_{2\,3}, 1) \Big\}, \text{ with } \Delta_{1\,2} = 1 \text{ and } \Delta_{2\,3} \in \mathbb{H}^2_-; \tag{69}$$

- $p_3 \in \partial U_{4,5}$, the $(3,0)$–configuration tree is

$$\Lambda_{X(p_3,z)} = \Big\{ ①, ②, ③; ⓵; (\Delta_{1\,2}, 0),\ (\Delta_{1\,3}, 1) \Big\}, \text{ with } \Delta_{1\,2} = 1 \text{ and } \Delta_{1\,3} > 0; \tag{70}$$

- $p_3 \in \partial U_{1,2} \cap (1/2, 1)$, the $(3,0)$–configuration tree is

$$\Lambda_{X(p_3,z)} = \Big\{ ①, ②, ③; ⓵; (\Delta_{1\,3}, 0),\ (\Delta_{3\,2}, 1) \Big\}, \text{ with } \Delta_{1\,3} > 1 \text{ and } \Delta_{3\,2} < 0; \tag{71}$$

- $p_3 \in \partial U_{7,8} \cap (1, 2)$, the $(3,0)$–configuration tree is

$$\Lambda_{X(p_3,z)} = \Big\{ ①, ②, ③; ⓵; (\Delta_{1\,2}, 0),\ (\Delta_{2\,3}, 1) \Big\}, \text{ with } \Delta_{1\,2} = 1 \text{ and } -1 < \Delta_{2\,3} < 0; \tag{72}$$

- $p_3 \in \partial U_{1,6}$, the $(3,0)$–configuration tree is

$$\Lambda_{X(p_3,z)} = \Big\{ ①, ②, ③; ⓵; (\Delta_{1\,3}, 0),\ (\Delta_{3\,2}, 0) \Big\}, \text{ with } 0 < \Delta_{1\,3} < 1 \text{ and } 0 < \Delta_{3\,2} < 1; \tag{73}$$

- $p_3 \in \partial U_{3,8}$, the $(3,0)$–configuration tree is

$$\Lambda_{X(p_3,z)} = \Big\{ ①, ②, ③; ⓵; (\Delta_{1\,2}, 0),\ (\Delta_{2\,3}, 0) \Big\}, \text{ with } \Delta_{1\,2} = 1 \text{ and } \Delta_{2\,3} > 0; \tag{74}$$

- $p_3 \in \partial U_{2,3}$, the $(3,0)$–configuration tree is

$$\Lambda_{X(p_3,z)} = \Big\{ ①, ②, ③; ⓵; (\Delta_{1\,3}, 0),\ (\Delta_{3\,2}, 0) \Big\}, \text{ with } 0 < \Delta_{1\,3} < 1 \text{ and } \Delta_{1\,3} > 0; \tag{75}$$

- $p_3 \in \partial U_{6,7}$, the $(3,0)$–configuration tree is

$$\Lambda_{X(p_3,z)} = \Big\{ ①, ②, ③; ⓵; (\Delta_{1\,2}, 0),\ (\Delta_{2\,3}, 0) \Big\}, \text{ with } \Delta_{1\,2} = 1 \text{ and } \Delta_{2\,3} > 0. \tag{76}$$

□

As an advantage of Proposition (8.2), recalling the complex analytic action (53), then the quotient map

$$\begin{array}{rcl} \Pi : \mathscr{E}(r,d) & \longrightarrow & \dfrac{\mathscr{E}(r,d)}{Aut(\mathbb{C})} \\ X & \longmapsto & [X] \end{array}$$

determines the analytic classes of vector fields. In particular, $\mathscr{E}(3,0)/Aut(\mathbb{C})$ is a complex analytic space of complex dimension two, having singularities originated from the vector fields in $\mathscr{E}(3,0)$ with non-trivial isotropy group under the $Aut(\mathbb{C})$–action. See [2] for general theory on $\mathscr{E}(r,d)$ and [23], [33] for the rational case. Hence the family $\mathfrak{F}$ gives origin to a curve $\Pi \circ X(p_2, z)$ of $Aut(\mathbb{C})$–classes of vector fields.

Corollary 8.4. *1) The complex analytic curve*

$$\Pi \circ X(p_3, z) : \mathbb{C}\backslash\{-1, 0, 1/2, 1, 2\} \longrightarrow \frac{\mathscr{E}(3,0)}{Aut(\mathbb{C})}$$

is injective.

2) The parameter plane $\mathbb{C}_{p_3}\backslash\{0,\ 1/2,\ 1\}$ provides a bifurcation diagram. There appear 12 (orientation preserving) topological classes of phase portraits of $\mathfrak{Re}\,(X(p_3, z))$.

The notions of topological equivalence and bifurcation appear as Definition 11.1. We shall study the general problem of the number of topological classes of phase portraits of $\mathfrak{Re}\,(X)$, for $X \in \mathscr{E}(r,d)$, in §11, see Theorem 11.3.

Proof. In order to describe the $Aut(\mathbb{C})$–equivalent the vector fields $X(p_3, z)$, consider the action $(T, X(p_3, z)) \longmapsto T^*X(p_3, z)$. It lifts to the action on distinguished parameters, as

$$(T, \Psi(p_3, z)) \longmapsto T^*\Psi(p_3, z) = \Psi(p_3, \ ) \circ T^{-1}(z).$$

The polynomial $\Psi(p_3, z)$ has branch points $\{(0,0), (1,1), (p_3, \widetilde{p}_3)\} \subset \mathbb{C}^2$. For $T \neq Id \in Aut(\mathbb{C})$, the polynomial $\Psi(p_3, \ ) \circ T^{-1}(z)$ gives rise to a permutation of $\{(0,0), (1,1), (p_2, \widetilde{p}_3)\}$. This is possible if and only if $\widetilde{p}_3 = 0$ or 1. Using the definition of $\widetilde{p}_3$, Equation (54), we have $p_3 = -1$ or 2. In fact the polynomials $\Psi(-1, z)$ and $\Psi(2, z)$ are $Aut(\mathbb{C})$–equivalent (using the translation map T^{-1} that sends $\{-1, 0, 1\}$ to $\{0, 1, 2\}$ in $\mathbb{C}_z$).

The assertion (2) uses careful inspection of Figure 10. We convene that $\sim$ means topologically equivalence. For p_3 the topologies are as follows:

• $U_1, \ldots, U_8$ determine eight topological classes. Clearly the topology remains without change for p_3 on each open set. For example, U_1, U_2 determine two horizontal strip flows for the corresponding $\mathfrak{Re}\,(X(p_3, z))$, however the orientation of the flows are different.

• $\partial U_{1,2} \cap (0, 1/2) \sim \partial U_{4,5}$, $\partial U_{7,8} \cap (1, 1/2) \sim \partial U_{7,8} \cap (2, \infty)$ determine two topological classes. In fact the corresponding $\mathfrak{Re}\,(X(p_3, z))$ have two saddle connections, the orientation determines two non-equivalent cases.

• $\partial U_{3,4} \sim \partial U_{1,6} \sim \partial U_{3,8}$, $\partial U_{5,6} \sim \partial U_{2,3} \sim \partial U_{6,7}$ determine two topological classes. The corresponding $\mathfrak{Re}\,(X(p_3, z))$ have two saddle connections that have a common half plane as boundary (this is the difference with respect to the above case), and the orientation determines two non-equivalent cases.

Hence we have 12 different topological classes of phase portraits. □

The general problem of of computing Ψ_X starting with a configuration of preassigned critical values $\{\widetilde{p}_1, \ldots, \widetilde{p}_r\}$ is treated in §14, Corollary 14.1.

8.2. **The vector field $X \in \mathscr{E}(0,d)$ has an isolated essential singularity at $\infty \in \widehat{\mathbb{C}}_z$, no zeros or poles.** The simplest example corresponds to a $(0,1)$–configuration tree; only one essential vertex and no edges.

Example 8.3. Consider once again Example 4.1, that is

$$X(z) = \mathrm{e}^{\mu(z+c_1)} \frac{\partial}{\partial z} \in \mathscr{E}(0,1),$$

with $\mu \in \mathbb{C}^*$, $c_1 \in \mathbb{C}$ as in (7). There is an isolated essential singularity at $\infty \in \widehat{\mathbb{C}}_z$ with finite asymptotic value a_1 given by (22).

The $(0,1)$–configuration tree consists of one essential vertex and no edges

$$\Lambda_X = \Big\{ \textcircled{1} = (\infty_1, a_1, -\infty); \textcircled{\textcircled{1}};\ \varnothing \Big\}.$$

See Figure 11 and 4.a. The vertices are branch points of the Riemann surface $\mathcal{R}_X$, and since there is only one branch point/vertex, then no weighted edges appear. The soul of $\mathcal{R}_X$ is a sheet, recall Remark 8.1, and coincides with the global zero level. It is to be noted that the semi–infinite helicoids, even though they are part of $\mathcal{R}_X$, are not necessary in the combinatorial description of the surface. The complete $\mathcal{R}_X$ is constructed by making the natural convention to glue two semi–infinite helicoids to each vertical tower, one on the top and one on the bottom. Hence the semi–infinite helicoids will have no counterpart in the combinatorial description as graphs. However, to remind the reader of their existence in $\mathcal{R}_X$ we have schematically represented them in the figures by the “springs” or “coils” attached to the vertical towers.

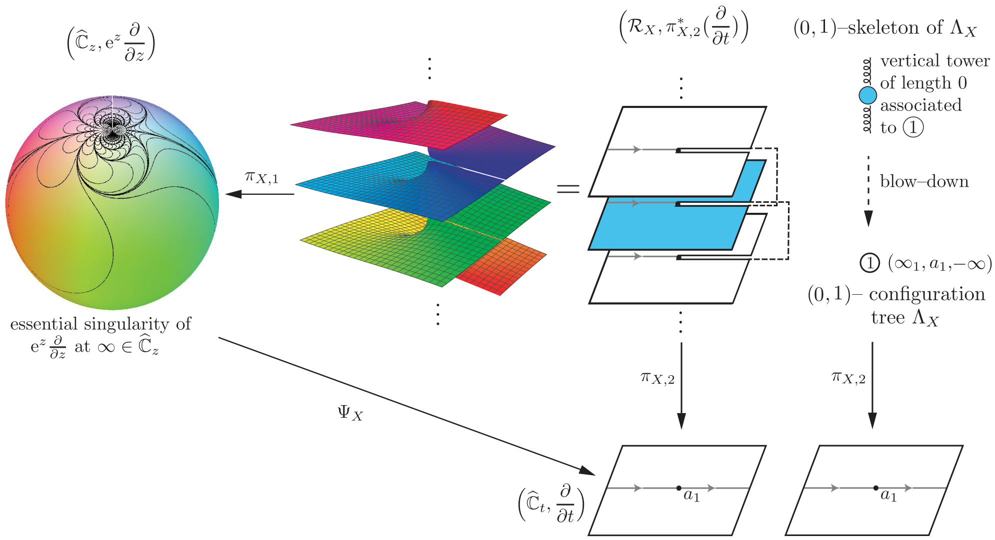

FIGURE 11. **Vector field $X(z) = e^{\mu(z+c_1)} \frac{\partial}{\partial z}$ with an essential singularity at $\infty \in \widehat{\mathbb{C}}_z$.** The surface $\mathcal{R}_X$ is formed by two semi–infinite helicoids glued to the global zero level sheet. This sheet is the soul, Definition 9.7, shaded blue. See Example 8.3, and §9.2 for the combinatorial elements on the right column.

In the following example there are $d \geq 2$ essential vertices and $d-1$ edges, all sharing the same sheet.

Example 8.4. Consider the vector field

$$X(z) = e^{z^d} \frac{\partial}{\partial z} \in \mathscr{E}(0, d), \text{ for } d \geq 2.$$

If $z_0 = 0$, the distinguished parameter is

$$\Psi_X(z) = \int_0^z e^{-\zeta^d} d\zeta.$$

Note that $a_1 \doteq \int_0^\infty e^{-\zeta^d} d\zeta \in \mathbb{R}^+$. Moreover Ψ_X has d finite asymptotic values given by[3] (see [39] p. 168)

$$a_\sigma = e^{i2\pi(\sigma-1)/d} a_1 \quad \text{for} \quad \sigma = 1 \ldots d,$$

each with multiplicity one, and a logarithmic branch point $(\infty_\sigma, a_\sigma, -\infty) \in \mathcal{R}_X$ over each finite asymptotic value. For each of the finite asymptotic values a_σ, the exponential tracts $U_\sigma(\rho)$ are given by

$$U_\sigma(\rho) = \left\{ z \in \mathbb{C}_z \mid \left| \arg z - \tfrac{2\pi(\sigma-1)}{d} \right| < \tfrac{\pi}{d}, |z| < R(\rho) \right\}, \quad \text{for } \sigma = 1, \ldots, d,$$

where $R(\rho) > 0$ is a suitable function of ρ.

Thus the $(0, d)$–configuration tree Λ_X will have d essential vertices

$$V_H = \{ \sigma = (\infty_\sigma, a_\sigma, -\infty) \}_{\sigma=1}^d$$

with root $1 = (\infty_1, a_1, -\infty)$. Recalling Definition 7.6.1, the $d-1$ edges E_H are selected such that we obtain a left–right–top–bottom linear directed tree of the vertices V_H, where the index

[3]Our numbering of the indices σ differ from the ones in [39] so that they agree with the conventions outlined in Remark 4.6.3.

σ_0 for the top and left most vertex will be given by the simple formula

$$\sigma_0 = \left\lceil \left\lfloor \frac{d}{2} \right\rfloor /2 \right\rceil + 1,$$

where $\lceil \cdot \rceil$ and $\lfloor \cdot \rfloor$ are the ceiling and floor functions respectively. Recalling Definition 7.6.2, we obtain $\Lambda_{H,①}$ the linear directed rooted tree with incoming vertex ①. Moreover, all d branch points share the same sheet in $\mathcal{R}_X$, hence by assigning weight 0 to each of the edges $\Delta_{\mathfrak{ar}} \in \widehat{E}_H$ we obtain the $(0, d)$–configuration tree of X. In Figure 12 the case $d = 9$ is illustrated, the $(0, 9)$–configuration tree is

$$\Lambda_X = \Big\{ ①, \dots, ⑨; ①; (\Delta_{1\,5}, 0), (\Delta_{5\,2}, 0), (\Delta_{2\,4}, 0), (\Delta_{4\,3}, 0), \\ (\Delta_{1\,6}, 0), (\Delta_{6\,9}, 0), (\Delta_{9\,7}, 0), (\Delta_{7\,8}, 0) \Big\}. \tag{77}$$

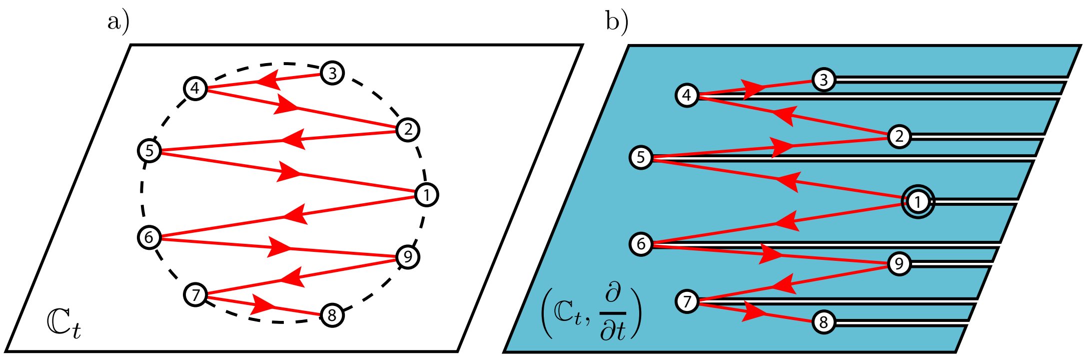

FIGURE 12. **Vector field $X(z) = e^{z^9} \frac{\partial}{\partial z}$ with essential singularity at ∞ and no poles.** In this case the top and left most vertex is σ_0 with $\sigma_0 = \lceil \lfloor 9/2 \rfloor /2 \rceil + 1 = 3$. (a) Represents the left–right–top–bottom linear directed tree of the vertices $V_H = \{①, \dots, ⑨\}$. (b) Represents the $(0, 9)$–configuration tree Λ_X where all the edges have weight 0. The soul, Definition 9.7, is shaded blue. The Riemann surface $\mathcal{R}_X$ consists of gluing 18 semi–infinite helicoids, one above and one below each logarithmic branch point/vertex. All the branch points and diagonals belong to the global zero level sheet.

The soul of $\mathcal{R}_X$ is a sheet and coincides with the global zero level.

The following example is a family of vector fields in $\mathscr{E}(0, 3)$ whose $(0, 3)$–configuration trees have two edges, one of which can assume a non–zero weight. Recall that the weight of an edge indicates the number of sheets one has to go up or down, at the starting branch point, in order to reach the sheet that shares both the starting and ending branch point of the diagonal/edge (*i.e.* the sheet containing the diagonal).

Example 8.5. Consider the vector field

$$X(z) = 2\pi i \exp\left(-\frac{1}{3}z^3 + c_2 z\right) \frac{\partial}{\partial z}, \quad c_2 \in \mathbb{C}. \tag{78}$$

We shall need some background on Airy functions and integrals, for full details see [1], pp. 200–203 and references therein. Let

$$\mathcal{A}i(p,z) = \frac{1}{2\pi i}\int\limits_{\mathcal{L}(z)} \mathrm{e}^{\frac{1}{3}\zeta^3 - p\zeta} d\zeta,$$

be the *Airy integral*, where $A = \{z \in \mathbb{C} \mid \arg(z) \in (\pi/6, 3\pi/6)\}$ and $\mathcal{L}(z) := \mathcal{L}(z,\tau) : [0,1] \longrightarrow A$ is a simple C^1 path starting at 0 and ending at $z \in A$. The relationship between the Airy function Ai and the Airy integral is given by

$$\mathrm{Ai}(p) = \mathcal{A}i(p) - \mathrm{e}^{-i2\pi/3}\mathcal{A}i(\mathrm{e}^{-i2\pi/3}p), \qquad \mathcal{A}i(p) = \lim_{\substack{z\to\infty\\ z\in A}} \mathcal{A}i(p,z). \tag{79}$$

Choosing $z_0 = 0$, the distinguished parameter of X is

$$\Psi_X(z) = \int_0^z \omega_X = \frac{1}{2\pi i}\int_0^z \mathrm{e}^{\frac{1}{3}\zeta^3 - c_2\zeta} d\zeta,$$

so the 3 finite asymptotic values of $\Psi_X(z)$ are given by

$$a_{j+1}(c_2) = \eta^j \mathcal{A}i(\eta^j c_2), \qquad j = 0,1,2, \quad \eta = \mathrm{e}^{i2\pi/3}, \tag{80}$$

with asymptotic paths ending in the exponential tracts

$$U_j(\rho) = \eta^j A \cap D\big(0, R(\rho)\big),$$

for $j = 0$, 1 and 2 respectively, where $R(\rho)$ is a suitable function of ρ.
The $(0,3)$–configuration trees for X as in (78) are

$$\Lambda_X = \Big\{ ① = (\infty_1, a_1, -\infty), ② = (\infty_2, a_2, -\infty), ③ = (\infty_3, a_3, -\infty); \\ ① ; (\Delta_{1\,2}, 0), (\Delta_{1\,3}, K(1,3)) \Big\}, \tag{81}$$

where

$$\begin{aligned} \Delta_{1\,2} &= a_2 - a_1 = \eta\,\mathrm{Ai}(\eta\, c_2), \\ \Delta_{1\,3} &= a_3 - a_1 = -\mathrm{Ai}(c_2), \end{aligned} \tag{82}$$

with $K(1,3) \in \mathbb{Z}$. See Figure 13. The dependency of $\Delta_{1\,2}$ and $\Delta_{1\,3}$ on c_2 is clear from (82), however the dependency of $K(1,3)$ on c_2 is much more intricate, any $K(1,3) \in \mathbb{Z}$ appears: for a full description see [1] §8.6.1, particularly figure 14.

8.3. **The vector field $X \in \mathscr{E}(r,d)$ has $r \geq 1$ poles on $\mathbb{C}_z$ and an isolated essential singularity at $\infty \in \widehat{\mathbb{C}}_z$.** The next example shows a simple case where the soul is non–trivial: it consists of more than one sheet.

Example 8.6. Consider the vector field

$$X(z) = \frac{\mathrm{e}^z}{(z-p_1)(z-p_2)}\frac{\partial}{\partial z} \in \mathscr{E}(2,1),$$

with $p_1 = 9i\frac{\pi}{2}$ and $p_2 = -i\frac{\pi}{2}$. Its distinguished parameter is then

$$\Psi_X(z) = \int_{z_0}^z \omega_X = \frac{\mathrm{e}^{-z}}{4}\big(-8 - 9\pi^2 + 16i\pi(1+z) - 4z(2+z)\big).$$

The vector field X has an isolated essential singularity at $\infty \in \widehat{\mathbb{C}}_z$ and Ψ_X has one finite asymptotic value

$$a_1 = \Psi_X(\infty) = 0$$

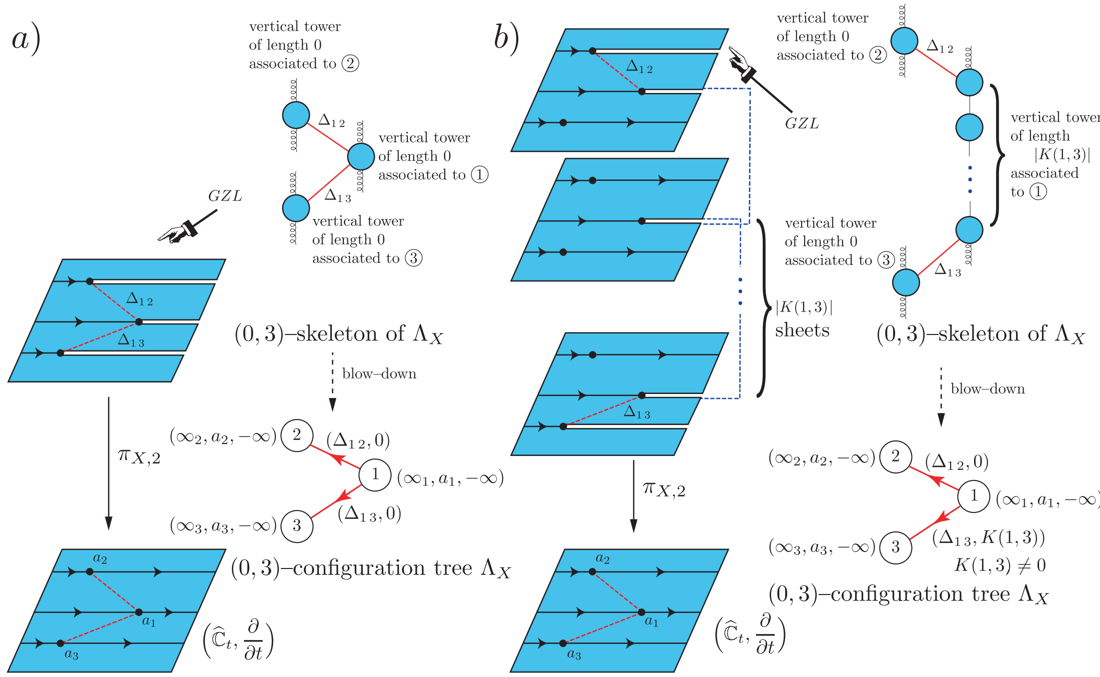

FIGURE 13. **Vector field** $X(z) = 2\pi i \exp\left(-\frac{1}{3}z^3 + c_2 z\right)\frac{\partial}{\partial z} \in \mathscr{E}(0,3)$ **with essential singularity at** ∞ **and no poles.** In (a) we have the case when $K(1,2) = K(1,3) = 0$ so the diagonals $\Delta_{1\,2}$ and $\Delta_{1\,3}$ share the same sheet of $\mathcal{R}_X$. Case (b) is when $K(1,2) = 0$ and $K(1,3) \in \mathbb{Z}\backslash\{0\}$, thus the diagonals $\Delta_{1\,2}$ and $\Delta_{1\,3}$ lie on two different sheets of $\mathcal{R}_X$. We illustrate the case $K(1,3) < 0$. Note that the global zero level sheet is the one containing the diagonal $\Delta_{1\,2}$. When starting on the global zero level sheet and in order to reach the sheet containing the diagonal $\Delta_{1\,3}$, it is necesarry to go around the branch point $(\infty_1, a_1, -\infty)$ exactly $K(1,3)$ times (see Remark 5.19.3). For case (b) the global zero level sheet is non-canonical: if we instead choose as the global zero level sheet the one containing the diagonal $\Delta_{1\,3}$, then the integer parameters would be $K(1,3) = 0$ and $K(1,2) > 0$.

with asymptotic path inside the exponential tract $\{z \in \mathbb{C}_z \mid \mathfrak{Re}(z) > 0\}$. The poles p_1, p_2 have associated critical values $\widetilde{p}_1 = -5\pi + 2i$ and $\widetilde{p}_2 = -5\pi - 2i$ respectively.
According to the labelling conventions in Definition 7.7, the (2, 1)–configuration tree

$$\Lambda_X = \Big\{①=(p_1,\widetilde{p}_1,-1), ②=(\infty_1,a_1,-\infty), ③=(p_2,\widetilde{p}_2,-1); \quad ①; (\Delta_{1\,2},0),(\Delta_{2\,3},-3)\Big\}, \tag{83}$$

has two pole vertices ①, ③, an essential vertex ②, and two edges

$$\Delta_{1\,2} = a_1 - \widetilde{p}_1 = 5\pi - 2i \quad \text{with weight } 0,$$
$$\Delta_{2\,3} = \widetilde{p}_2 - a_1 = -5\pi - 2i \quad \text{with weight } -3.$$

In this case, the (2, 1)–soul of Λ_X is a flat Riemann surface consisting of:

• 12 half planes,
• 2 finite height horizontal strips,
• two cone points with cone angle 4π (equivalent to the two simple poles),
• a cone point with cone angle 8π (associated to the infinitely ramified branch point $(\infty_1, a_1, -\infty)$) and
• a horizontal branch cut starting at the branch point $(\infty_1, a_1, -\infty)$.
See Figures 14 and 4.

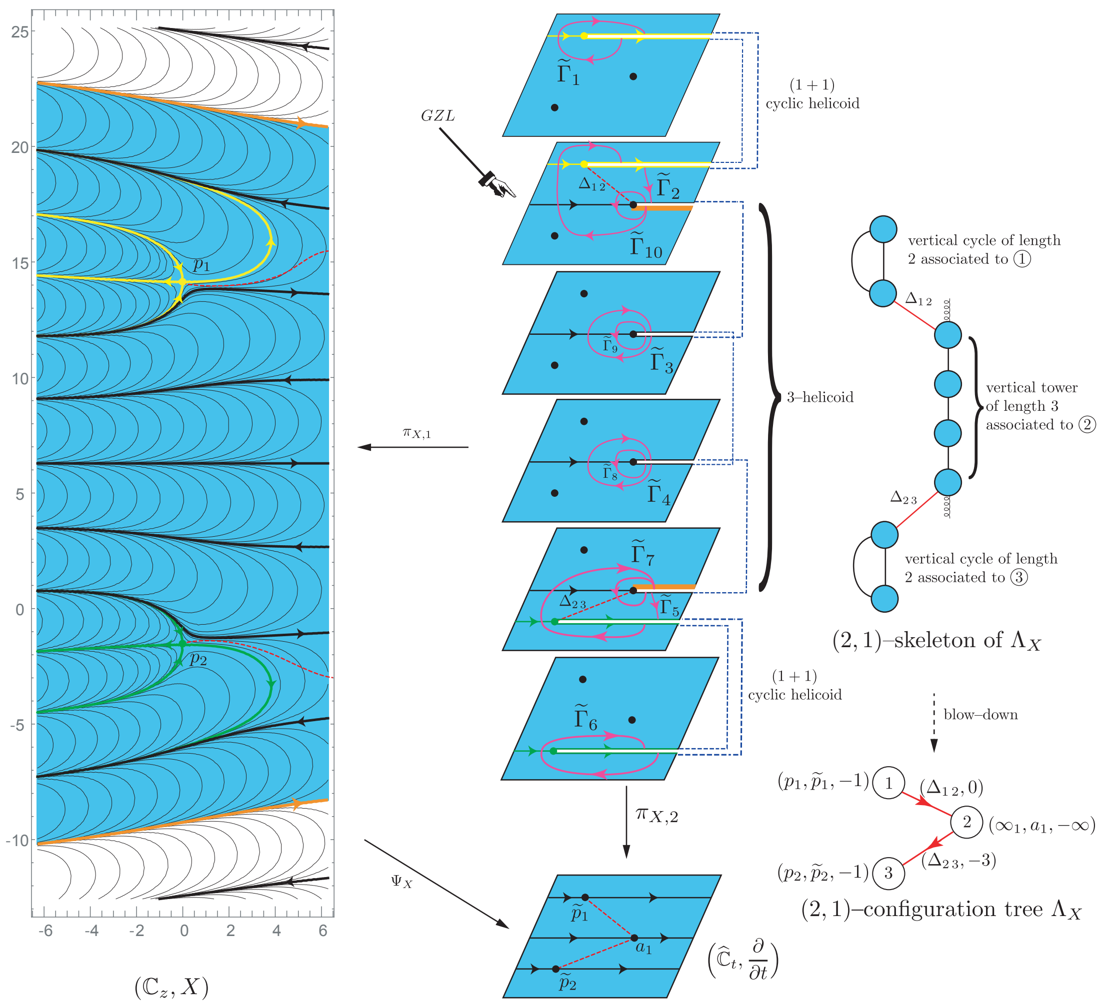

FIGURE 14. **Vector field** $X(z) = \dfrac{e^z}{(z-9i\frac{\pi}{2})(z+i\frac{\pi}{2})}\dfrac{\partial}{\partial z}$ **with essential singularity at** ∞ **and two simple poles at** $p_1 = 9i\frac{\pi}{2}$ **and** $p_2 = -i\frac{\pi}{2}$**.** The Riemann surface $\mathcal{R}_X$ consists of two semi–infinite helicoids, two $(1+1)$–cyclic helicoids and a 3–helicoid. The soul, Definition 9.7, is shaded blue and consists of the Riemann surface $\mathcal{R}_X$ minus the semi–infinite helicoids. The boundary (where the two semi–infinite helicoids should be glued) is coloured orange.

The next examples present (r,d)–configuration trees with more than one weighted edge.

Example 8.7. Consider the vector field

$$X(z) = -\frac{\mathrm{e}^{z^3}}{3z^2}\frac{\partial}{\partial z} \in \mathscr{E}(2,3).$$

If $z_0 = 0$ the distinguished parameter is

$$\Psi_X(z) = \mathrm{e}^{-z^3} - 1.$$

Thus the pole $p_1 = 0$ has order $-\nu_1 = -2$ and critical value $\widetilde{p}_1 = 0$, while the essential singularity at $\infty \in \widehat{\mathbb{C}}_z$ has finite asymptotic value $a_1 = -1$, with multiplicity 3. In order to distinguish each of the three finite asymptotic values, one has to consider the asymptotic path associated to each and see on which of the following exponential tracts each lies in

$$\begin{aligned} U_1(\rho) &= \{z \in \mathbb{C} \mid \arg(z) \in (-\pi/6, \pi/6),\ |z| < R(\rho)\}, \\ U_2(\rho) &= \{z \in \mathbb{C} \mid \arg(z) \in (\pi/2, 5\pi/6),\ |z| < R(\rho)\}, \\ U_3(\rho) &= \{z \in \mathbb{C} \mid \arg(z) \in (7\pi/6, 3\pi/2),\ |z| < R(\rho)\}, \end{aligned} \tag{84}$$

for suitable $R(\rho) > 0$. That is $(\infty_1, -1, -\infty), (\infty_2, -1, -\infty), (\infty_3, -1, -\infty) \in \mathcal{R}_X$ are 3 logarithmic branch points corresponding to the above exponential tracts as in Definition 4.3.
The $(2,3)$–configuration tree has three essential vertices, and one pole vertex. According to Definition 7.7.4, since $r \neq 0$ the root must be the unique pole vertex, so we conveniently label the vertices as follows

$$\begin{array}{rclcrcl} ① = (z_1, t_1, -\nu_1) &=& (p_1, \widetilde{p}_1, -2), && ② = (z_2, t_2, -\nu_2) &=& (\infty_1, a_1, -\infty), \\ ③ = (z_3, t_3, -\nu_3) &=& (\infty_2, a_1, -\infty), && ④ = (z_4, t_4, -\nu_4) &=& (\infty_3, a_1, -\infty). \end{array}$$

In this way the $(2,3)$–configuration tree is

$$\Lambda_X = \Big\{①, ②, ③, ④; ①;\ (\Delta_{1\,2}, 0), (\Delta_{1\,3}, 1), (\Delta_{1\,4}, -1)\Big\}. \tag{85}$$

Once again the edges $\Delta_{1\,2}$, $\Delta_{1\,3}$ and $\Delta_{1\,4}$ correspond to the diagonals/semi–residues between the branch points associated to the corresponding vertices:

$$\begin{aligned} &\Delta_{1\,2} = \int_{p_1}^{\infty_1} \omega_X = a_1 - \widetilde{p}_1 = -1, \quad \Delta_{1\,3} = \int_{p_1}^{\infty_2} \omega_X = a_1 - \widetilde{p}_1 = -1, \\ &\Delta_{1\,4} = \int_{p_1}^{\infty_3} \omega_X = a_1 - \widetilde{p}_1 = -1. \end{aligned} \tag{86}$$

The weight $K(1,2) = 0$ since the branch points corresponding to the root ① and the vertex ② share the same sheet in $\mathcal{R}_X$, $K(1,3) = 1$ since in order to reach the diagonal $\Delta_{1\,3}$ one has to go up one sheet, at the branch point corresponding to ① (*i.e.* $\Delta_{1\,3}$ is one sheet above the diagonal $\Delta_{1\,2}$ in $\mathcal{R}_X$), and $K(1,4) = -1$ since in order to reach the diagonal $\Delta_{1\,4}$ one has to go down one sheet, at the branch point corresponding to ① (*i.e.* $\Delta_{1\,4}$ is one sheet below the diagonal $\Delta_{1\,2}$ in $\mathcal{R}_X$).
Recalling Remark 7.8.2 and the definition of semi–residues (42), note that it is possible to calculate the weights $K(\mathfrak{a}, \mathfrak{r})$ by considering the phase portrait of X: the path of integration from p_1 to ∞_1 stays on the same angular sector about p_1 so $K(1,2) = 0$, the path of integration from ∞_1 to ∞_2 necessarily crosses two angular sectors going counterclockwise around p_1 corresponding to going up a sheet in $\mathcal{R}_X$ so $K(1,3) = 1$, and the path of integration from ∞_1 to ∞_3 crosses two angular sectors going clockwise around p_1 corresponding to going down a sheet in $\mathcal{R}_X$ so $K(1,4) = -1$.
In this case the decomposition, provided by Lemma 7.4, into horizontal subtrees is

$$\Lambda_X = \Lambda_{H(1)} \cup \Lambda_{H(1,3)} \cup \Lambda_{H(1,4)},$$

where

$$\Lambda_{H(1)} = \Big\{①, ②; ⓵; (\Delta_{1\,2}, 0)\Big\}, \qquad \Lambda_{H(1,3)} = \Big\{①, ③; ⓵; (\Delta_{1\,3}, 1)\Big\},$$
$$\Lambda_{H(1,4)} = \Big\{①, ④; ⓵; (\Delta_{1\,4}, -1)\Big\}.$$

See Figure 15 and the left hand side of Figure 17.

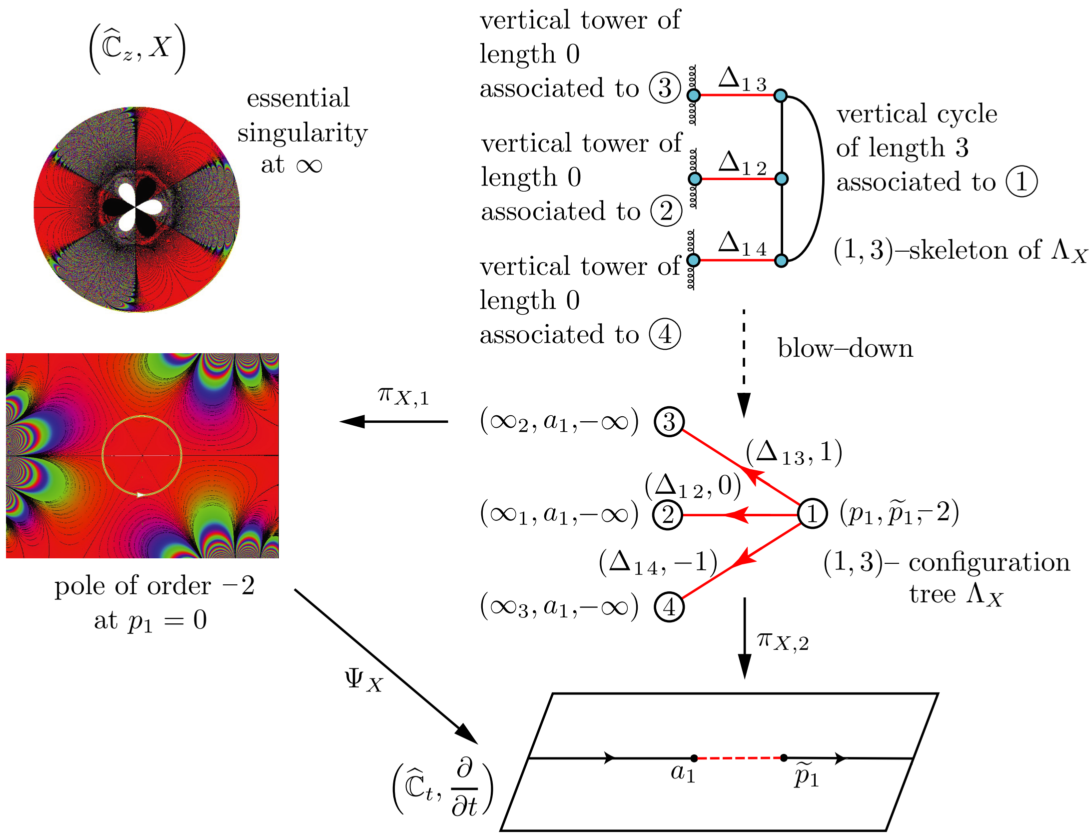

FIGURE 15. **Vector field** $X(z) = -\frac{e^{z^3}}{3z^2}\frac{\partial}{\partial z}$ **with an essential singularity at** ∞ **and pole** $p_1 = 0$ **of order** -2**.** The diagonals $\Delta_{1\,2}$, $\Delta_{1\,3}$ and $\Delta_{1\,4}$, and their projections are shown as red segments. The Riemann surface $\mathcal{R}_X$ is not drawn. See Example 8.7, and §9.2 for the right drawing.

Example 8.8. In a similar vein as the previous example consider the vector field

$$X(z) = \frac{e^{z^3}}{3z^3 - 1}\frac{\partial}{\partial z} \in \mathscr{E}(3,3),$$

with simple poles at $p_1 = \frac{1}{\sqrt[3]{3}}$, $p_2 = \frac{e^{i2\pi/3}}{\sqrt[3]{3}}$, $p_3 = \frac{e^{-i2\pi/3}}{\sqrt[3]{3}}$, and an essential singularity at $\infty \in \widehat{\mathbb{C}}_z$. Its distinguished parameter is

$$\Psi_X(z) = \int_0^z \omega_X = -ze^{-z^3}.$$

Thus the critical values corresponding to the poles are

$$\widetilde{p}_1 = -\frac{1}{\sqrt[3]{3\mathrm{e}}},\ \ \widetilde{p}_2 = -\frac{\mathrm{e}^{i2\pi/3}}{\sqrt[3]{3\mathrm{e}}}\ \text{ and }\ \widetilde{p}_3 = -\frac{\mathrm{e}^{-i2\pi/3}}{\sqrt[3]{3\mathrm{e}}}.$$

The essential singularity at ∞ has $a_1 = 0$ as its finite asymptotic value with multiplicity 3, once again with the same exponential tracts as the previous example, see equation (84), hence $(\infty_1, 0, -\infty), (\infty_2, 0, -\infty), (\infty_3, 0, -\infty) \in \mathcal{R}_X$ are the 3 logarithmic branch points corresponding to the mentioned exponential tracts.

The $(3, 3)$–configuration tree has three essential vertices and three pole vertices, which we label as

$$\begin{array}{lllllll} \text{(87)} & ① = (z_1, t_1, -\nu_1) & = & (p_2, \widetilde{p}_2, -1), & ② = (z_2, t_2, -\nu_2) & = & (p_1, \widetilde{p}_1, -1), \\ & ③ = (z_3, t_3, -\nu_3) & = & (p_3, \widetilde{p}_3, -1), & ④ = (z_4, t_4, -\nu_4) & = & (\infty_1, a_1, -\infty), \\ & ⑤ = (z_5, t_5, -\nu_5) & = & (\infty_2, a_1, -\infty), & ⑥ = (z_6, t_6, -\nu_6) & = & (\infty_3, a_1, -\infty). \end{array}$$

Thus the $(3, 3)$–configuration tree (see Figure 16) is[4]

$$\text{(88)} \qquad \Lambda_X = \Big\{①,②,③,④,⑤,⑥;\circledcirc\!③;\ (\Delta_{3\,6}, 0), (\Delta_{3\,2}, 1), (\Delta_{2\,4}, 1), (\Delta_{4\,1}, 0), (\Delta_{1\,5}, 1)\Big\},$$

with edges given by the diagonals/semi–residues

$$\text{(89)} \qquad \begin{aligned} \Delta_{3\,6} &= \int_{p_3}^{\infty_3} \omega_X = a_1 - \widetilde{p}_3 = \frac{\mathrm{e}^{-i2\pi/3}}{\sqrt[3]{3\mathrm{e}}}, \\ \Delta_{3\,2} &= \int_{p_3}^{p_1} \omega_X = (\widetilde{p}_1 - \widetilde{p}_3) = -\Big(\frac{1 - \mathrm{e}^{-i2\pi/3}}{\sqrt[3]{3\mathrm{e}}}\Big), \\ \Delta_{2\,4} &= \int_{p_1}^{\infty_1} \omega_X = a_1 - \widetilde{p}_1 = \frac{1}{\sqrt[3]{3\mathrm{e}}}, \\ \Delta_{4\,1} &= \int_{\infty_1}^{p_2} \omega_X = \widetilde{p}_2 - a_1 = -\frac{1}{\sqrt[3]{3\mathrm{e}}}\mathrm{e}^{i2\pi/3}, \\ \Delta_{1\,5} &= \int_{p_2}^{\infty_2} \omega_X = a_1 - \widetilde{p}_2 = \frac{\mathrm{e}^{i2\pi/3}}{\sqrt[3]{3\mathrm{e}}}, \end{aligned}$$

and weights $K(3, 6) = 0$, $K(3, 2) = 1$, $K(2, 4) = 1$, $K(4, 1) = 0$, $K(1, 5) = 1$.

Once again it is instructive to examine in detail how these weights are calculated, Figures 16 and 17 will facilitate the discussion.

Consider the phase portrait of X: for the calculation of the weight $K(3, 6) = 0$, consider the projection of the diagonal $\Delta_{3\,6}$ onto $\mathbb{C}_z$, clearly this path remains on one angular sector about p_3 (that corresponds to the exponential tract $U_3(\rho)$ containing $\infty_3 \in \overline{\mathbb{C}}_z$). Thus the logarithmic branch point $(\infty_3, a_1, -\infty)$ and the finitely ramified branch point $(p_3, \widetilde{p}_3, -1)$ share the same sheet on $\mathcal{R}_X$.

Now consider the projection onto $\mathbb{C}_z$ of the diagonals $\Delta_{3\,6}$ and $\Delta_{3\,2}$: the projection of $\Delta_{3\,6}$ lies on the exponential tract $U_3(\rho)$ associated to ∞_3 while the projection of the diagonal $\Delta_{3\,2}$ lies on the strip flow determined by p_1 and p_3. In order to go from the exponential tract $U_3(\rho)$ to the strip flow just mentioned, one must go through three half planes about p_3. This is equivalent to going up (or down) one level on $\mathcal{R}_X$, hence $K(3, 2) = 1$.

Similarly, considering the projections of $\Delta_{3\,2}$ and $\Delta_{2\,4}$ we note that when coming from the pole

[4] The root is ③ so as to agree with the conventions of Definition 7.7.

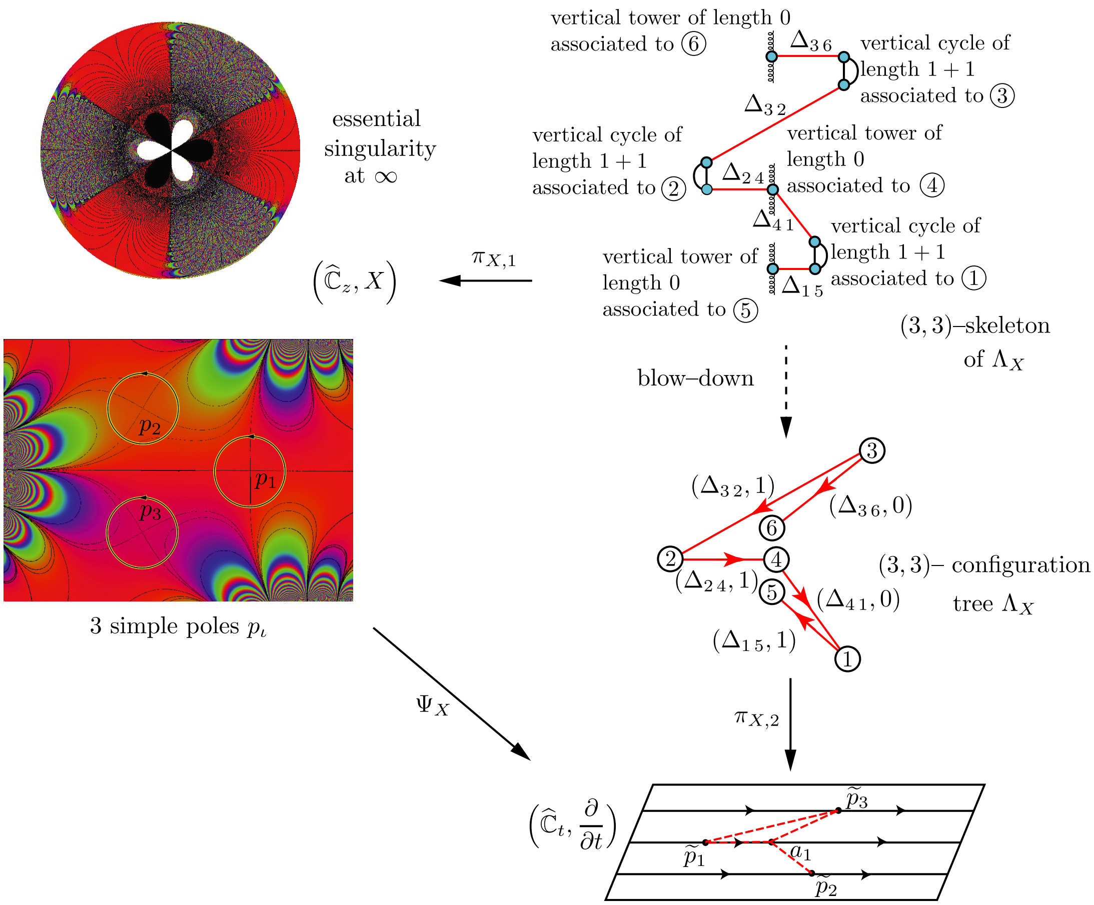

FIGURE 16. **Vector field $X(z) = \dfrac{e^{z^3}}{3z^3-1}\frac{\partial}{\partial z}$ with an essential singularity at ∞ and 3 simple poles p_ι.** The five diagonals and their projections are shown in red. The Riemann surface $\mathcal{R}_X$ is not drawn. See Example 8.8, and §9.2 for the drawing on the right.

p_3 to the pole p_1 and then to ∞_1 contained in $U_1(\rho)$, we go around p_1 and touch upon three half planes (since ∞_1 lies on the real axis), thus $K(2,4) = 1$.

For $K(2,1) = 0$, note that the projection of $\Delta_{4\,1}$ lies entirely within the strip flow determined by p_1 and p_2, thus the logarithmic branch point $(\infty_1, a_1, -\infty)$ and the finitely ramified branch point $(p_2, \widetilde{p}_2, -1)$ share the same sheet on $\mathcal{R}_X$.

Finally, by considering the projections of $\Delta_{4\,1}$ and $\Delta_{1\,5}$, we see that the projection of $\Delta_{1\,5}$ lies on the exponential tract associated to ∞_2 while the projection of the diagonal $\Delta_{4\,1}$ lies on the exponential tract associated to ∞_1. In order to go from one exponential tract to another one must cross at least three angular sectors (but no more than four), this is equivalent to the fact that one must go up or down one level on $\mathcal{R}_X$ to get from the sheet containing $\Delta_{4\,1}$ to the sheet containing $\Delta_{1\,5}$. Hence $K(1,5) = 1$.

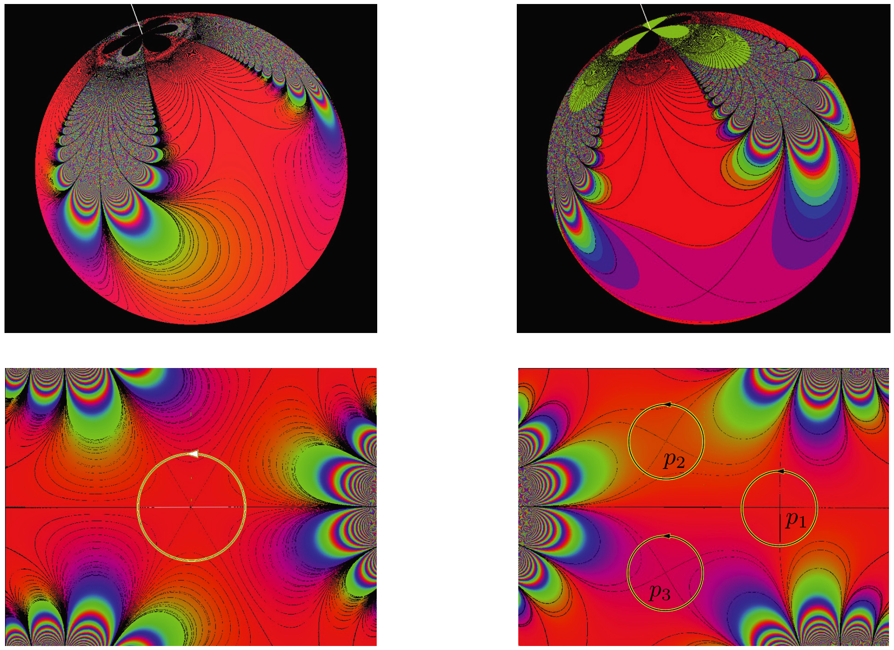

FIGURE 17. **Detail of vector fields in Examples 8.7 and 8.8.** The left hand side shows the vector field $X(z) = -\frac{e^{z^3}}{3z^2}\frac{\partial}{\partial z}$, the right hand side the vector field $X(z) = \frac{e^{z^3}}{3z^3-1}\frac{\partial}{\partial z}$. Each angular sector around the poles corresponds to a half plane on $\mathcal{R}_X$. Note that the dynamics of $\mathfrak{Re}(X)$ in a neighbourhood of $\infty \in \widehat{\mathbb{C}}$ are different. The images contain the information needed to construct the corresponding (r, d)–configuration trees, as explained in the text.

In this case the decomposition, provided by Lemma 7.4, into horizontal subtrees is

$$\Lambda_X = \Lambda_{H(3)} \cup \Lambda_{H(3,2)} \cup \Lambda_{H(2,4)} \cup \Lambda_{H(1,5)},$$

where

$$\Lambda_{H(3)} = \Big\{ ③, ⑥; ③; (\Delta_{3\,6}, 0) \Big\}, \qquad \Lambda_{H(3,2)} = \Big\{ ②, ③; ③; (\Delta_{3\,2}, 1) \Big\},$$
$$\Lambda_{H(2,4)} = \Big\{ ①, ②, ④; ②; (\Delta_{2\,4}, 1)(\Delta_{4\,1}, 0) \Big\}, \quad \Lambda_{H(1,5)} = \Big\{ ①, ⑤; ①; (\Delta_{1\,5}, 1) \Big\}.$$

Example 8.9. Recall Example 4.2, where the vector fields

$$X(z) = \frac{e^{z^d}}{z^r}\frac{\partial}{\partial z} \in \mathscr{E}(r, d), \qquad \text{for } d \geq 1,$$

are approximated by the rational vector fields

$$X_{\mathtt{n}}(z) = \frac{1}{z^r \left(1 - \frac{z^d}{\mathtt{n}}\right)^{\mathtt{n}}}\frac{\partial}{\partial z} \in \mathscr{E}(r + \mathtt{n}d, 0), \qquad \text{for } \mathtt{n} \geq 1.$$

We wish to explore (some of) the (r, d)–configuration trees for X and $X_{\mathtt{n}}$.

First note that the answer will heavily depend on the parameters r and d. For instance, (37) shows that there is only one finite asymptotic value a with multiplicity d (as in Example 8.7) if and only if $r = -1 \pmod{d}$, *i.e.* $(r + 1)/d = k \in \mathbb{N}$.

In this case the unique finite asymptotic value is $a = (k-1)!/d$. Thus $\mathcal{R}_X$ has a branch point $① = (p_1, \widetilde{p_1}, -\nu_1) = (0, 0, -r)$ of ramification index $\nu_1 = r = kd - 1$ and logarithmic branch points $\textcircled{1+\sigma} = (\infty_\sigma, a, -\infty) \in \mathcal{R}_X$, with asymptotic paths $\alpha_\sigma(\tau) = \tau e^{i2\pi\sigma/d}$ for $\sigma = 1, \ldots, d$.
On the other hand the Riemann surfaces $\mathcal{R}_{X_{\mathtt{n}}}$ associated to $X_{\mathtt{n}}(z)$ have a branch point at $① = (p_1, \widetilde{p_1}, -r) = (0, 0, -r)$ of ramification index $r + 1 = kd$ and branch points at

$$\textcircled{1+\sigma}_{\mathtt{n}} = \big(\widehat{e}_\sigma(\mathtt{n}), \widetilde{e}_\sigma(\mathtt{n}), -\mathtt{n}\big) = \big(e^{i2\pi\sigma/d}\mathtt{n}^{1/d}, a\, \mathtt{n}^k \mathtt{n}!/(\mathtt{n}+k)!, -\mathtt{n}\big)$$

of ramification index $\mathtt{n} + 1$, for $\sigma = 1, \ldots, d$. Hence by examining the corresponding phase portraits we can see that the (r, d)–configuration trees are given by

$$\Lambda_{X_{\mathtt{n}}} = \Big\{①, ②_{\mathtt{n}}, \ldots, \textcircled{1+\sigma}_{\mathtt{n}}, \ldots, \textcircled{1+d}_{\mathtt{n}}; \textcircled{①}; \\ (\Delta_{1\,2}, 0), (\Delta_{1\,3}, k), \ldots, \big(\Delta_{1\,(1+\sigma)}, (\sigma-1)k\big), \ldots, \big(\Delta_{1\,(1+d)}, (d-1)k\big)\Big\}, \tag{90}$$

$$\Lambda_X = \Big\{①, ②, \ldots, \textcircled{1+\sigma}, \ldots, \textcircled{1+d}; \textcircled{①}; \\ (\Delta_{1\,2}, 0), (\Delta_{1\,3}, k), \ldots, \big(\Delta_{1\,(1+\sigma)}, (\sigma-1)k\big), \ldots, \big(\Delta_{1\,(1+d)}, (d-1)k\big)\Big\}, \tag{91}$$

whose skeletons are as in Figure 18.

Example 8.10. *A prototypical* $(r, 4)$*–configuration tree.* Consider a vector field

$$X(z) = \frac{e^{E(z)}}{(z-p_1)^{\nu_1}(z-p_2)^{\nu_2}} \frac{\partial}{\partial z}, \quad r = \nu_1 + \nu_2, \tag{92}$$

$E(z)$ a polynomial of degree 4, and $\mathfrak{Im}\,(p_1) > \mathfrak{Im}\,(p_2)$. The singularity at $\infty \in \widehat{\mathbb{C}}_z$ has four finite asymptotic values (∞_1, a_1), (∞_2, a_2), (∞_3, a_2) and (∞_4, a_3); note that two of them differ exclusively by their exponential tract, sharing the asymptotic value $a_2 \in \mathbb{C}_z$. The existence of such a polynomial $E(z)$ will be proved in §9.3, in particular this involves solving the system of equations (45).
The following $(r, 4)$–configuration tree Λ_X, will be used to exemplify some constructions and possible complexities that arise in the proof of the Main Theorem. Thus the $(r, 4)$–configuration tree has three essential vertices and two pole vertices, which we label as follows

$$\begin{aligned} ① &= (p_1, \widetilde{p}_1, -\nu_1), & ② &= (\infty_2, a_2, -\infty), & ③ &= (\infty_1, a_1, -\infty), \\ ④ &= (p_2, \widetilde{p}_2, -\nu_2), & ⑤ &= (\infty_3, a_2, -\infty), & ⑥ &= (\infty_4, a_3, -\infty). \end{aligned} \tag{93}$$

Let

$$\Lambda_X = \Big\{①, ②, ③, ④, ⑤, ⑥; \textcircled{①}; \\ (\Delta_{1\,2}, 0), (\Delta_{1\,5}, -2), \big(\Delta_{2\,3}, K(2,3)\big), \big(\Delta_{2\,4}, K(2,4)\big), \big(\Delta_{2\,6}, K(2,6)\big)\big)\Big\}, \tag{94}$$

with edges given by the diagonals/semi–residues

$$\begin{aligned} \Delta_{1\,2} &= \int_{p_1}^{\infty_2} \omega_X = a_2 - \widetilde{p}_1, & \Delta_{1\,5} &= \int_{p_1}^{\infty_3} \omega_X = a_2 - \widetilde{p}_1, \\ \Delta_{2\,3} &= \int_{\infty_2}^{\infty_1} \omega_X = a_1 - a_2, & \Delta_{2\,4} &= \int_{\infty_2}^{p_2} \omega_X = \widetilde{p}_2 - a_2, \\ \Delta_{2\,6} &= \int_{\infty_2}^{\infty_4} \omega_X = a_3 - a_2, \end{aligned} \tag{95}$$

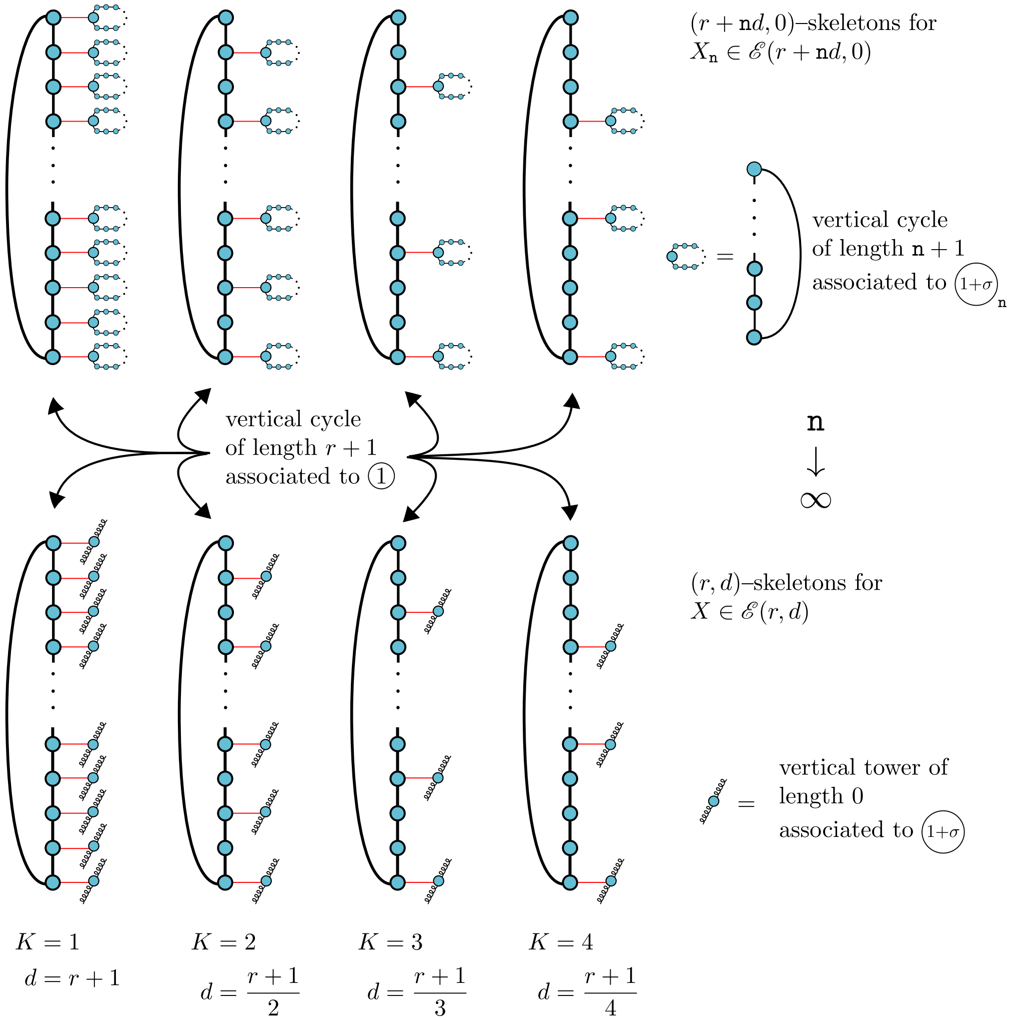

FIGURE 18. Regarding Example 8.9; the top figures are the $(r+\mathtt{n}d,0)$–skeletons for $X_\mathtt{n} \in \mathscr{E}(r+\mathtt{n}d,0)$ approximating $X \in \mathscr{E}(r,d)$, when $r = -1 \pmod d$. Bottom figures are the (r,d)–skeletons for $X \in \mathscr{E}(r,d)$. Note that for $X_\mathtt{n}$ the critical values are 0 and $a\,\mathtt{n}^k\mathtt{n}!/(\mathtt{n}+k)!$ and for X the only critical value is 0 and the only finite asymptotic value is $a = (k-1)!/d$. Further note that $k = (r+1)/d$ is the number of sheets that separate the different diagonals both in $\mathcal{R}_{X_\mathtt{n}}$ and $\mathcal{R}_X$.

and weights $K(1,2) = 0$, $K(1,5) = -2$, $K(2,6) < K(2,4) < K(2,3) \leq -1$. Figure 19 shows the $(r,4)$–configuration tree Λ_X together with the corresponding $(r,4)$–skeleton. This figure will be used as a guide in the proof of the Main Theorem.
In this case the decomposition, provided by Lemma 7.4, into horizontal subtrees is

$$\Lambda_X = \Lambda_{H(1)} \cup \Lambda_{H(1,5)} \cup \Lambda_{H(2,3)} \cup \Lambda_{H(2,4)} \cup \Lambda_{H(2,6)},$$

where

$$\Lambda_{H(1)} = \Big\{ ①, ②; ①; (\Delta_{1\,2}, 0) \Big\}, \qquad \Lambda_{H(1,5)} = \Big\{ ①, ⑤; ①; (\Delta_{1\,5}, -2) \Big\},$$
$$\Lambda_{H(2,3)} = \Big\{ ②, ③; ②; (\Delta_{2\,3}, K(2,3)) \Big\}, \quad \Lambda_{H(2,4)} = \Big\{ ②, ④; ②; (\Delta_{2\,4}, K(2,4)) \Big\},$$
$$\Lambda_{H(2,6)} = \Big\{ ②, ⑥; ②; (\Delta_{2\,6}, K(2,6)) \Big\}.$$

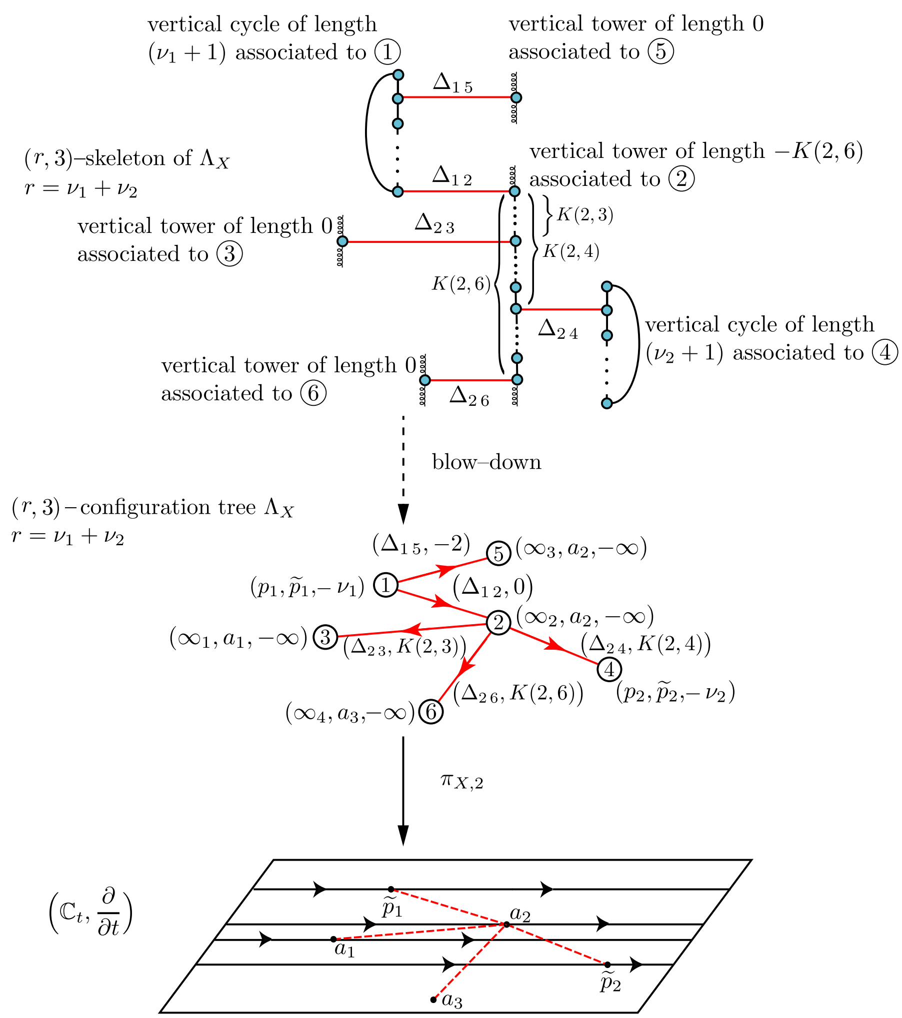

FIGURE 19. **The $(r, 4)$–configuration tree Λ_X and its $(r, 4)$–skeleton corresponding to Example 8.10.** The root is ①, the weight $K(1,2) = 0$ (hence the branch points ①, ② which are the endpoints of the diagonal $\Delta_{1\,2} \subset \mathcal{R}_X$, share the global zero level (GZL) sheet), $K(1,5) = -2 \pmod{\nu_1+1}$, and $K(2,6) < K(2,4) < K(2,3) \leq -1$. The information about how many sheets we have gone "up" or "down" on the Riemann surface is given by the weights. The asymptotic value a_2 has multiplicity 2.

9. Proof of Main Theorem: description of the family $\mathscr{E}(r,d)$ via combinatorial scheme

Plan for proof. Obviously $\mathscr{E}(r,d)$ is a complex manifold of dimension $r+d+1$, see [2] for more general discussion.

The proof of the bijection $\mathscr{E}(r,d) \cong \{[\Lambda_X]\}$ shall proceed as follows:
Note that our Dictionary Proposition 2.5 provides the correspondence between $\mathcal{R}_X$, Ψ_X and $X \in \mathscr{E}(r,d)$.

1) In §9.1 starting from Ψ_X, we construct the (r,d)–configuration tree Λ_X.
2) In §9.2, we start with an abstract (r,d)–configuration tree Λ_X, Definition 7.7, and construct the (r,d)–skeleton of Λ_X (as an associated combinatorial object).
3) In §9.3 from the (r,d)–skeleton of Λ_X, we proceed to construct a Riemann surface $\mathcal{R}_X$ in $\mathscr{E}(r,d)$.
4) The suitable equivalence class $[\Lambda_X]$ of (r,d)–configuration trees Λ_X will be explained in §9.4.

9.1. From $X \in \mathscr{E}(r,d)$ to an (r,d)–configuration tree Λ_X.

Recalling Definition 7.7 of (r,d)–configuration tree, we have:
• The trivial case: Ψ_X *has exactly one finite asymptotic or critical value:*
From Lemma 5.3, only the following two cases are possible,
1) $X(z) = \frac{\mu}{(z-p_1)^r}\frac{\partial}{\partial z}$, *i.e.* $(r,d)=(r,0)$, or
2) $X(z) = \mu^{-1}\mathrm{e}^z\frac{\partial}{\partial z}$, *i.e.* $(r,d)=(0,1)$,
where $p_1 \in \mathbb{C}_z$ and $\mu \neq 0$.
For (1), $\Lambda_X = \left\{ ① = (p_1, \widetilde{p}_1, -r); ①; \varnothing \right\}$, see Example 8.1.
For (2), $\Lambda_X = \left\{ ① = (\infty_1, a_1, -\infty); ①; \varnothing \right\}$, see Example 8.3.
• The non–trivial case: Ψ_X *has two or more finite asymptotic or critical values, i.e.* $d+n \geq 2$*:*
Considering the surface $\mathcal{R}_X$, recall Equation (31) and the reduced divisor, Definition 5.1.

1. Vertices of Λ_X. Let the vertices be those obtained from the reduced divisor of X,

$$V = \left\{ \textcircled{\iota} = \big(p_\iota, \widetilde{p}_\iota, -\nu_\iota\big) \right\}_{\iota=1}^{n} \cup \left\{ \textcircled{n+\sigma} = \big(\infty_\sigma, a_\sigma, -\infty\big) \right\}_{\sigma=1}^{d} \tag{96}$$
$$= \left\{ \textcircled{\mathfrak{a}} = \big(z_\mathfrak{a}, t_\mathfrak{a}, -\nu_\mathfrak{a}\big) \right\}_{\mathfrak{a}=1}^{n+d}.$$

There are $n+d$ vertices.
Note that the essential vertices $\textcircled{n+\sigma}$ are labelled as in Remark 4.6.2, that is according to the natural counterclockwise cyclic order of the exponential tracts in a small circle about $\infty \in \widehat{\mathbb{C}}_z$.
Root choice:
If $r=0$ let the root be $\textcircled{\varrho} \doteq ① = \big(\infty_1, a_1, -\infty\big)$.
If $r \neq 0$ let the vertex $\big(p_\varrho, \widetilde{p}_\varrho, -\nu_\varrho\big)$ be such that $\mathfrak{Im}\,(\widetilde{p}_\varrho) \geq \mathfrak{Im}\,(\widetilde{p}_\iota)$ and $\mathfrak{Re}\,(\widetilde{p}_\varrho) \leq \mathfrak{Re}\,(\widetilde{p}_\iota)$ for $1 \leq \iota \leq n$; *i.e.* $\widetilde{p}_\varrho \in \mathbb{C}_t$ is the top & left–most critical value, following the root condition in Definition 7.7. In this case, choose the root to be $\textcircled{\varrho} \doteq \big(p_\varrho, \widetilde{p}_\varrho, -\nu_\varrho\big)$.

2. Edges of Λ_X. From Definition 5.4, the diagonals, associated to different pairs $t_\mathfrak{a}, t_\mathfrak{r}$ of finite asymptotic or critical values, are *oriented* segments

$$\Delta_{\mathfrak{a}\mathfrak{r}} = \overline{(z_\mathfrak{a}, t_\mathfrak{a}, -\nu_\mathfrak{a})(z_\mathfrak{r}, t_\mathfrak{r}, -\nu_\mathfrak{r})} \quad \text{in } \mathcal{R}_X,$$

whose endpoints project down, via π_2, to the finite asymptotic or critical values $t_\mathfrak{a}$, $t_\mathfrak{r}$. From Lemma 5.6 it follows that there are at least two[5] diagonals associated to each finite asymptotic

[5] This is so because diagonals are oriented.

or critical value. As a first step, we ignore orientation and consider the diagonals as undirected edges[6], which without loss of generality we shall simply denote by $E = \{\Delta_{\mathfrak{ar}}\}$. In this way we obtain a connected graph, say $G = \{V; E\}$.

A subgraph formed by the set of vertices associated to branch points that share the same sheet in $\mathcal{R}_X$ will be called a *horizontal subgraph.* Note that each horizontal subgraph, consisting of the vertices (branch points) sharing a same sheet of $\mathcal{R}_X$, say $\{\textcircled{\ell} = (z_\ell, t_\ell, -\nu_\ell)\}_{\ell=1}^{s}$ together with the corresponding set of edges (undirected diagonals) on the same sheet, forms a complete graph K_s with $s(s-1)$ edges. Moreover, by eliminating appropriate edges from K_s we can always obtain an (undirected) left–right–top–bottom linear tree of vertices $\{\textcircled{\ell} = (z_\ell, t_\ell, -\nu_\ell)\}_{\ell=1}^{s}$, recall Definition 7.6.

Now replace each of the horizontal subgraphs of G by the corresponding (undirected) left–right–top–bottom linear tree. As a consequence, the diagonals $\Delta_{\mathfrak{ar}}$ and finite height horizontal strips

$$\Big(\big\{\mathfrak{Im}\,(t_{\mathfrak{a}}) \leq \mathfrak{Im}\,(t) \leq \mathfrak{Im}\,(t_{\mathfrak{r}})\big\}, \frac{\partial}{\partial t}\Big) \subset \mathcal{R}_X$$

are in bijective correspondence, as in Lemma 5.9.2–3.

This produces a connected (undirected) graph $\overline{\Lambda}_X$ whose horizontal subgraphs are (undirected) left–right–top–bottom linear subtrees. The next lemma shows its shape.

Lemma 9.1. *If $X \in \mathscr{E}(r, d)$ then the graph $\overline{\Lambda}_X$ is a tree.*

Proof. Recall the decomposition of $\mathbb{C}_z$ in half planes and finite height horizontal strips, Lemma 5.9.

Assume that all the asymptotic and critical values $t_{\mathfrak{a}}$, associated to the branch points $(z_{\mathfrak{a}}, t_{\mathfrak{a}})$, lie on different horizontal trajectories of $(\mathbb{C}_t, \frac{\partial}{\partial t})$ (we leave the general case for the interested reader, see for instance the discussion preceding Proposition 9.9).

Note that the intersection of the interior of any two finite height horizontal strips is empty.

Since $\mathbb{C}_z$ is simply connected and each diagonal determines a finite height horizontal strip, there is no loop/cycle of diagonals. □

Finally, assign an orientation to $\overline{\Lambda}_X$ by choosing the appropriate orientation so that the edges point away from the root vertex $\textcircled{\varrho}$.

We thus obtain a non–weighted, directed rooted tree

$$\Big\{\big\{\textcircled{\mathfrak{a}} = \big(z_{\mathfrak{a}}, t_{\mathfrak{a}}, -\nu_{\mathfrak{a}}\big)\big\}_{\mathfrak{a}=1}^{d+n}; \textcircled{\varrho}; \big\{\Delta_{\mathfrak{ar}}\big\}\Big\}, \tag{97}$$

satisfying conditions (1–6) of Definition 7.7.

By simple inspection, it is clear that each diagonal in (97) falls into one of the cases mentioned in Remark 5.5.

3. Weights of Λ_X. At this point of the description of the surface $\mathcal{R}_X$, branch points and the diagonals between them are in correspondence with vertices of a non–weighted tree and its edges, respectively. However, as mentioned in Remark 5.19, an important part of the description of the Riemann surface $\mathcal{R}_X$ as a pasting of geometric pieces, corresponds to the number of sheets in $\mathcal{R}_X$ that separate the diagonals (pairwise). Recalling that in a rooted tree there is a unique (simple) path from each vertex to the root, allows us to assign a weight to each edge/diagonal of the tree.

As an aid, the reader can follow the construction by considering Example 8.10. [We will include such references inside square brackets.]

For the assignment of weights $\{K(\mathfrak{a}, \mathfrak{r})\}$ to the edges $\{\Delta_{\mathfrak{ar}}\}$ we shall proceed by induction on the depth of the vertices as follows.

[6] We agree to leave only one undirected edge for each pair of oriented edges.

a) We start by considering the vertices contiguous to the root $\circledcirc{\varrho}$ (*i.e.* vertices of depth 1 in (97)), say $\{\textcircled{\mathfrak{z}}\}$. Since all the branch points corresponding to $\{\textcircled{\mathfrak{z}}\}$ share a sheet with the branch point corresponding to the root $\circledcirc{\varrho}$, any of the corresponding edges can be assigned a weight zero. Choose one, say $\textcircled{\mathfrak{z}_0}$, and assign the weight $K(\varrho, \mathfrak{z}_0) = 0$ to the edge $\Delta_{\varrho\mathfrak{z}_0}$ and call this sheet in $\mathcal{R}_X$ the *global zero level (GZL)* sheet.
If there are more vertices in $\{\textcircled{\mathfrak{z}}\}$ whose branch points share the global zero level sheet, then the corresponding edges are also assigned the weight 0.
[Referring to Example 8.10, our first edge is $\Delta_{1\,2}$ with weight $K(1, 2) = 0$; note that the diagonal is as in case (3) of Remark 5.5. Moreover, there are no more vertices sharing the GZL sheet.]

b) Now consider the vertices of depth 1 that do not share the GZL sheet, say $\{\textcircled{\mathfrak{r}}\} \subset \{\textcircled{\mathfrak{z}}\}$. For each of these vertices consider their edge $\Delta_{\varrho\mathfrak{r}}$: we assign the weight $K(\varrho, \mathfrak{r})$ such that

$$2\pi K(\varrho, \mathfrak{r}) \text{ is the } \textit{argument between the sheets containing } \Delta_{\varrho\mathfrak{z}_0} \textit{ and } \Delta_{\varrho\mathfrak{r}}.$$

[Referring to Example 8.10, the vertex of depth 1 not sharing the GZL sheet is $\textcircled{5}$. In this case the weight $K(1, 5) = -2 \pmod{\nu_1 + 1}$.]
If (97) has only vertices contiguous to the root $\circledcirc{\varrho}$, then we have completed the construction of Λ_X.

c) We now consider the set of vertices of depth 2. Of course there is an edge from a vertex of depth 1, say $\textcircled{\mathfrak{z}}$ to a vertex of depth 2, say $\textcircled{\mathfrak{a}}$. The associated weight for the edge $\Delta_{\mathfrak{z}\mathfrak{a}}$ is defined as $K(\mathfrak{z}, \mathfrak{a})$ such that

$$2\pi K(\mathfrak{z}, \mathfrak{a}) \text{ is the } \textit{argument between the sheets containing } \Delta_{1\mathfrak{z}} \textit{ and } \Delta_{\mathfrak{z}\mathfrak{a}}.$$

d) Continue the assignment of weights as in (c) for all the edges that contain vertices of depth 2.
[Referring to Example 8.10, the weight $K(2, 3) \leq -1$ since on $\mathcal{R}_X$ the diagonal $\Delta_{2\,3}$ is $|K(2, 3)|$ sheets below the diagonal $\Delta_{1\,2}$; similarly the weight $K(2, 4) \leq -2$, since on $\mathcal{R}_X$ the diagonal $\Delta_{2\,4}$ is $|K(2, 4)|$ sheets below the diagonal $\Delta_{1\,2}$.]

e) Repeat (c) and (d) with vertices of depth ≥ 3, assigning the weights until all the vertices are exhausted.
[Referring to Example 8.10, the last edge to be considered is $\Delta_{3\,5}$ with corresponding weight $K(3, 5) = -2$.]

We have thus constructed an (r, d)–configuration tree

$$\Lambda_X = \Big\{ \big\{ \textcircled{\mathfrak{a}} = \big(z_{\mathfrak{a}}, t_{\mathfrak{a}}, -\nu_{\mathfrak{a}}\big) \big\}_{\mathfrak{a}=1}^{d+n}; \circledcirc{\varrho}; \big\{ (\Delta_{\mathfrak{a}\mathfrak{r}},\ K(\mathfrak{a}, \mathfrak{r})) \big\} \Big\} \tag{98}$$

associated to Ψ_X.

Remark 9.2. [Remark 5.19 revisited.] The integer weight $K(\mathfrak{a}, \mathfrak{r})$ associated to the edge $\Delta_{\mathfrak{a}\mathfrak{r}}$ can be incorporated into a continuous "edge" by considering

$$\widetilde{\Delta}_{\mathfrak{a}\mathfrak{r}} \doteq \Delta_{\mathfrak{a}\mathfrak{r}} \mathrm{e}^{i2\pi K(\mathfrak{a},\mathfrak{r})} \in \widetilde{\mathbb{C}^*},$$

where $\widetilde{\mathbb{C}^*} = \{|z|\, \mathrm{e}^{i \arg(z)}\}$ is the universal cover of $\mathbb{C}^*$ and $\arg(z)$ is the multivalued argument. This will provide the compatibility of "continuous coordinates/parameters" for the manifold structure of $\mathscr{E}(r, d)$.

9.2. **From an (r, d)–configuration tree Λ_X to the (r, d)–skeleton of Λ_X.** Let Λ_X be an abstract (r, d)–configuration tree as in Definition 7.7. We want to show the existence of a vector field X. In order to achieve this goal, we construct the (r, d)*–skeleton of* Λ_X (as a certain *"blow–up"* of Λ_X, see Definition 9.5).

The (r, d)*–skeleton of* Λ_X will contain the same information as Λ_X.

a) With the disadvantage of being more cumbersome to express.
b) With the advantage that it will enable us to identify the equivalence classes of Λ_X in §9.4.
c) Also note that the (r, d)–skeleton of Λ_X describes the "embedding" of Λ_X in $\overline{\mathbb{C}}_z \times \mathbb{C}_t$.

Figure 19 presents a particular example that will help the reader follow the construction.

A priori, Λ_X has two types of vertices: essential vertices $(n+\sigma) = (\infty_\sigma, a_\sigma, -\infty)$ and pole vertices $(\iota) = (p_\iota, \widetilde{p}_\iota, -\nu_\iota)$.

Before proceeding to the construction of the (r, d)–skeleton of Λ_X, we shall need the following two definitions/constructions.

Associated to the pole vertices, recalling Definition 5.17, the following construction is natural. See right hand side of Figures 4.c, 7, 8 and the blow up of vertices (1) and (4) in Figure 19.

Remark 9.3. For each pole vertex $(\iota) = (p_\iota, \widetilde{p}_\iota, -\nu_\iota)$ of Λ_X, the

vertical cycle of length $\nu_\iota + 1$ associated to (ι)

is a cyclic graph consisting of exactly $\nu_\iota + 1$ copies of the vertex (ι) joined by $\nu_\iota + 1$ vertical edges (without weights). The vertices on the vertical cycle are also assigned a local level: in this case arithmetic modulo $(\nu_\iota + 1)$ is to be used.

The vertical cycle of length $\nu_\iota + 1$ will only have vertices of valence 2. Once again, call one direction of the vertical cycle *up* and the other direction *down*. To be precise, up corresponds to the anti–clockwise direction of $\beta(\theta) = \pi_2^{-1}\big(t_{\mathfrak{a}} + \rho\, \mathrm{e}^{i2\pi\theta}\big)$ considered in Remark 5.19.2.

Similarly, associated to essential vertices, recalling Definition 5.15, the following construction is natural.

Remark 9.4. For each essential vertex $(n+\sigma) = (\infty_\sigma, a_\sigma, -\infty)$, of Λ_X, let

$$K_{\max}(\sigma) = \max_{\mathfrak{r}}\{0, K(\sigma, \mathfrak{r})\} \quad \text{and} \quad K_{\min}(\sigma) = \min_{\mathfrak{r}}\{0, K(\sigma, \mathfrak{r})\},$$

where the maximum and minimum are taken over all the edges that start at $(n+\sigma)$ and end at the respective $\{(\mathfrak{r})\}$. Then by letting

$$K(\sigma) \doteq K_{\max}(\sigma) - K_{\min}(\sigma)$$

we shall say that the

vertical tower of length $K(\sigma)$ associated to $(n+\sigma)$

is a linear graph consisting of exactly $K(\sigma) + 1 \geq 1$ copies of the vertex $(n+\sigma)$ joined by $K(\sigma)$ *vertical edges* (without weights). Each of the vertices of the vertical tower will have a *local level* assigned to it: the local level assigned to the first vertex of the vertical tower will be $K_{\min}(\sigma)$, the local level assigned to the second vertex of the vertical tower will be $K_{\min}(\sigma)+1$, continuing in this way the local level assigned to the last vertex of the vertical tower will be $K_{\max}(\sigma)$. We shall call the increasing direction, using $\beta(\theta) = \pi_2^{-1}\big(t_{\mathfrak{a}} + \rho\, \mathrm{e}^{i2\pi\theta}\big)$, of the local level *up* and the decreasing direction *down*.

The vertical tower will have vertices of valence 1 at the extreme local levels $K_{\min}(\sigma)$ and $K_{\max}(\sigma)$, otherwise of valence 2.

On the right hand side of Figure 4.b a simple example of a vertical tower is presented. However in Example 8.10 and Figure 19 a more complex $(r, 4)$–skeleton is shown: vertex $(2) \in \Lambda_X$ blows up into the vertical tower of length $-K(2, 6)$. Moreover,

the local zero level is assigned to the vertex where the edge $\Delta_{1\,2}$ is attached;
the local $K(2, 3) \leq -1$ level is assigned to the vertex where the edge $\Delta_{2\,3}$ is attached;
the local $K(2, 4) \leq -2$ level is assigned to the vertex where the edge $\Delta_{2\,4}$ is attached; and
the local $K(2, 6) \leq -3$ level is assigned to the vertex where the edge $\Delta_{2\,6}$ is attached.

We can now define the associated combinatorial object.

Definition 9.5. Let Λ_X be an (r,d)–configuration tree. The (r,d)*–skeleton of* Λ_X is the undirected graph obtained by:

a) Replacing each essential and pole vertices $\textcircled{\mathfrak{a}} = (z_{\mathfrak{a}}, t_{\mathfrak{a}}, -\nu_{\mathfrak{a}}) \in \Lambda_X$, with their associated vertical tower or vertical cycle respectively.

b) For each directed weighted edge, $(\Delta_{\mathfrak{a}\mathfrak{r}}, K(\mathfrak{a},\mathfrak{r})) \in \Lambda_X$, eliminate the weight and consider it an undirected *horizontal edge* $\pm\Delta_{\mathfrak{a}\mathfrak{r}}$.

c) The undirected $\pm\Delta_{\mathfrak{a}\mathfrak{r}}$ edge is to have as its ends the local level 0 vertex of the vertical tower or vertical cycle associated to $\textcircled{\mathfrak{r}}$, and the local level $K(\mathfrak{a},\mathfrak{r})$ vertex of the vertical tower or vertical cycle associated to $\textcircled{\mathfrak{a}}$; noting that if $\textcircled{\mathfrak{a}}$ is a pole vertex, modular arithmetic is to be used.

Remark 9.6. The (r,d)–skeleton of Λ_X has the following properties (also see Diagram 99):

1. The edges of the (r,d)–skeleton of Λ_X are divided in two sets:
   • the vertical edges (alluded to in Definitions 9.4 and 9.3 above), and
   • the *horizontal edges* $\pm\Delta_{\mathfrak{a}\mathfrak{r}}$, which form a finite set of connected subtrees, that correspond precisely to the horizontal subtrees of the (r,d)–configuration tree Λ_X (recall Definition 7.7.7).
2. Consider two horizontal edges $\Delta_{\mathfrak{z}\mathfrak{a}}$ and $\Delta_{\mathfrak{a}\mathfrak{r}}$ in the (r,d)–skeleton of Λ_X that share the vertex $\textcircled{\mathfrak{a}}$ in the original (r,d)–configuration tree Λ_X. We shall say that:
   In the (r,d)–skeleton of Λ_X, the (horizontal) edge $\Delta_{\mathfrak{a}\mathfrak{r}}$, relative to
   the (horizontal) edge $\Delta_{\mathfrak{z}\mathfrak{a}}$, is $\begin{cases} \text{at the } \textit{same (global) level} \text{ if } K(\mathfrak{a},\mathfrak{r}) = 0, \\ K(\mathfrak{a},\mathfrak{r}) \text{ levels } \textit{up} \text{ if } K(\mathfrak{a},\mathfrak{r}) > 0, \\ K(\mathfrak{a},\mathfrak{r}) \text{ levels } \textit{down} \text{ if } K(\mathfrak{a},\mathfrak{r}) < 0. \end{cases}$
   Hence, using geometry and combinatorics, $K(\mathfrak{a},\mathfrak{r})$ can be recognized as
   · the number of sheets in $\mathcal{R}_X$ separating the diagonals $\Delta_{\mathfrak{z}\mathfrak{a}}$ and $\Delta_{\mathfrak{a}\mathfrak{r}}$, or equivalently
   · the number of levels in the (r,d)–skeleton of Λ_X separating the edges $\Delta_{\mathfrak{z}\mathfrak{a}}$ and $\Delta_{\mathfrak{a}\mathfrak{r}}$.
3. Note that even though one can recognize which is the global zero level (GZL) sheet on the (r,d)–skeleton of Λ_X, this is a property inherited from Λ_X: it is not intrinsic to the (r,d)–skeleton.
4. Roughly speaking, the (r,d)–configuration tree Λ_X is a *blow–down* of the (r,d)–skeleton of Λ_X, see Diagram 99 and Figure 19 for an example.

9.3. **From the (r,d)–skeleton of Λ_X to a Riemann surface $\mathcal{R}_X$.** We proceed in two steps: In the first step, from the (r,d)–skeleton of Λ_X we will construct a connected Riemann surface with boundary, the (r,d)–soul of Λ_X (see Definition 9.7).
As the second and final step, we shall glue $2d$ semi-infinite helicoids on the boundaries of the (r,d)–soul of Λ_X to obtain the simply connected Riemann surface $\mathcal{R}_X$ (without boundary).

Definition 9.7. Given an (r,d)–skeleton of Λ_X as above, the associated (r,d)*–soul of* Λ_X is a flat Riemann surface

1) constructed from the gluing of half planes $(\mathbb{H}^2_{\pm}, \frac{\partial}{\partial t})$ and finite height horizontal strips

$$\big(\{0 < \mathfrak{Im}\,(z) < h\}, \frac{\partial}{\partial t}\big),$$

2) having two families of cone points:

a) the first with n conic points $\{(p_\iota, \widetilde{p}_\iota)\}_{\iota=1}^{n}$ each with cone angle $2(\nu_\iota + 1)\pi$ and $r = \sum_\iota \nu_\iota$,

b) the second with d conic points $\{(z_\sigma, a_\sigma)\}_{\sigma=1}^{d}$ each with cone angle $2\big(K(\sigma)+1\big)\pi$, $K(\sigma) \geq 0$,

3) d horizontal branch cuts starting at the cone points of the second family.

The branch cuts determine the boundary of the (r,d)–soul, $2d$ horizontal boundaries, recall Equation (43).

Remark 9.8. For $X \in \mathscr{E}(r,d)$, the (r,d)–soul of Λ_X is a simply connected Riemann surface with boundary. The boundary consists of the $2d$ horizontal segments $\{[a_\sigma,\infty)_- \cup\ [a_\sigma,\infty)_+\}$. Furthermore, it has two families of cone points:

a) n cone points $\{(p_\iota,\widetilde{p}_\iota)\}_{\iota=1}^n$ with cone angles $\{2(\nu_\iota+1)\pi\}_{\iota=1}^n$. Each of these cone point corresponds to a vertical cycle of the (r,d)–skeleton. Hence each of these cone points is equivalent to a pole p_ι of X of order $-\nu_\iota$.

b) d cone points $\{(\infty_\sigma,a_\sigma)\}_{\sigma=1}^d$ each with cone angle $2\big(K(\sigma)+1\big)\pi$. Each of these cone points corresponds to a vertical tower of the (r,d)–skeleton. These cone points are associated to X via the logarithmic branch points of Ψ_X^{-1}.

1. Construction of the (r,d)–*soul of* Λ_X from the (r,d)–*skeleton of* Λ_X.

From Remark 9.6.2, we see that the (r,d)–skeleton of Λ_X has two types of vertices: those that do not share horizontal edges and those that share horizontal edges (the vertices that belong to a horizontal subtree).

Generic horizontal subtrees assumption. For simplicity, let us first assume that on any given horizontal subtree the asymptotic and critical values, associated to the vertices of the horizontal subtree, all lie on different horizontal trajectories of $(\mathbb{C}_t,\frac{\partial}{\partial t})$. Figure 12 illustrates this assumption.

Starting from the (r,d)–skeleton of Λ_X consider the following construction.

a) Replace each vertex[7] of the (r,d)–skeleton of Λ_X that does not share a horizontal edge with a sheet $\mathbb{C}_t\backslash L_{\mathfrak{a}}$.

b) Given a horizontal subtree with s vertices, say $\big\{\mathfrak{a}_1,\dots,\mathfrak{a}_s\big\}$, replace the given horizontal subtree with a sheet
$$\mathbb{C}_t\backslash\{L_{\mathfrak{a}_\ell}\}_{\ell=1}^s,$$
where each $L_{\mathfrak{a}_\ell}$ is the horizontal branch cut associated to the vertex $\mathfrak{a}_\ell$, recall Equation (43).
By the generic horizontal subtrees assumption, all the values $\{t_{\mathfrak{a}_\ell}\}$ lie on different horizontal trajectories of $\frac{\partial}{\partial t}$, then none of the horizontal branch cuts $L_{\mathfrak{a}_\ell}$ intersect in $\mathbb{C}_t$.
Continue this replacement process for every horizontal subtree.
Note that we obtain stacked copies of $\mathbb{C}_t\backslash L_{\mathfrak{a}}$ and $\mathbb{C}_t\backslash\{L_{\mathfrak{a}_\ell}\}_{\ell=1}^s$, but they retain their relative position respect to the (r,d)–skeleton of Λ_X, by the fact that we still have not removed the vertical edges of the d–skeleton of Λ_X.

c) We now replace the vertical towers and vertical cycles in the (r,d)–skeleton of Λ_X with $|K|$–helicoids or $(\nu+1)$–cyclic helicoids respectively (recall Definitions 5.15 and 5.17). On each vertical tower or vertical cycle, say the one associated to the vertex $\mathfrak{a}$, apply Corollary 5.8 to glue the horizontal branch cuts by alternating the boundaries of $\mathbb{C}_t\backslash L_{\mathfrak{a}}$; so as to form finite helicoids or cyclic helicoids over the vertex $\mathfrak{a}$, making sure that all the finite helicoids go up when turning counter–clockwise around the vertex.
In the case where a vertical tower is involved, the finite helicoid has two boundaries consisting of $[t_{\mathfrak{a}},\infty)_+$ and $[t_{\mathfrak{a}},\infty)_-$; in the case where a vertical cycle is involved we obtain a cyclic helicoid, that is a finite helicoid whose boundaries have been identified/glued.

Non–generic (degenerate) horizontal subtrees. We now turn our attention to the particular case when on some horizontal subtree there are at least two asymptotic or critical values $\{t_{\mathfrak{a}}\}_{\mathfrak{a}=1}^{d+n}\subset(\mathbb{C},\frac{\partial}{\partial t})$ arising from the vertices $\mathfrak{a}$, that lie on the same horizontal trajectory of $\frac{\partial}{\partial t}$. Since there are only a finite set of asymptotic or critical values, then for any small enough angle

[7] Recall that all the vertices of the (r,d)–skeleton of Λ_X are either the vertices $\mathfrak{a}$ of the original (r,d)–configuration tree Λ_X, or copies of them. Thus any vertex in the (r,d)–skeleton of Λ_X projects to a unique vertex on Λ_X.

$\theta > 0$, the set of values $\{t_{\mathfrak{a}}\} \subset (\mathbb{C}, \mathrm{e}^{i\theta}\frac{\partial}{\partial t})$ lie on $m+n$ different trajectories of the rotated vector field $\mathfrak{Re}\left(\mathrm{e}^{i\theta}\frac{\partial}{\partial t}\right)$. Proceed with the construction (a)–(e) as above but using $\mathrm{e}^{i\theta}L_{\mathfrak{a}}$ instead of $L_{\mathfrak{a}}$ for the construction. Note that for small enough $\theta > 0$ all the surfaces obtained are homeomorphic. Finally let $\theta \to 0^+$ and consider the limiting surface.

According to Definition 9.7 we have:

Proposition 9.9. *Every Λ_X has a canonically associated (r,d)–soul.*

Proof. The (r,d)*–soul of the* (r,d)*–configuration tree* Λ_X is the Riemann surface with boundary, described by (a)–(c) above. ☐

Example 9.1. The (r,d)–soul is shaded blue in all the figures.
1) $X \in \mathscr{E}(r,0)$, so Ψ_X is a polynomial, in which case the $(r,0)$–soul of Λ_X is $\mathcal{R}_X$. See Figure 8.
2) $X(z) = \mathrm{e}^z\frac{\partial}{\partial z} \in \mathscr{E}(0,1)$, so Ψ_X is an exponential, in which case the $(0,1)$–soul of Λ_X consists of $\mathbb{C}_t \backslash L_1$, a single sheet with exactly one branch cut. See Figure 11 and figure 11.a in [1].
3) $X(z) = \mathrm{e}^{z^2}\frac{\partial}{\partial z} \in \mathscr{E}(0,2)$, so Ψ_X is the error function, in which case the $(0,2)$–soul of Λ_X consists of $\mathbb{C}_t \backslash (L_1 \cup L_2)$, a single sheet with exactly two branch cuts. See Figure 22 and figure 11.b in [1].
4) An (r,d)–configuration tree has all $K(\mathfrak{a},\mathfrak{r}) \equiv 0$ if and only if on the corresponding Riemann surface $\mathcal{R}_X$ all the diagonals share the same sheet $\mathbb{C}_t \backslash \{L_{\mathfrak{a}}\}_{\mathfrak{a}=1}^{d+n}$. In this case the (r,d)–soul of Λ_X is this sheet. See Figure 12.b.

2. Construction of $\mathcal{R}_X$ from the (r,d)–soul of Λ_X. To each of the $2d$ boundaries of the (r,d)–soul of Λ_X, glue a semi–infinite helicoid to obtain a simply connected Riemann surface $\mathcal{R}_X$. This surface has exactly:
d logarithmic branch points of Ψ_X^{-1} over d finite asymptotic values of Ψ_X, and
n finitely ramified branch points with ramification indices that add up to $r+n$.

We can recognize that our isometric glueing Corollary 5.8 in the above cases coincides with the Maskit surgery as is defined by M. Taniguchi [45] p. 68, [46] p. 110–115. In fact, $\mathcal{R}_X$ is realized via Maskit surgeries with
- d exp–blocks (in our language $2d$ semi–infinite helicoids) and
- r quadratic blocks,

hence following[8] [45] theorem 1 and [46] theorem 2.14, there exist polynomials $E(z)$ of degree d and $P(z)$ of degree r arising from $\mathcal{R}_X$, which characterize the function

$$\Psi_X \in SF_{r,d} = \left\{ \int_{z_0}^{z} P(\zeta)\,\mathrm{e}^{-E(\zeta)} d\zeta \; + b \;\Big|\; P, E \in \mathbb{C}[z],\ \deg P = r,\ \deg E = d \right\}.$$

Alternatively[9], since $\mathcal{R}_X$ is a log–Riemann surface with d logarithmic branch points over d finite asymptotic values and n finitely ramified branch points with ramification indices that add up to $r+n$ whose finite completion is simply connected, by theorem 1.1 of [13], it follows that $\Psi_X \in SF_{r,d}$.

Finally assign to $\mathcal{R}_X$ a flat metric $\left(\mathcal{R}_X, \pi_2^*(\frac{\partial}{\partial t})\right)$ induced by π_2. By the dictionary in Proposition 2.5, our sought after vector field is

$$X(z) = \Psi_X^*(\tfrac{\partial}{\partial t})(z) = \tfrac{1}{P(z)}\,\mathrm{e}^{E(z)}\tfrac{\partial}{\partial z} \in \mathscr{E}(r,d)$$

as required.

We have essentially proved the following.

[8] It is to be noted that in the case of $X \in \mathscr{E}(r,0)$, $r \geq 1$, there is no need to use M. Taniguchi's results involving exponential blocks.

[9] Note that these results are classical, in particular R. Nevanlinna [39], [40] and G. Elfving [20] essentially proved the correspondence between $\mathcal{R}_X$ and Ψ_X.

Proposition 9.10. *Consider the following set of (r,d)–configuration trees*
$$\left\{ \begin{array}{l} \Lambda_X \textit{ has at least two branch points} \\ \textit{over different values in } \mathbb{C}_t \end{array} \right\},$$
then the (r,d)–soul of Λ_X determines a unique vector field $X \in \mathscr{E}(r,d)$.

Proof. If Λ_X has only one ramification value in $\mathbb{C}_t$, then by simple inspection it is
$$\Lambda_X = \Big\{ ① = (p_1, \widetilde{p}_1, -r); ①; \varnothing \Big\} \ \text{ or } \ \Lambda_X = \Big\{ ① = (\infty_1, a_1, -\infty); ①; \varnothing \Big\},$$
see Examples 8.1, 8.3. The corresponding vector fields
$$X(z) = \frac{\mu}{(z-p_1)^r}\frac{\partial}{\partial z} \in \mathscr{E}(r,0) \ \text{ and } \ X(z) = \mu^{-1}\mathrm{e}^{z}\frac{\partial}{\partial z} \in \mathscr{E}(0,1),$$
are not uniquely determined, since $\mu \neq 0$ is not unique.

On the other hand, if Λ_X has at least two branch points over different values, say $t_1, t_2 \in \mathbb{C}_t$, then the diagonal $\Delta_{1\,2}$ satisfies the Equation (42),
$$\int_{z_1}^{z_2} P(\zeta)\mathrm{e}^{-E(\zeta)} d\zeta = t_2 - t_1.$$
It allows us the computation of the factors λ, μ in Equation (8), obtaining the uniqness of $P(z)$ and $E(z)$. $\square$

Remark 9.11. Note that the (r,d)–configuration tree Λ_X has an embedding as a subset of $\overline{\mathbb{C}}_z \times \widehat{\mathbb{C}}_t$. However, it does not have an embedding in $\mathcal{R}_X$, since the logarithmic branch points of Ψ_X^{-1} are not in fact part of the surface $\mathcal{R}_X \subset \mathbb{C}_z \times \widehat{\mathbb{C}}_t$ (see also Definition 4.3). On the other hand, on the (r,d)–skeleton of Λ_X, the branch points of $\mathcal{R}_X$ are replaced by a vertical tower or vertical cycle during the blow–up process of Λ_X (the vertical edges of the (r,d)–skeleton of Λ_X indicate how many sheets separate the diagonals).
In this sense, both the (r,d)–configuration tree Λ_X and the (r,d)–skeleton of Λ_X project to a graph $\pi_2(\Lambda_X) \subset \mathbb{C}_t$. See Figures 8–16 and 19, in particular $\pi_2(\Lambda_X)$ need not be a tree as in Figure 16. This is represented by the diagram:

$$\begin{array}{ccccc} & & & (r,d)\text{–skeleton of } \Lambda_X & \\ & & & \text{blow–up} \big\uparrow \big\downarrow \text{blow–down} & \\ \widehat{\mathbb{C}}_z \times \widehat{\mathbb{C}}_t & \hookleftarrow & \mathcal{R}_X \text{ “}\hookleftarrow\text{” } & (r,d)\text{–configuration tree } \Lambda_X & \hookrightarrow \overline{\mathbb{C}}_z \times \widehat{\mathbb{C}}_t \\ & & & \big\downarrow \pi_2 & \\ & & & \pi_2(\Lambda_X) \subset \mathbb{C}_t. & \end{array} \tag{99}$$

9.4. **The equivalence relation on (r,d)–configuration trees.**

Remark 9.12. *Non–uniqueness of (r,d)–configuration trees Λ_X associated to Ψ_X.*
1. Even though condition (4) of Definition 7.7 provides a clear choice for the root ϱ of $\Lambda(r,d)$; if the branch point corresponding to the root shares more than one sheet with other branch points, then each of these sheets could be the global zero level sheet. Hence each choice provides a different global zero level subtree and thus a different (r,d)–configuration tree Λ_X.
2. When considering an edge that connects a pole vertex with any other type of vertex, the choice of the weight is not unique because of the modular arithmetic involved. For instance, if we have a weighted edge $(\Delta_{\iota\mathfrak{r}}, K(\iota,\mathfrak{r}))$ connecting a pole vertex $\iota = (p_\iota, \widetilde{p}_\iota, -\nu_\iota)$ to any other vertex $\mathfrak{r}$, then changing $K(\iota,\mathfrak{r})$ to $K(\iota,\mathfrak{r}) + \ell\nu$ for $\ell \in \mathbb{Z}$, will give rise to a different (r,d)–configuration tree associated to the same Ψ_X.
3. However, recalling Remark 9.6.2–3, it is to be noted that for fixed $X \in \mathscr{E}(r,d)$, even though there are choices in the construction of Λ_X, up to re–labelling of the vertices, the (r,d)–skeletons associated to each choice will be the same as undirected graphs.

Following is an example that illustrates (1)–(3).

Example 9.2 (Example 8.8 revisited)**.** Let us consider once again

$$X(z) = \frac{\mathrm{e}^{z^3}}{3z^3 - 1}\frac{\partial}{\partial z} \in \mathscr{E}(3,3).$$

However we shall now re–label the vertices, choose a different global zero level and assign different weights to some edges.

$$\begin{array}{rclrcl} ① = (z_1, t_1, \nu_1) & = & (p_2, \widetilde{p}_2, -1), & ④ = (z_4, t_4, \nu_4) & = & (p_1, \widetilde{p}_1, -1), \\ ⑤ = (z_5, t_5, \nu_5) & = & (p_3, \widetilde{p}_3, -1), & ② = (z_2, t_2, \nu_2) & = & (\infty_1, a_1, -\infty), \\ ③ = (z_3, t_3, \nu_3) & = & (\infty_2, a_1, -\infty), & ⑥ = (z_6, t_6, \nu_6) & = & (\infty_3, a_1, -\infty). \end{array} \tag{100}$$

Thus the $(3,3)$–configuration tree (see Figure 20) is

$$\Lambda_X = \Big\{①,②,③,④,⑤,⑥;⑤; \\ (\Delta_{5\,4}, 0), (\Delta_{5\,6}, -5), (\Delta_{4\,2}, -1), (\Delta_{2\,1}, 0), (\Delta_{1\,3}, -1)\Big\}, \tag{101}$$

with edges given by the diagonals/semi–residues

$$\begin{aligned} \Delta_{5\,4} &= \int_{p_3}^{p_1} \omega_X = \widetilde{p}_1 - \widetilde{p}_3 = -\Big(\frac{1 - \mathrm{e}^{-i2\pi/3}}{\sqrt[3]{3\mathrm{e}}}\Big), \\ \Delta_{5\,6} &= \int_{p_3}^{\infty_3} \omega_X = a_1 - \widetilde{p}_3 = \frac{\mathrm{e}^{-i2\pi/3}}{\sqrt[3]{3\mathrm{e}}}, \\ \Delta_{4\,2} &= \int_{p_1}^{\infty_1} \omega_X = a_1 - \widetilde{p}_1 = \frac{1}{\sqrt[3]{3\mathrm{e}}}, \\ \Delta_{2\,1} &= \int_{\infty_1}^{p_2} \omega_X = \widetilde{p}_2 - a_1 = -\frac{1}{\sqrt[3]{3\mathrm{e}}}\mathrm{e}^{i2\pi/3}, \\ \Delta_{1\,3} &= \int_{p_2}^{\infty_2} \omega_X = a_1 - \widetilde{p}_2 = \frac{\mathrm{e}^{i2\pi/3}}{\sqrt[3]{3\mathrm{e}}}, \end{aligned} \tag{102}$$

and weights $K(5,4) = 0,\ K(5,6) = -5,\ K(4,2) = -1,\ K(2,1) = 0,\ K(1,3) = -1$.

Of course this $(3,3)$–configuration tree is different from the one of Example 8.8; however *their corresponding* $(3,3)$*–skeletons are the same up to re-labelling the vertices.* Compare Figures 16 and 20.

Summarizing, the following choices and/or conventions have been made for the (r,d)–skeleton of Λ_X.
1) Because of condition (4) of Definition 7.7 and Remark 4.6.3 the root ϱ is unique.
2) The choice of $z_0 \in \mathbb{C}_z$ as the initial point of integration of $\Psi_X(z) = \int_{z_0}^{z} \omega_X$, allows the critical and asymptotic values to be well defined (and thus the vertices of the (r,d)–skeleton of Λ_X).
3) Condition (7) of Definition 7.7 provides a unique choice of the subset of diagonals needed to specify the (r,d)–skeleton of Λ_X.
4) The "blow–up" of the pole and essential vertices (of the (r,d)–configuration tree Λ_X) into vertical cycles and vertical towers (of the (r,d)–skeleton of Λ_X) respectively, eliminates the weights $K(\mathfrak{a},\mathfrak{r})$ for each diagonal $\Delta_{\mathfrak{a}\,\mathfrak{r}}$ on the (r,d)–skeleton of Λ_X.

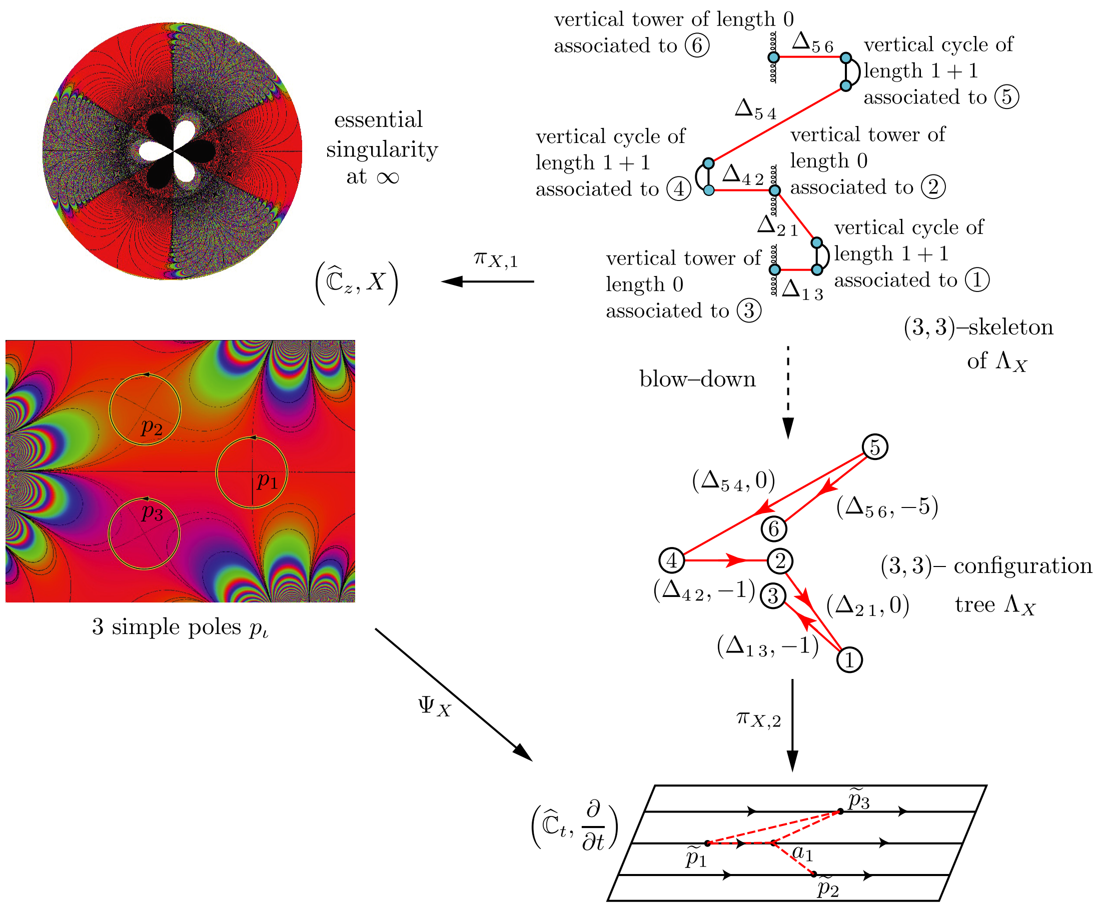

FIGURE 20. **Vector field $\frac{e^{z^3}}{3z^3-1}\frac{\partial}{\partial z}$ with an essential singularity at ∞ and 3 simple poles p_ι.** The five diagonals and their projections are shown in red. The Riemann surface $\mathcal{R}_X$ is not drawn. See Example 9.2.

Thus, as stated in Remark 9.12.3, an immediate consequence is the following.

Definition 9.13. *Two (r,d)–configuration trees Λ_1 and Λ_2 are equivalent* if their corresponding (r,d)–skeletons are the same up to re–labelling of the vertices.

This finishes the proof of the Main Theorem. □

10. Decomposition of the phase portraits into invariant components

Recall Lemma 5.9 providing a decomposition in half planes and finite height horizontal strips related to $\mathfrak{Re}\,(X)$. The interior of these pieces are invariant open components under the real vector field $\mathfrak{Re}\,(X)$.

Theorem 10.1. *Let $X \in \mathscr{E}(r,d)$, its phase portrait decomposes into $\mathfrak{Re}\,(X)$–invariant components as follows*

$$(\mathbb{C}_z, X) = \underbrace{\left(\overline{\mathbb{H}}^2_{\pm}, \frac{\partial}{\partial z}\right) \cup \ldots \cup \left(\overline{\mathbb{H}}^2_{\mp}, \frac{\partial}{\partial z}\right)}_{2(r+1)\leq N_p \leq 4r} \tag{103}$$
$$\bigcup_{a_\sigma} \Bigg[\left(\Big\{ 0 \leq |\mathfrak{Im}\,(z)| \leq 2\pi(K_\sigma+1) \Big\}, \mathrm{e}^z \frac{\partial}{\partial z} \right)_{a_\sigma}$$
$$\cup \left(\overline{\mathbb{H}}^2_{\pm}, \mathrm{e}^z \frac{\partial}{\partial z}\right)_{a_\sigma, upper} \cup \left(\overline{\mathbb{H}}^2_{\pm}, \mathrm{e}^z \frac{\partial}{\partial z}\right)_{a_\sigma, lower} \Bigg]$$
$$\bigcup_{\ell}^{M\leq\infty} \left(\Big\{ 0 \leq \mathfrak{Im}\,(z) \leq h_\ell \Big\}, \frac{\partial}{\partial z} \right),$$

where $\{a_\sigma\}$ are the finite asymptotic values of Ψ_X, N_p is the number of half planes associated to the poles of X (equivalently the number of hyperbolic sectors around the poles of X) and M is the number of diagonals (equivalently the number of finite height strips in the phase portrait of $\mathfrak{Re}\,(X)$).
There are an infinite number of half planes $\left(\overline{\mathbb{H}}^2_{\pm}, \frac{\partial}{\partial z}\right)$ in the decomposition if and only if $d \geq 1$.

Proof. Decomposition (103) follows by recalling Definition 5.7, the biholomorphism π_1 presented in Diagram 5 and the fine structure of the (r,d)–skeleton of Λ_X. It is an accurate description of the phase portrait decomposition of $\mathfrak{Re}\,(X)$:
The first row depicts the, at least $2(r+1)$ and at most $4r$, half planes associated to the r poles.
On the second row are the d finite helicoids arising from the d finite asymptotic values $\{a_\sigma\}$, where it is to be noticed that this can be an empty collection.
On the third row are the $2d$ semi–infinite helicoids.
Finally, on the fourth row the finite height strips associated to the diagonals in $\mathcal{R}_X$. □

Definition 10.2. An *incomplete trajectory* $z(\tau)$ of X is such that its maximal domain is a strict subset of $\mathbb{R}$.

Corollary 10.3. *Let $X \in \mathscr{E}(r,d)$, $d \geq 1$. Then, the incomplete trajectories of $\mathfrak{Re}\,(X)$ in $\widehat{\mathbb{C}}_z$ are infinite, numerable and have Lebesgue measure zero in $\widehat{\mathbb{C}}_z$.* □

Obviously, the number of incomplete trajectories is finite if and only if $r \geq 1$ and $d = 0$. Compare with [32] and [31].

11. On the topology of $\mathfrak{Re}\,(X)$

Consider the group of orientation preserving homeomorphisms of $\mathbb{C}$,

$$Homeo(\mathbb{C})^+ = \{h : \widehat{\mathbb{C}}_z \to \widehat{\mathbb{C}}_z \mid \text{ preserving orientation and fixing } \infty \in \widehat{\mathbb{C}}\}.$$

Definition 11.1. 1. Let $X_1, X_2 \in \mathscr{E}(r,d)$ be two singular analytic vector fields.
They are *topologically equivalent* or *the phase portraits of* $\mathfrak{Re}\,(X_1)$, $\mathfrak{Re}\,(X_2)$ *determine the same (orientation preserving) topological class* if there exists $h \in Homeo(\mathbb{C})^+$ which takes the trajectories of $\mathfrak{Re}\,(X_1)$ to trajectories of $\mathfrak{Re}\,(X_2)$, preserving real time orientation, but not necessarily the parametrization.
2. A *bifurcation for* $\mathfrak{Re}\,(X_1)$ *occurs*, when its phase portrait topologically changes under small deformation of X_1 in the family $\mathscr{E}(r,d)$, otherwise $\mathfrak{Re}\,(X_1)$ is *structurally stable* in $\mathscr{E}(r,d)$.

Let $\Lambda_X = \Big\{ \big\{ (\mathfrak{a}) = \big(z_{\mathfrak{a}}, t_{\mathfrak{a}}, -\nu_{\mathfrak{a}}\big) \big\}_{\sigma=1}^{d+n}; (\varrho); \big\{ (\Delta_{\mathfrak{a}\mathfrak{r}}, K(\mathfrak{a}, \mathfrak{r})) \big\} \Big\}$ be a (r,d)–configuration tree. By simple inspection we have

Theorem 11.2 (Structural stability of $\mathfrak{Re}\,(X)$ for $X \in \mathscr{E}(r,d)$)**.** *The real vector field $\mathfrak{Re}\,(X)$ is structurally stable in $\mathscr{E}(r,d)$ if and only if*
1) X has only simple poles and
2) $\mathfrak{Im}\,(\Delta_{\mathfrak{a}\mathfrak{r}}) \neq 0$ for all the weighted edges of Λ_X.

Proof. Recall that, a diagonal $\Delta_{\mathfrak{a}\mathfrak{r}}$ has $\mathfrak{Im}\,(\Delta_{\mathfrak{a}\mathfrak{r}}) = 0$ and poles of X at its two extreme points, if and only if $\Delta_{\mathfrak{a}\mathfrak{r}}$ determines a saddle connection of $\mathfrak{Re}\,(X)$, see Lemma 5.9.3. If in addition, X has only simple poles, then this is the unique bifurcation scenario for $\mathfrak{Re}\,(X)$.
We leave the converse implication to the reader. □

Recall that an (r,d)–skeleton of Λ_X is a graph embedded in $\overline{\mathbb{C}}_z \times \mathbb{C}_t$, with a specific complex parameter associated to each edge and having horizontal and vertical attributes. As a direct consequence of the structure of the (r,d)–skeleton of Λ_X we have:

Theorem 11.3 (Number of (orientation preserving) topological classes of phase portraits of $\mathfrak{Re}\,(X)$, for $X \in \mathscr{E}(r,d)$)**.** *Given a fixed pair (r,d):*
1) The number of topological classes of $\mathfrak{Re}\,(X)$ is infinite when
$$(r,d) \in \big\{(r \geq 2, 1), (r \geq 1, 2), (r \geq 0, d \geq 3)\big\}.$$
2) The number of topological classes is
- *a) one when $(r,d) = (0,1), (1,0)$;*
- *b) two when $(r,d) = (0,2)$, $(1,1)$;*
- *c) finite when $(r,0)$.*

For $X \in \mathscr{E}(r,0)$, the phase portrait $\mathfrak{Re}\,(X)$ on $\mathbb{C}_z$ only has a finite number $n \leq r$ of multiple saddle points. These phase portraits were first studied by W. M. Boothby [15], [16], showing that they appear as the real part of certain harmonic functions (non-necessarily polynomials); in our framework, the imaginary part of $\Psi_X(z) = \int^z P(\zeta) \mathrm{e}^{-E(\zeta)} d\zeta$.

Proof. Let (r,d) be as in assertion (1). There will be at least one $X \in \mathscr{E}(r,d)$ such that the (r,d)–skeleton of Λ_X has at least one vertical tower with two horizontal subgraphs attached to the *same* vertical tower. These horizontal subgraphs are vertically separated from each other by an integer number $K(\sigma,\rho)$, of degree 2 vertices on the vertical tower. Hence there are an infinite number of different ways, described by $\{K(\sigma,\rho) \geq 1\}$, we can attach these two subgraphs to the vertical tower; each of which represents a different configuration in $\mathcal{R}_X$.

The remaining cases are $(r,d) \in \big\{(0,1), (0,2), (1,1), (r \geq 1, 0)\big\}$.
The cases $(0,1), (1,0)$ are trivial by Lemma 5.3. For cases $(0,2)$ and $(1,1)$: $\mathcal{R}_X$ has two branch points hence they must share the same sheet. Thus each one of these cases have exactly two topologies. Case (0,2) is illustrated in Figure 22. Case $(r \geq 2, 0)$ corresponds to Ψ_X being a polynomial, hence the number of topological classes is finite. □

Table 2 presents a summary of the non-topologically equivalent vector fields $\mathfrak{Re}\,(X)$, for $X \in \mathscr{E}(r,d)$, that arise for different pairs (r,d).

Remark 11.4. For Ψ_X and X in $\mathscr{E}(r,d)$, Theorem 11.3 and Proposition 8.2 show that the topological classification of functions is coarser than the topological classification of phase portraits of vector fields.

TABLE 2. Topologies of $\mathfrak{Re}(X)$ for different pairs (r,d).

r	d	# of topologies of $\mathfrak{Re}(X)$	(r,d)–configuration trees Λ_X chosen as a representative for the topological class
1	0	1	$\Lambda_X = \{(p_1, \widetilde{p}_1, -1); \varnothing\}$
0	1	1	$\Lambda_X = \{(\infty_1, a_1, -\infty); \varnothing\}$
0	2	2	$\Lambda_X = \{(\infty_1, a_1, -\infty), (\infty_1, a_2, -\infty); \big(\Delta_{1\,2}, K(1,2)\big)\}$, with $\Delta_{1\,2} \in \mathbb{C}^*$, two topologies: $\Delta_{1\,2} \in \mathbb{R}, \Delta_{1\,2} \notin \mathbb{R}$
1	1	2	$\Lambda_X = \{(\infty_1, a_1, -\infty), (p_1, \widetilde{p}_1, -1); \big(\Delta_{1\,2}, K(1\,2)\big)\}$, with $\Delta_{1\,2} \in \mathbb{C}^*$, two topologies: $\Delta_{1\,2} \in \mathbb{R}, \Delta_{1\,2} \notin \mathbb{R}$
2	0	3	$\Lambda_X = \{(p_1, \widetilde{p}_1, -2); \varnothing\}$, gives rise to one topology. $\Lambda_X = \{(p_1, \widetilde{p}_1, -1), (p_2, \widetilde{p}_2, -1); \big(\Delta_{1\,2}, K(1\,2)\big)\}$, with $\Delta_{1\,2} \in \mathbb{C}^*$, two topologies: $\Delta_{1\,2} \in \mathbb{R}, \Delta_{1\,2} \notin \mathbb{R}$
$r \geq 3$	0	finite	$\Lambda_X = \Big\{(p_1, \widetilde{p}_1, -\nu_1), \dots, (p_n, \widetilde{p}_n, -\nu_n); \{\big(\Delta_{\iota\kappa}, K(\iota,\kappa)\big) \mid \iota, \kappa \in \{1, \dots, n-1\}\}\Big\}$, $1 \leq n \leq r$ being the number of distinct poles
$r \geq 2$	1	infinite	$\Lambda_X = \Big\{(\infty_1, a_1, -\infty), (p_1, \widetilde{p}_1, -\nu_1), \dots, (p_n, \widetilde{p}_n, -\nu_n); \{\big(\Delta_{\mathfrak{a}\mathfrak{r}}, K(\mathfrak{a},\mathfrak{r})\big) \mid \mathfrak{a}, \mathfrak{r} \in \{1, \dots, n+1\}\}\Big\}$, $1 \leq n \leq r$ being the number of distinct poles
$r \geq 1$	2	infinite	$\Lambda_X = \Big\{(\infty_1, a_1, -\infty), (\infty_2, a_2, -\infty), (p_1, \widetilde{p}_1, -\nu_1), \dots, (p_n, \widetilde{p}_n, -\nu_n); \{\big(\Delta_{\mathfrak{a}\mathfrak{r}}, K(\mathfrak{a},\mathfrak{r})\big) \mid \mathfrak{a}, \mathfrak{r} \in \{1, \dots, n+2\}\}\Big\}$, $1 \leq n \leq r$ being the number of distinct poles
$r \geq 0$	$d \geq 3$	infinite	$\Lambda_X = \Big\{(\infty_1, a_1, -\infty), (\infty_2, a_2, -\infty), (\infty_3, a_3, -\infty), \dots, (\infty_d, a_d, -\infty), (p_1, \widetilde{p}_1, -\nu_1), \dots, (p_n, \widetilde{p}_n, -\nu_n); \{\big(\Delta_{\mathfrak{a}\mathfrak{r}}, K(\mathfrak{a},\mathfrak{r})\big) \mid \mathfrak{a}, \mathfrak{r} \in \{1, \dots, d+n\}\}\Big\}$, $0 \leq n \leq r$ being the number of distinct poles

12. THE ESSENTIAL SINGULARITY AT ∞

Our naive question in the introduction;

how can we describe the essential singularity of $X \in \mathscr{E}(r,d)$ at $\infty \in \widehat{\mathbb{C}}_z$?

is answered in this section. The available tools are as follows. In [1] §5, germs of singular analytic vector fields X are studied; the Poincaré–Hopf index theory and a certain version of the decomposition in angular sectors for essential isolated singularities are established for the phase portrait of $\mathfrak{Re}(X)$.

In fact, starting with a simple closed anticlockwise orientated path γ enclosing

$$z_\vartheta \in \{p_1, \dots, p_r, \infty\} \subset \widehat{\mathbb{C}}_z$$

a pole, zero or essential singularity, of X, the notion of an admissible cyclic word $\mathcal{W}_X$ in the alphabet $\{H, E, P, \mathscr{E}\}$ is well defined,

$$\big((\widehat{\mathbb{C}}, z_\vartheta), \mathfrak{Re}\,(X)\big) \longmapsto \mathcal{W}_X. \tag{104}$$

The letters in the alphabet are the usual angular sectors for vector fields as follows: hyperbolic H, elliptic E, parabolic P (see [4] p. 304, [5] p. 86). Moreover, a *class 1 entire sector* $\mathscr{E}$ based upon $\mathrm{e}^z \frac{\partial}{\partial z}$ at infinity, see Figure 21. Recalling Diagram 12, $\mathscr{E}$ can be thought as the image under π_1 of a semi–infinite helicoid contained in $\mathcal{R}_X$, see Example 8.3, Figures 4.a and 11. For full details see [1] p. 151.

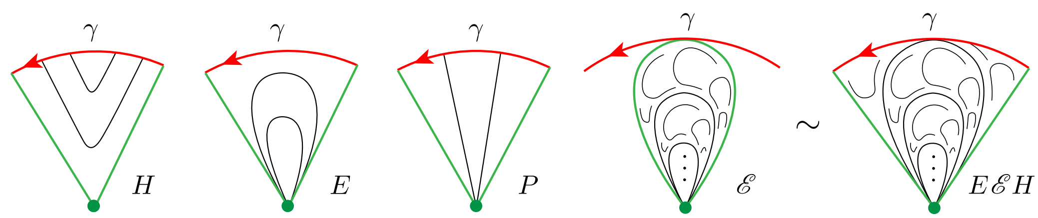

FIGURE 21. Hyperbolic H, elliptic E, parabolic P and entire $\mathscr{E}$ sectors at a singular point $(\widehat{\mathbb{C}}_z, z_\vartheta)$ of a vector field $\mathfrak{Re}\,(X)$. The point z_ϑ is green, the path γ is shown in red. The equivalence relation $\mathscr{E} \sim E\mathscr{E}H$ is illustrated on the right.

Specific attributions encoded by the word $\mathcal{W}_X$ in (104) are as follows.

1) *Equivalence classes.* The word $\mathcal{W}_X$ is well defined up to the relations
$$E\mathscr{E}H \sim \mathscr{E} \quad \text{and} \quad H\mathscr{E}E \sim \mathscr{E},$$
according to [1] pp. 166–167. Under this equivalence the word becomes independent of the choice of the path γ enclosing the singularity.

2) *Poincaré–Hopf index.* If the number of letters H, E and $\mathscr{E}$ that appear in a word $\mathcal{W}_X$ at z_ϑ, is denoted by h, e and ε respectively, then the Poincaré–Hopf index formula is
$$PH(X, z_\vartheta) = 1 + \frac{e - h + \varepsilon}{2}. \tag{105}$$
Furthermore, in theorem A p. 130 and §6 of [1], the Poincaré–Hopf index theorem
$$\chi(\widehat{\mathbb{C}}) = \sum_z PH(X, z) \tag{106}$$
is extended to include germs of singular analytic vector fields X that determine an admissible cyclic word.

3) *Displacement of parabolic sectors.* As matter of record, each parabolic sector P_ν of $\mathcal{W}_X$ has a displacement number $\nu \in \mathbb{C}\backslash\mathbb{R}$, see [1] pp. 149–150.

4) *The residue.* The residue of the vector field germ is
$$Res(\omega_X) \doteq Res(X, z_\vartheta) = \tfrac{1}{2\pi i} \int_\gamma \omega_X,$$
recall that $\omega_X(X) = 1$, also see [1] p. 167.
In fact, for $X \in \mathscr{E}(r, d)$ all the residues are zero, since $\omega_X = P(z)\mathrm{e}^{-E(z)}dz$ is holomorphic on $\mathbb{C}_z$.

Clearly, for each singularity $z_\vartheta \in \{p_1, \ldots, p_r, \infty\}$ of X, the germ $\big((\widehat{\mathbb{C}}_z, z_\vartheta), X(z)\big)$ is

- a local analytic invariant (under the local biholomorphisms of $(\widehat{\mathbb{C}}_z, z_\vartheta)$, and
- an analytic invariant under the action of $Aut(\mathbb{C})$,

$$\mathcal{A} : Aut(\mathbb{C}) \times \mathscr{E}(r, d) \longrightarrow \mathscr{E}(r, r), \quad (T, X) \longmapsto T^*X.$$

Example 12.1 (Cyclic words at poles)**.** For $X(z) = \frac{1}{(z-p_\iota)^{\nu_\iota}}\frac{\partial}{\partial z}$, the cyclic word $\mathcal{W}_X$ consists of exactly $2(\nu_\iota + 1)$ hyperbolic sectors H, see Figure 1:

$$\Big((\mathbb{C}_z, p_\iota), \mathfrak{Re}\,(X)\Big) \longmapsto \mathcal{W}_X = \underbrace{HH\cdots HH}_{2(\nu_\iota+1)}. \tag{107}$$

The Poincaré–Hopf index is $PH(X, p_\iota) = -\nu_\iota$.

Example 12.2 (A cyclic word at ∞, from a zero of X)**.** Recall the rational vector field

$$X(z) = \frac{1}{(z-p_1)^{\nu_1}(z-p_1)^{\nu_2}}\frac{\partial}{\partial z}$$

in Example 8.2, in our language the description of the singularity at infinity is

$$\Big((\widehat{\mathbb{C}}_z, \infty), \mathfrak{Re}\,(X)\Big) \longmapsto \mathcal{W}_X = \underbrace{EE\cdots EE}_{\nu_1+\nu_2+2}. \tag{108}$$

The Poincaré–Hopf index is $PH(X, \infty) = \nu_1 + \nu_2 + 2$, also see Figure 1.

Example 12.3 (The cyclic word at ∞ of the exponential vector field has two entire sectors)**.** Recall the exponential vector field $X(z) = \mathrm{e}^z\frac{\partial}{\partial z}$ in Example 8.3 and Figure 11, we have

$$\Big((\widehat{\mathbb{C}}_z, \infty), \mathfrak{Re}\,(X)\Big) \longmapsto \mathcal{W}_X = E\mathscr{E}H\mathscr{E} \sim \mathscr{E}\mathscr{E}. \tag{109}$$

The Poincaré–Hopf index of X at ∞ is 2.

Example 12.4 (The error function)**.** The vector field

$$X(z) = \mu\tfrac{\sqrt{\pi}}{4}\mathrm{e}^{z^2}\tfrac{\partial}{\partial z}, \quad \mu \in \mathbb{C}^*,$$

has associated the error function

$$\Psi(z) = \mu^{-1}\tfrac{2}{\sqrt{\pi}}\textstyle\int_0^z \mathrm{e}^{-\zeta^2}d\zeta.$$

Case $\mu = 1$, the logarithmic branch points are

$$\{(\infty_1, -1, -\infty), (\infty_2, 1, -\infty), (\infty_3, \infty, -\infty), (\infty_4, \infty, -\infty)\},$$

using the notation in equations (31), and the $\mathfrak{Re}\,(X)$–invariant decomposition is

$$(\widehat{\mathbb{C}}_z, X) = \textstyle\bigcup_{\sigma=1}^{\infty}\big(\overline{\mathbb{H}}^2_\sigma, \tfrac{\partial}{\partial z}\big).$$

The cyclic word is

$$\Big((\widehat{\mathbb{C}}_z, \infty), \mathfrak{Re}\,(X)\Big) \longmapsto \mathcal{W}_X = E\mathscr{E}HH\mathscr{E}E\mathscr{E}HH\mathscr{E}.$$

See Figure 22.

Case $\mu = i$, the logarithmic branch points are

$$\{(\infty_1, -i, -\infty), (\infty_2, i, -\infty), (\infty_3, \infty, -\infty), (\infty_4, \infty, -\infty)\},$$

and the $\mathfrak{Re}\,(X)$–invariant decomposition is

$$(\widehat{\mathbb{C}}_z, X) = \Big(\textstyle\bigcup_{\sigma=1}^{\infty}\big(\overline{\mathbb{H}}^2_\sigma, \tfrac{\partial}{\partial z}\big)\Big) \ \cup\ \big(\{-1 \leq \mathfrak{Im}\,(z) \leq 1\}, \tfrac{\partial}{\partial z}\big).$$

The cyclic word is

$$\Big((\widehat{\mathbb{C}}_z, \infty), \mathfrak{Re}\,(X)\Big) \longmapsto \mathcal{W}_X = E\mathscr{E}HH\mathscr{E}P_{2i}E\mathscr{E}HH\mathscr{E}P_{-2i},$$

note that the appearance of two opposite parabolic sectors having displacements $\pm 2i$ is due the horizontal strip in the decomposition. See Figure 22.

In both cases the Poincaré–Hopf index of X at ∞ is 2.

Remark 12.1. *The singularity at infinity does not determine the analytic class of X.* 1. For $X \in \mathscr{E}(3,0)$ having simple zeros, all the germs $\big((\widehat{\mathbb{C}}_z, \infty), X\big)$ are analytically equivalent. Thus the singularity at infinity does not determine the analytic class of X even in $\mathscr{E}(3,0)/Aut(\mathbb{C})$.

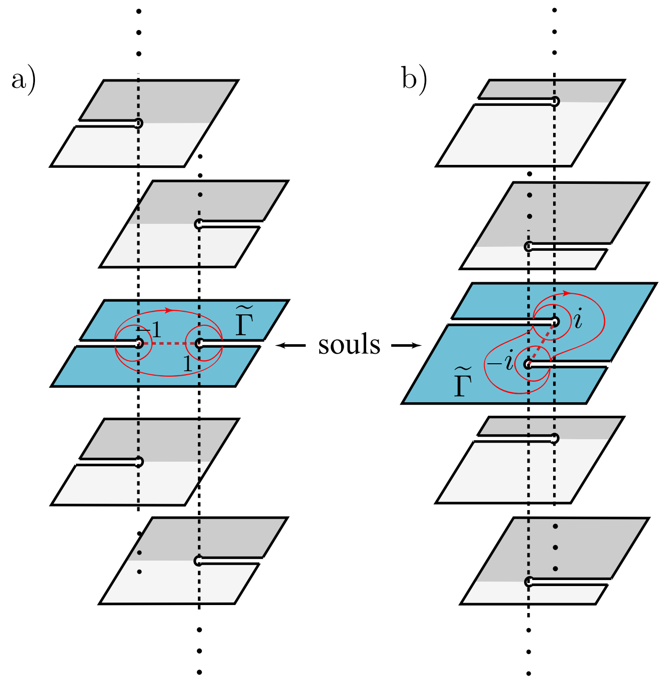

FIGURE 22. The Riemann surfaces of X and $e^{i\pi/2}X$ for $X \in \mathscr{E}(0,2)$. In (a) is the one associated to the error function $\Psi_{X_1}(z) = \frac{2}{\sqrt{\pi}}\int_0^z e^{-\zeta^2}d\zeta$, having a diagonal $\Delta_{1\,2}$ which determines a homoclinic trajectory of $\mathfrak{Re}\,(X)$. In (b) is the one corresponding to $\Psi_{X_2}(z) = \frac{2i}{\sqrt{\pi}}\int_0^z e^{-\zeta^2}d\zeta$. The red curves represent taut $\widetilde{\Gamma}$'s that allow the recognition of the words. The global topologies of the corresponding $\mathfrak{Re}\,(X)$, $X \in \mathscr{E}(0,2)$, are described in the third row of Table 2, and the germ of singularities at ∞ in Example 12.4.

2. We further note that the vector field

$$\widetilde{X}(p_3,z) = \mu\frac{2p_3-1}{12z(z-1)(z-p_3)}e^{z^4}\frac{\partial}{\partial z} \in \mathscr{E}(3,4),$$

has the same behaviour in $\{z \in \mathbb{C} \mid |z| < R\} \subset \mathbb{C}_z$, for adequate choices of $\mu \in \mathbb{C}^*$ and $R > 0$, as $X(p_3,z)$ given by (51), hence the singularity at infinity does not determine the analytic class of X in $\mathscr{E}(3,4)/Aut(\mathbb{C})$, see [1] §9 and §10.

Thus, for vector fields in $\mathscr{E}(r,d)$, $r+d \geq 3$, the $Aut(\mathbb{C})$–equivalence notion from (53) is very rigid.

We now have that for the essential singularity:

Theorem 12.2.
1) Let $X \in \mathscr{E}(r,d)$, the cyclic word $\mathcal{W}_X$ at ∞ is recognized as

$$\big((\widehat{\mathbb{C}}_z,\infty),\mathfrak{Re}\,(X)\big) \longmapsto \mathcal{W}_X = W_1W_2\cdots W_k, \quad W_\iota \in \{H,E,P,\mathscr{E}\}, \tag{110}$$

with exactly $\varepsilon = 2d$ letters $W_\iota = \mathscr{E}$.
Moreover, $h - e = 2(d-r-1)$.

2) The word $\mathcal{W}_X$ is a local topological invariant of the germ $\big((\widehat{\mathbb{C}}_z,\infty),\mathfrak{Re}\,(X)\big)$.
3) Conversely, a germ of a singular complex analytic vector field $\big((\mathbb{C},0),Y\big)$ is the restriction of an $X\in\mathscr{E}(r,d)$ at ∞ if and only if the point 0 is an isolated essential singularity of Y and satisfies that
i) the residue of ω_Y is zero,
ii) the Poincaré–Hopf index of the word $PH(Y,0)=2+r$,
iii) $\mathcal{W}_Y$ is an admissible cyclic word having exactly $2d$ entire sectors $\mathscr{E}$.

Proof. The proof of statement (1) follows the arguments in §5, §9 and §10 of [1].
Step 1: Take a simple path $\gamma\subset(\widehat{\mathbb{C}}_z,\infty)$ enclosing only ∞ (γ does not enclose any pole of X).
Step 2: Lift γ to $\Gamma\doteq\pi_1^{-1}(\gamma)$ in $\mathcal{R}_X\subset\widehat{\mathbb{C}}_z\times\widehat{\mathbb{C}}_t$. Note that a priori, Γ does not lie completely in the soul of $\mathcal{R}_X$, recall Definition 9.7.
Step 3: The singularity at ∞ of X has a certain self–similarity (as the examples in §8 show), hence in order to recognize a simple word describing it, an appropriate choice of Γ is required. That is, we deform Γ to a *taut deformation* $\widetilde{\Gamma}$ in the soul of $\mathcal{R}_X$. For examples of a taut deformation $\widetilde{\Gamma}$ see Figures 22 and 25. For the appropriate technical definitions and another example see pp. 211–212 of [1], in particular figure 17.

The taut deformation $\widetilde{\Gamma}$ recognizes letters W_ι at ∞ as follows:
- letters P when $\widetilde{\Gamma}$ crosses finite height strip flows,
- letters H when $\widetilde{\Gamma}$ makes a half circle around a branch point of $\mathcal{R}_X$,
- letters E when $\widetilde{\Gamma}$ makes a half circle around (the branch point at) ∞ on a sheet of $\mathcal{R}_X$,
- letters $\mathscr{E}$ when $\widetilde{\Gamma}$ touches a component of the boundary of the soul; see Figures 21 and 22.

As for the difference $h-e$ between the number of sectors H and E appearing in the cyclic word $\mathcal{W}_X$ at ∞, we shall use the Poincaré–Hopf index theory extended to these kinds of singularities (theorem A in §6 of [1] with $M=\widehat{\mathbb{C}}_z$).
From the fact that $X\in\mathscr{E}(r,d)$ has exactly r poles (counted with order) in $\mathbb{C}_z$ and since $PH(X,p_\iota)=-\nu_\iota$ for a pole p_ι of order $-\nu_\iota$, then equation (6.6) of [1] gives us

$$2=\chi(\widehat{\mathbb{C}})=PH(X,\infty)+\sum_{p_\iota\in\mathcal{P}}PH(X,p_\iota)=PH(X,\infty)-r. \tag{111}$$

On the other hand from equation (6.5) of [1]
$$PH(X,\infty)=1+\tfrac{e-h+2d}{2},$$
the result follows.

Assertion (2) is clear. by simple inspection.

For assertion (3), use a slight modification of corollary 10.1 of [1]. The only change arises from the fact that $X\in\mathscr{E}(r,d)$ has exactly r poles (counted with order) in $\mathbb{C}_z$. Once again, by (111) the result follows. ☐

Example 12.5 (Cyclic words at ∞)**.** 1. Recall the vector field in Example 8.6

$$X(z)=\frac{\mathrm{e}^z}{(z-9i\frac{\pi}{2})(z+i\frac{\pi}{2})}\frac{\partial}{\partial z}.$$

Figure 14 shows the $(2,1)$–skeleton of Λ_X together with the soul of Λ_X. Here we also show a *taut* curve $\widetilde{\Gamma}_1\cup\cdots\cup\widetilde{\Gamma}_{10}=\widetilde{\Gamma}(\tau)=\big(\gamma(\tau),(\Psi_X\circ\gamma)(\tau)\big)\subset\mathcal{R}_X$ where $\gamma(\tau)$ is a simple closed curve enclosing $\infty\in\widehat{\mathbb{C}}_z$ with $p_1=9i\frac{\pi}{2}$ and $p_2=-i\frac{\pi}{2}$ lying in its exterior. As shown in [1] §9.1, we can read the admissible cyclic word

$$\mathcal{W}_X = \underbrace{EE}_{\widetilde{\Gamma}_1}\underbrace{P}_{\widetilde{\Gamma}_2}\underbrace{EE}_{\widetilde{\Gamma}_3}\underbrace{EE}_{\widetilde{\Gamma}_4}\underbrace{P}_{\widetilde{\Gamma}_5}\underbrace{EE}_{\widetilde{\Gamma}_6}\underbrace{EPE\mathscr{E}HH}_{\widetilde{\Gamma}_7}\underbrace{HH}_{\widetilde{\Gamma}_8}\underbrace{HH}_{\widetilde{\Gamma}_9}\underbrace{HH\mathscr{E}EPE}_{\widetilde{\Gamma}_{10}}, \tag{112}$$

so that the number of elliptic, hyperbolic and entire sectors are $e = 12$, $h = 8$ and $\varepsilon = 2$ respectively. The Poincaré–Hopf index at ∞, in this case turns out to be

$$PH(X, \infty) = 1 + \frac{e - h + \varepsilon}{2} = 1 + 3 = 4.$$

2. Recall the vector field $X(z) = \frac{-e^{z^3}}{3z^2}\frac{\partial}{\partial z}$ in Example 8.7,

$$\Big((\widehat{\mathbb{C}}_z, \infty), \mathfrak{Re}\,(X)\Big) \longmapsto \mathcal{W}_X = \mathscr{E}\mathscr{E}\mathscr{E}\mathscr{E}\mathscr{E}\mathscr{E} \tag{113}$$

The Poincaré–Hopf index of X at ∞ is 4.

3. Recall the vector field $X(z) = \frac{e^{z^3}}{3z^3-1}\frac{\partial}{\partial z}$ in Example 8.8,

$$\Big((\widehat{\mathbb{C}}_z, \infty), \mathfrak{Re}\,(X)\Big) \longmapsto \mathcal{W}_X = \mathscr{E}EE\mathscr{E}\mathscr{E}\mathscr{E}\mathscr{E}\mathscr{E}. \tag{114}$$

The Poincaré–Hopf index of X at ∞ is 5.

In the next example we show that it is possible to calculate, among other things, the Poincaré–Hopf index.

Example 12.6. [Example 8.10 revisited.] Considering Example 8.10 once again, Figure 23 shows the $(r, 4)$–skeleton of Λ_X together with the soul of Λ_X. Here we also show a *taut* curve $\widetilde{\Gamma}(\tau) = \big(\gamma(\tau), (\Psi_X \circ \gamma)(\tau)\big) \subset \mathcal{R}_X$ where $\gamma(\tau)$ is a simple closed curve enclosing $\infty \in \widehat{\mathbb{C}}_z$ with p_1 and p_2 lying in its exterior. As shown in [1] §9.1 and §6, we can read the admissible cyclic word

$$\begin{aligned}\mathcal{W}_X = {} & \underbrace{EE}_{\widetilde{\Gamma}_1}\ \underbrace{P\mathscr{E}HH\mathscr{E}EPE}_{\widetilde{\Gamma}_2}\ \underbrace{EE}_{\substack{\widetilde{\Gamma}_3\\(\nu_1-2)\\\text{copies}}}\ \underbrace{P}_{\widetilde{\Gamma}_4}\ \underbrace{EE}_{\substack{\widetilde{\Gamma}_5\\-K(2,3)-1\\\text{copies}}}\ \underbrace{P\mathscr{E}HH\mathscr{E}EPE}_{\widetilde{\Gamma}_6}\\ & \underbrace{EE}_{\substack{\widetilde{\Gamma}_7\\-K(2,4)+K(2,3)-1\\\text{copies}}}\ \underbrace{P}_{\widetilde{\Gamma}_8}\ \underbrace{EE}_{\substack{\widetilde{\Gamma}_9\\\nu_2\\\text{copies}}}\ \underbrace{EPE}_{\widetilde{\Gamma}_{10}}\ \underbrace{EE}_{\substack{\widetilde{\Gamma}_{11}\\-K(2,6)+K(2,4)-1\\\text{copies}}}\ \underbrace{P\mathscr{E}HH\mathscr{E}EPE\mathscr{E}HH}_{\widetilde{\Gamma}_{12}}\\ & \underbrace{HH}_{\substack{\widetilde{\Gamma}_{13}\\-K(2,6)+K(2,4)-1\\\text{copies}}}\ \underbrace{HH}_{\widetilde{\Gamma}_{14}}\ \underbrace{HH}_{\substack{\widetilde{\Gamma}_{15}\\-K(2,4)+K(2,3)-1\\\text{copies}}}\ \underbrace{HH}_{\widetilde{\Gamma}_{16}}\ \underbrace{HH}_{\substack{\widetilde{\Gamma}_{17}\\-K(2,3)-1\\\text{copies}}}\ \underbrace{HH\mathscr{E}EPE}_{\widetilde{\Gamma}_{18}},\end{aligned} \tag{115}$$

and thus calculate the Poincaré–Hopf index at ∞, which in this particular case turns out to be

$$\begin{aligned} PH(X, \infty) &= 1 + \frac{1}{2}\big(2\big(\nu_1 + \nu_2 - K(2,6) + 1\big) - 2\big(-K(2,6) + 4\big) + 8\big)\\ &= 2 + \nu_1 + \nu_2.\end{aligned}$$

13. Relations with other works

13.1. **The case that all critical and asymptotic values are real.** Recall the following result.

Theorem (Eremenko *et al.*, [21], [22])**.** *If all critical points of a rational function $\frac{Q}{P}(z)$ are real, then it is equivalent to a real rational function.*

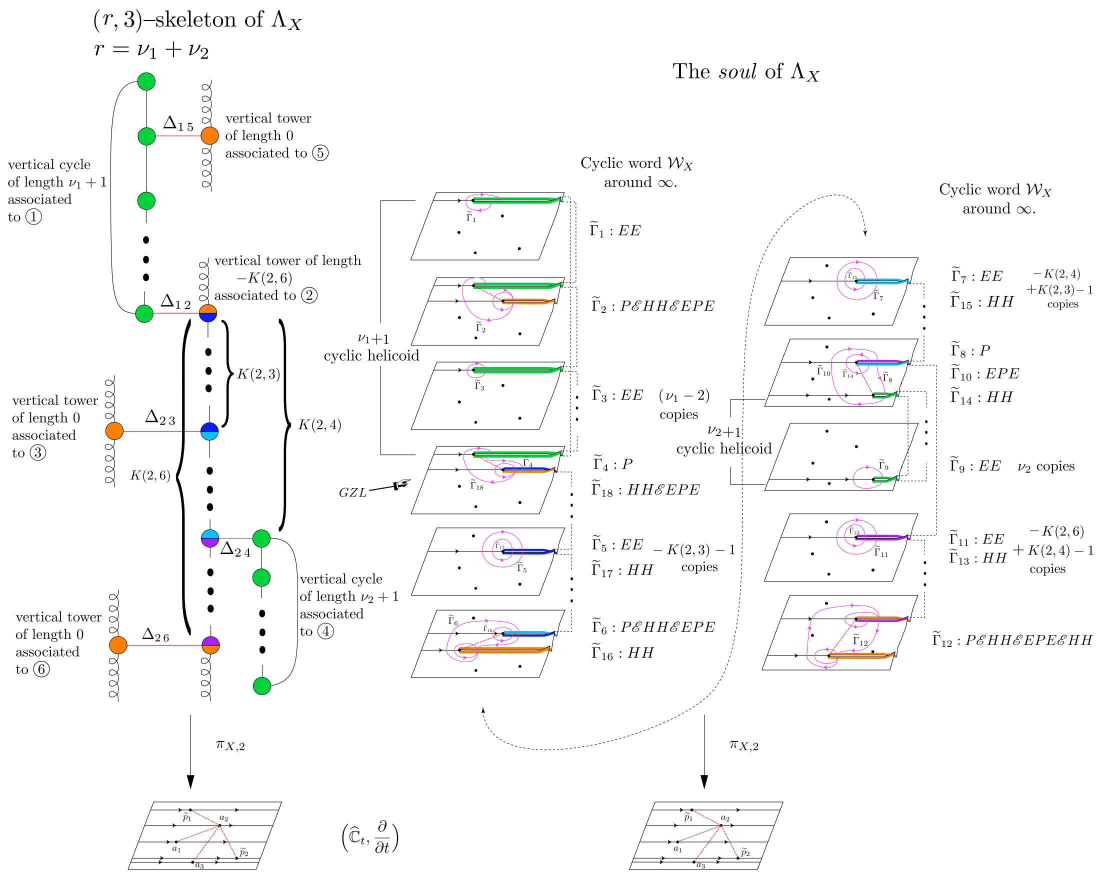

FIGURE 23. **The soul of Λ_X and the cyclic word $\mathcal{W}_X$.** The left hand side shows the $(r,4)$–skeleton of Λ_X of Example 8.10, in the middle the corresponding soul together with the curve $\widetilde{\Gamma}$ decomposed into the corresponding $\widetilde{\Gamma}_\iota$ on each sheet of the soul. On the right hand side are the corresponding syllables of the cyclic word $\mathcal{W}_X$ around $\infty \in \widehat{\mathbb{C}}_z$. See Example 12.6.

This immediately implies that for such a rational function all the critical values are also real.

Motivated by the above, we have.

Corollary 13.1 (Real critical and asymptotic values)**.**

1) If all critical and asymptotic values of Ψ_X for $X \in \mathscr{E}(r,d)$ are in $\mathbb{R}$, then the following assertions hold.

a) $\mathcal{R}_X$, as in (103), is the union of half planes.

b) $\Psi_X : U \subset \widehat{\mathbb{C}} \longrightarrow \mathbb{H}^2$ is a Schwarz–Christoffel map, for each half plane U.

c) All the diagonals $\Delta_{\mathfrak{a}\mathfrak{r}}$ of Λ_X satisfy $\mathfrak{Im}(\Delta_{\mathfrak{a}\mathfrak{r}}) = 0$.

d) X is structurally unstable in $\mathscr{E}(r,d)$, thus a bifurcation for $\mathfrak{Re}(X)$ occurs.

2) The critical and asymptotic values are in $\mathbb{R}$ if and only if the family of rotated vector fields $\{\mathfrak{Re}(e^{i\theta}X) \mid \theta \in \mathbb{R}/2\pi n\}$ bifurcates exactly at $\theta = n\pi$ for $n \in \mathbb{Z}$.

□

13.2. **Relations with Belyĭ's functions.** Recall that a *rational function* $\frac{Q}{P}(z)$ *is Belyĭ* if it has only three critical values $\{0, 1, \infty\}$, the original source is [6], see [30] Ch. 2 for current developments. Recently Ch. J. Bishop [11] develops analogous combinatorial and analytic ideas for entire functions.

The construction of a certain $\Psi_X(z)$ having three asymptotic values, say at $\{0, 1, \infty\}$ set theoretically, as in Belyĭ's theory, is possible. It is natural to call these functions *Transcendental Belyĭ*.

Example 13.1. Let $X(z) = \frac{\sqrt{\pi}}{4} \mathrm{e}^{z^2} \frac{\partial}{\partial z}$ be as in Example 12.4, having associated the error function $\Psi(z) = \frac{2}{\sqrt{\pi}} \int_0^z \mathrm{e}^{-\zeta^2} d\zeta$ with logarithmic branch points of Ψ_X^{-1},

$$\{(\infty_1, -1, -\infty), (\infty_2, 1, -\infty), (\infty_3, \infty, -\infty), (\infty_4, \infty, -\infty)\},$$

using the notation in Equations (31) and Definition 5.1. In set theoretically language, its asymptotic values are $\{-1, 1, \infty\}$, hence it is a Transcendental Belyĭ function.

Example 13.2. *A transcendental Belyĭ function that does not belong to the family Ψ_X, for $X \in \mathscr{E}(r, d)$.* With the present techniques, we can describe the following vector field arising from a transcendental Belyĭ function. Let $\mathcal{R}$ be the Riemann surface that consists of half a Riemann sphere (cut along the extended real line $\mathbb{R} \cup \{\infty\} \subset \widehat{\mathbb{C}}$) glued to three semi–infinite towers of copies of $\widehat{\mathbb{C}} \backslash (a, b]$ where $(a, b] \in \{(-\infty, 0], (0, 1], (1, \infty]\}$, as in Figure 25. The general version of the dictionary ([1] lemma 2.6) shows that a transcendental function $\Upsilon(z) : \mathbb{C}_z \longrightarrow \widehat{\mathbb{C}}_t$ and a vector field $X(z) = \frac{1}{\Upsilon'(z)} \frac{\partial}{\partial z}$ are associated to $\mathcal{R}$.
The logarithmic branch points of Υ^{-1} are

$$\{(\infty_1, 0), (\infty_2, 1), (\infty_3, \infty)\}.$$

Compare also with the description using line complexes, as in p. 292 of [39].
The cyclic word is

$$\Big((\widehat{\mathbb{C}}_z, \infty), \mathfrak{Re}\,(X)\Big) \longmapsto \mathcal{W}_X = H\mathscr{E}E\mathscr{E}H\mathcal{T}.$$

Note the appearance of a new kind of angular sector $\mathcal{T}$ having an accumulation point of double zeros of X: the phase portrait of $\mathfrak{Re}\,(X)$ is obtained by considering the pullback of $\mathfrak{Re}\left(\frac{\partial}{\partial t}\right)$ via Υ, see Figure 24.c. The 1–order of X is finite and at least 1.

13.3. **Relation with complex correspondence principle in mechanics.** C. Bender *et al.* studies the relation between classical and quantum mechanics using a $\mathbb{C}$ complex framework, see [7], [8] and [9]. Motivated by the correspondence principle, asserting that quantum mechanics resembles classical mechanics in the high–quantum–number limit. These works introduce the concept of a local quantum probability density $\rho(z)$ in the complex plane. C. Bender proposes the novel approach of constructing a complex contour C on which $\rho(z)dz$ is an infinitesimal probability measure. Thus, C must satisfy

$$\begin{aligned} \text{condition I:} \quad & \mathfrak{Im}\,(\rho(z)dz) = 0, \\ \text{condition II:} \quad & \mathfrak{Re}\,(\rho(z)dz) > 0, \\ \text{condition III:} \quad & \textstyle\int_C \rho(z)dz = 1, \end{aligned}$$

see [7]. In our language, we consider $\rho(z)dz$ as an entire 1–form on $\mathbb{C}$. By using the singular complex analytic Dictionary Proposition 2.5 and conditions I–II, we have that C can be interpreted as a trajectory of

$$\mathfrak{Re}\left(\tfrac{1}{\rho(z)} \tfrac{\partial}{\partial z}\right), \text{ where } \tfrac{1}{\rho(z)} \tfrac{\partial}{\partial z} \in \mathscr{E}(r, 2),$$

condition III is a certain normalization. The works of C. Bender *et al.* illustrate the application of the corresponding trajectory structures of $\mathfrak{Re}\left(\frac{1}{\rho(z)} \frac{\partial}{\partial z}\right)$.

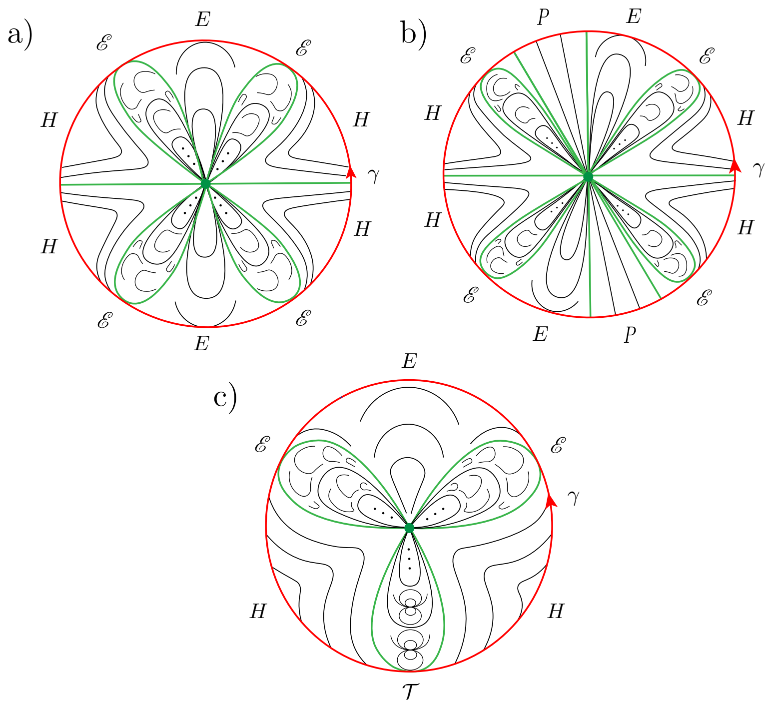

FIGURE 24. The cyclic words (a)–(b) appearing in Examples 12.4 and (c) in 13.2. Numerical models for (a)–(b) appeared as figures 15 and 16 in [1].

13.4. **Future work.**

13.4.1. *Relations with Dessin's d'enfants.* In the combinatorial framework, dessin's d'enfants are well known plane bipartite trees associated to Belyĭ functions; in their modern form were promoted and named by A. Grothendieck. Among other things, they have been used to study the action of the absolute Galois group of $\mathbb{Q}$, see [24].

By the singular complex analytic Dictionary Proposition 2.5, we may consider a polynomial Belyĭ function Ψ_X as the distinguished parameter of the associated vector field $X \in \mathscr{E}(r, 0)$, $r \geq 2$. That is, up to action of $Aut(\mathbb{C})$ on the target, we assume that the critical values of Ψ_X are $\{0, 1, \infty\}$. By assigning the color black to the vertices associated to the critical value 0 and the color white to the vertices associated to the critical value 1, we see that Λ_X is a bipartite graph, as in the usual theory.

The extension of the theory for Ψ_X, $X \in \mathscr{E}(r, d)$ with $r \geq 1$ is possible and is an interesting subject. In fact, *(r, d)–configuration trees Λ_X that lie over exactly three critical or asymptotic values are a natural extension of dessins d'enfant of the structurally finite Belyĭ functions Ψ_X.*

13.4.2. *Topological classification of $\mathfrak{Re}(X)$ for $X \in \mathscr{E}(r, d)$.* As suggested by the results of §11; a careful study of the (r, d)–skeleton of Λ_X allows for a global topological classification of $\mathfrak{Re}(X)$ for $X \in \mathscr{E}(r, d)$, in terms of the placement of the critical and asymptotic values. This study is in progress, however the technical language needed to provide a clear exposition would require too much space, thus it has been left for a future work. A particularly interesting case is the bound for the number of topological classes $\{\mathfrak{Re}(X) \mid \mathscr{E}(r, 0)\}$, for $r \geq 3$.

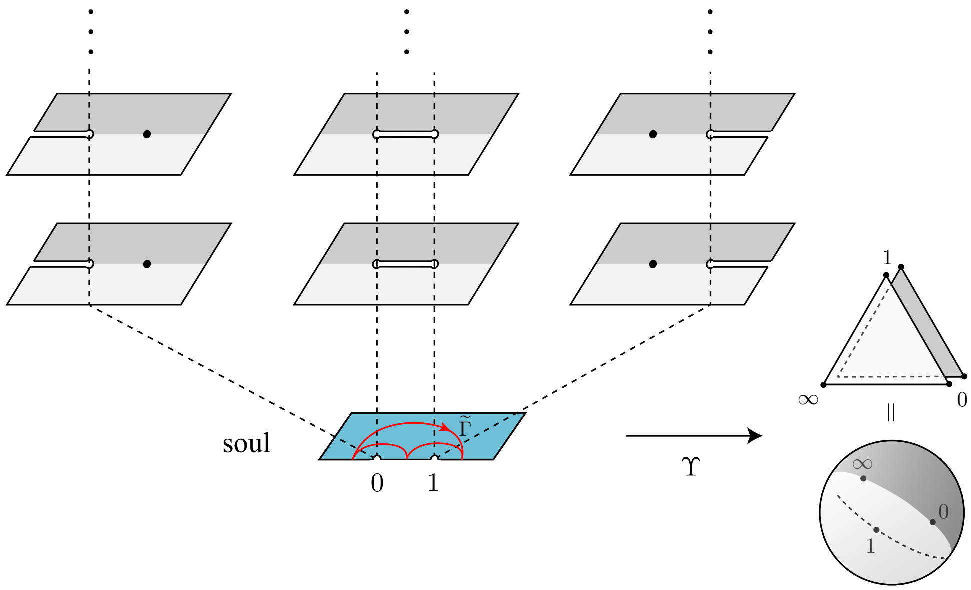

FIGURE 25. Riemann surface corresponding to a transcendental Belyĭ function Υ. The path $\widetilde{\Gamma}$ is a taut deformation of $\Gamma = (\Psi_X \circ \gamma)$ originated by a γ bounding the singularity $\big((\widehat{\mathbb{C}}, \infty), X_\Upsilon\big)$. Note that topologically this is the only possible surface with exactly three logarithmic branch points. Compare with Lemma 4.1 and note that the singularities in the central column are topologically different from semi–infinite helicoids in Figure 4.

13.4.3. *Dynamical coordinates for other families of vector fields.* As Example 13.2 suggests, there are other families of vector fields where the construction of the dynamical coordinates Λ_X is certainly possible.

For instance, when considering the family

$$\mathscr{E}(s,r,d) = \left\{ X(z) = \frac{Q(z)}{P(z)}\, \mathrm{e}^{E(z)} \frac{\partial}{\partial z} \;\middle|\; \begin{array}{l} Q,\ P,\ E \in \mathbb{C}[z], \\ \deg Q = s,\ \deg P = r,\ \deg E = d \end{array} \right\},$$

as in [2], we are presented with two intrinsically different cases:
1) If Ψ_X is single valued (this is equivalent to requiring that the associated 1–form ω_X have all its residues zero), then vertices $(q_\iota, \infty, \nu_\iota)$ with $\nu_\iota \geq 1$, corresponding to the zeros $\mathcal{Z} = \{q_\iota\}_{\iota=1}^{s}$ of X, need to be added to the description of Λ_X.

2) If Ψ_X is multivalued (there appear at least two non-zero residues for ω_X), then extra structure will be required. This is so because of the appearance of logarithmic branch points of Ψ_X^{-1}, over those $q_\iota \in \mathbb{C}_z$ where the associated 1–form has non–zero residue.

13.4.4. *On cyclic words.*
Cyclic words as topological or analytical invariants for germs. The word $\mathcal{W}_X$ (as in Theorem 12.2), is a local topological invariant of a germ $\big((\widehat{\mathbb{C}}_z, \infty), \mathfrak{Re}\,(X)\big)$, $X \in \mathscr{E}(r,d)$.

Moreover, the word $\mathcal{W}_X$ in general, is not a global topological invariant of $X \in \mathscr{E}(r,d)$. For example all the vector fields $X \in \mathscr{E}(r,0)$, $r \geq 3$, with all critical and asymptotic values in $\mathbb{R}$, have the same word $\mathcal{W}_X = \underbrace{EE\cdots EE}_{2r+2}$ at ∞.

However, it is possible to modify the definitions of angular sectors P_ν, E and $\mathscr{E}$ so that in fact the corresponding $\mathcal{W}_X$ is a *global analytic invariant* of X modulo $Aut(\mathbb{C})$. This is left for a future project.

Other angular sectors as letters for cyclic words. As shown in Example 13.2 and in examples 5.9, 5.12 and figures 2, 5 of [1]; there are certainly other possible angular sectors that can be used as letters for cyclic words. In this context and considering the above examples, it is clear that there are an infinite number of topologically different angular sectors (letters) that can appear in a cyclic word associated to an essential singularity for a vector field X.

However, it is not immediately clear *how many topologically different letters there are when we specify the p–order of* X, that is the coarse analytic invariant of functions and vector fields. For instance, by once again considering Example 13.2, $X(z) = \Upsilon^*(\frac{\partial}{\partial t})(z) = \frac{1}{\Upsilon'(z)}\frac{\partial}{\partial z}$; we may also consider $Y(z) = \Upsilon^*(\mu t\frac{\partial}{\partial t})(z) = \mu\frac{\Upsilon(z)}{\Upsilon'(z)}\frac{\partial}{\partial z}$ which provides a (very) different vector field.

14. Epilogue: parameters for families of vector fields

The second part of the proof of the Main Theorem provides a proof of the following result of independent interest. Recalling Equations (25), (28), (39) and (40) we have.

Corollary 14.1. *Given $r + d$ values*

$$\widetilde{p}_1, \ldots, \widetilde{p}_r, a_1, \ldots, a_d \in \mathbb{C}_t,$$

possibly repeated, with the exception that if $d \geq 1$ there are at least two non–repeated values. Then there exists a (non-unique) vector field $X \in \mathscr{E}(r,d)$ having these $r + d$ ramification values, i.e. a collection of $n + d$ realizable vertices, see (45),

$$\{(p_\iota, \widetilde{p}_\iota, -\nu_\iota)\}_{\iota=1}^{n} \cup \{(\infty_\sigma, a_\sigma, -\infty)\}_{\mathfrak{a}=1}^{d}$$

for the corresponding Ψ_X.

Remark 14.2. In our case, the complete collection of ramification values are

$$\{\widetilde{p}_1, \ldots, \widetilde{p}_r, a_1, \ldots, a_d, \underbrace{\infty, \ldots, \infty}_{d}\} \subset \widehat{\mathbb{C}}_t.$$

Moreover, the use of ramification values $t_\mathfrak{a}$ provides information of the moduli space of Ψ_X. Recalling the classical Riemann's idea that for ramified cover maps over $\widehat{\mathbb{C}}_t$ with $\mathfrak{n} \geq 4$ ramification values, we can specify three of them, and the other $\mathfrak{n}-3$ determine holomorphic deformations of the cover maps π_2.

Because of the singular complex analytic Dictionary Proposition 2.5, the works of R. Thom [47] and J. Mycielski [38], describes the situation for polynomials Ψ_X, *i.e.* the case $d = 0$. However the answer is not unique, that is given a set of preassigned critical values $\{\widetilde{p}_1, \ldots, \widetilde{p}_r\}$ there are a finite number of polynomials Ψ_X with the above set as critical values, namely

Theorem (Mycielski–Thom)**.** *Given r points $\widetilde{p}_1, \ldots, \widetilde{p}_r \in \mathbb{C}_t$, there exist r points $p_1, \ldots, p_r \in \mathbb{C}_z$ such that the (monic) polynomial of degree $r + 1$*

$$\Psi(z) = (r+1)\int^z \prod_{\iota=1}^{r}(\zeta - p_\iota)d\zeta$$

satisfies

1) $\Psi(p_\iota) = \widetilde{p}_\iota$ and $\Psi'(p_\iota) = 0$, for $\iota = 1, \ldots, r$.

2) If β occurs k times in the collection $p_1, \ldots, p_r$ then $(z-\beta)^{k+1}$ divides $\Psi(z) - \Psi(\beta)$. □

Proof of Corollary 14.1. Recalling Equation (45), we want to show that there exists:

a) r points $p_1, \ldots, p_r \in \mathbb{C}_z$, determining a (monic) polynomial $P(z) = \prod_{\iota=1}^{r}(z - p_\iota)$,

b) a polynomial $E(z)$ of degree d,

c) d asymptotic paths $\alpha_\sigma(\tau)$,

such that the distinguished parameter $\Psi_X(z) = \int^z P(\zeta)\mathrm{e}^{-E(\zeta)}\, d\zeta$ satisfies

i) $\Psi_X(p_\iota) = \widetilde{p}_\iota$ and $\Psi_X^{(\ell)}(p_\iota) = 0$, for $1 \leq \ell \leq \nu_\iota = 1$,

ii) $\lim_{\tau\to\infty} \Psi_X(\alpha_\sigma(\tau)) = a_\sigma$, for $\sigma = 1, \ldots, d$.

Furthermore, the polynomials $P(z)$ and $E(z)$ are non–unique.

Note that the *geometrical* construction carried out in §9.2 (the second part of the proof of the Main Theorem) can be carried out *by only specifying the critical and asymptotic values and the corresponding* $K(\mathfrak{a}, \mathfrak{r})$ of the (r, d)–configuration tree, this uses Lemma 5.3 actively.

That is we can construct a Riemann surface $\mathcal{R}$ by glueing sheets $\mathbb{C}_t$ with branch cuts starting at $\{\widetilde{p}_1, \ldots, \widetilde{p}_r, a_1, \ldots, a_d\}$. As before, $\mathcal{R}$ is recognized as a simply connected Riemann surface $\mathcal{R}_X$ corresponding to some $X \in \mathscr{E}(r, d)$. Thus showing that for every possible choice of $(\widetilde{p}_1, \ldots, \widetilde{p}_r, a_1, \ldots, a_d) \in \mathbb{C}^{r+d}$ there are polynomials $P(z)$ and $E(z)$ of degrees r and d respectively such that Ψ_X has precisely $\{\widetilde{p}_1, \ldots, \widetilde{p}_r, a_1, \ldots, a_d\}$ as critical and asymptotic values.

For the non–uniqueness of the polynomials $P(z)$ and $E(z)$ note that: when $d = 0$ generically, by Bezout's Theorem, there are $(r + 1)^r$ solutions of the system (45). For the case $r = 3$, $d = 0$ see Equation (52).
For $r = 0$, $d = 3$, recall Example 8.5 where there are an infinite number of solutions for each vertex of finite asymptotic values $a_1, a_2, a_3 \in \mathbb{C}_t$: each parameter $K(1, 3) \in \mathbb{Z}$ provides a different $X \in \mathscr{E}(0, 3)$.
The general case now follows easily from the above examples. □

Remark 14.3. 1. Corollary 14.1 gives rise to a complex analytic set in $\overline{\mathbb{C}}_z^{r+d} \times \mathbb{C}_t^{r+d}$ consisting of the sets of branch points that determine $\mathcal{R}_X$ with $X \in \mathscr{E}(r, d)$.
2. Corollary 14.1 can be interpreted as saying that the map from $\mathbb{C}[z]_{=r} \times \mathbb{C}[z]_{=d}$ to $\mathbb{C}_t^{r+d}$ given by the Equation (45) is surjective.

Recalling (6) and (7), there are two obvious ways of parametrizing $\mathscr{E}(r, d)$:

1) Specifying the coefficients of $P(z)$ and $E(z)$.

2) Specifying the roots of $P(z)$ and $E(z)$ together with the non-zero coefficient μ.

Noting that the roots of $P(z)$ correspond to the poles of X, equivalently to the critical points of Ψ_X. In the case $d = 0$, the usual geometrical/dynamical interpretation of (2) arises. However, we are not aware of a geometrical/dynamical interpretation of the roots of $E(z)$; compare with [2] where a study of the discrete symmetries of X is provided.

3) A third kind of "parametrization" is given by Corollary 14.1: given a set of critical and asymptotic values $\{\widetilde{p}_1, \ldots, \widetilde{p}_r, a_1, \ldots, a_d\}$, there are non–unique $X \in \mathscr{E}(r, d)$ such that the above set are precisely the critical and asymptotic values of Ψ_X.

Note that the non–uniqueness arises from the solution of the system of transcendental equations (45).

Recalling Diagram 12, parametrization (3) can be represented by specifying the bottom row of Diagram 116.

$$\begin{tikzcd}
\mathbb{C}_z \supset \{p_1,\dots p_n,\infty_1,\dots,\infty_d\} \arrow[drr, "\Psi_X"'] & & \big\{(p_\iota,\widetilde{p}_\iota,-\nu_\iota)\big\}_{\iota=1}^{n} \cup \big\{(\infty_\sigma,a_\sigma,-\infty)\big\}_{\sigma=1}^{d} \subset \mathcal{R}_X \arrow[ll, "\pi_1"'] \arrow[d, "\pi_2"] \\
& & \{\widetilde{p}_1,\dots,\widetilde{p}_r,a_1,\dots,a_d\} \subset \mathbb{C}_t .
\end{tikzcd} \tag{116}$$

Is there another way of parametrizing $X \in \mathscr{E}(r,d)$?

Striving for a unique geometrical/dynamical solution in the general case $r,d \geq 1$, (r,d)–configuration trees provide a "mixed approach". Further study of the above question and effective parameters from Diagram 116 is the goal of a future project.

References

[1] A. Alvarez–Parrilla, J. Muciño–Raymundo, *Dynamics of singular complex analytic vector fields with essential singularities I*, Conform. Geom. Dyn., 21 (2017), 126–224. http://dx.doi.org/10.1090/ecgd/306

[2] A. Alvarez–Parrilla, J. Muciño–Raymundo, *Symmetries of complex analytic vector fields with an essential singularity on the Riemann sphere*, Advances in Geom., 21, 4 (2021), 483–504. https://doi.org/10.1515/advgeom-2021-0002

[3] A. Alvarez–Parrilla, J. Muciño–Raymundo, S. Solorza and C. Yee–Romero, *On the geometry, flows and visualization of singular complex analytic vector fields on Riemann surfaces*, Proceedings of the 2018 Workshop in Holomorphic Dynamics, C. Cabrera *et al.* Eds., Instituto de Matemáticas, UNAM, México, *Serie Papirhos*, Actas 1 (2019), 21–109. https://arxiv.org/abs/1811.04157

[4] A. A. Andronov, E. A. Leontovich, I. I. Gordon, A. G. Maier, *Qualitative Theory of Second–Order Dynamic Systems*, J. Wiley & Sons, New–York, Toronto, 1973.

[5] V. I. Arnold, Y. Ilyashenko, *Ordinary Differential Equations*, in Dynamical Systems I, D. V. Anosov, V. I. Arnold Eds., Springer–Verlag, Berlin, 1994.

[6] G. V. Belyĭ, *On Galois extensions of a maximal cyclotonic field*, Math. USSR Izvestija, 193, 14 (1980), 247–256. https://doi.org/10.1070/IM1980v014n02ABEH001096

[7] C. M. Bender, D. W. Hook, P. N. Meisinger, Q.–H. Wang, *Complex correspondence principle*, Physical Review Letters PRL 104, 12 February (2010), 061601–0616014. https://doi.org/10.1103/PhysRevLett.104.061601

[8] C. M. Bender, D. W. Hook, P. N. Meisinger, Q.–H. Wang, *Probability density in the complex plane*, Annals of Physics 325 (2010), 2332–2362. https://doi.org/10.1016/j.aop.2010.02.011

[9] C. M. Bender, *PT Symmetry in Quantum and Classical Physics*, with contributions from P. E. Dorey, C. Dunning, A. Fring, D. W. Hook, H. F. Jones, S. Kuzhel, G. Lévai, R. Tateo, World Sci., Hackensack NJ, 2019. https://www.worldscientific.com/worldscibooks/10.1142/q0178

[10] W. Bergweiler, A. Eremenko, *On the singularities of the inverse to a meromorphic function of finite order*, Revista Matemática Iberoamericana, 11, 2, (1995), 355–373. http://dx.doi.org/10.4171/RMI/176

[11] Ch. J. Bishop, *Constructing entire functions by quasiconformal folding,* Acta Math., 214 (2015), 1–60. https://doi-org.pbidi.unam.mx:2443/10.1007/s11511-015-0122-0

[12] K. Biswas, R. Pérez–Marco, *Log–Riemann surfaces, Caratheodory convergence and Euler's formula*, Contemporary Math., 639 (2015), 197–203. http://de.doi.org/10.1090/com/639/12826

[13] K. Biswas, R. Pérez–Marco, *Uniformization of simply connected finite type Log–Riemann surfaces*, Contemporary Math., 639 (2015), 205–216. http://de.doi.org/10.1090/com/639/12827

[14] K. Biswas, R. Pérez–Marco, *The ramificant determinant*, SIGMA 15 (2019), Paper No, 086, 28 pp. https://www.emis.de/journals/SIGMA/2019/086/sigma19-086.pdf

[15] W. M. Boothby, *The topology of regular curve families with multiple saddle points*, Amer. J. Math., Vol. 73, No. 2, Apr., (1951), 405–438. https://www.jstor.org/stable/2372185

[16] W. M. Boothby, *The topology of the level curves of harmonic functions with critical points*, Amer. J. Math., Vol. 73, No. 3, Jul. (1951), 512–538. https://www.jstor.org/stable/2372305

[17] B. Branner, K. Dias, *Classification of complex polynomial vector fields in one complex variable*, J. Difference Equ. Appl., 16, 5–6, (2010), 463–517. https://doi.org/10.1080/10236190903251746

[18] J. Cheeger, D. Gromoll, *The structure of complete manifolds of nonnegative curvature*, Bull. Amer. Math. Soc., 74 (1968), 1147–1150. https://doi-org.pbidi.unam.mx:2443/10.1090/S0002-9904-1968-12088-9

[19] K. Dias, L. Tan, *On parameter space of complex polynomial vector fields in* $\mathbb{C}$, J. Differential Equations, 260, 1 (2016), 628–652. http://dx.doi.org/10.1016/j.jde.2015.09.001

[20] G. Elfving, *Über eine Klasse von Riemannschen Flächen und ihre Uniformisierung*, Acta Soc. Sci. Fennicae, N.S. 2, Nr. 3 (1934), 1–60.

[21] A. Eremenko, A. Gabrielov, *Rational functions with real critical points and the B. and M. Shapiro conjecture in real enumerative geometry*, Ann. of Math. (2) 155, no. 1 (2002), 105-–129. http://dx.doi.org/10.2307/3062151

[22] A. Eremenko, A. Gabrielov, *An elementary proof of the B. and M. Shapiro conjecture for rational functions*, In Notions of positivity and the geometry of polynomials, 167–178, Trends Math., Birkhäuser/Springer Basel AG, Basel, 2011. http://dx.doi.org/10.1007/978-3-0348-0142-3_10

[23] M. E. Frías–Armenta, J. Muciño–Raymundo, *Topological and analytic classification of vector fields with only isochronous centers*, J. Eqs. Appl., 19, 10, (2013), 1694–1728. https://doi.org/10.1080/10236198.2013.772598

[24] A. Grothendieck. *Equisse d'un program*, In Geometric Galois actions 1, L. Schneps *et al.* Ed., vol. 242 London Math. Soc. Lecture Note Ser., (1997), 7–48. https://doi.org/10.1017/CBO9780511758874.003

[25] K. Hockett, S. Ramamurti, *Dynamics near the essential singularity of a class of entire vector fields*, Transactions of the AMS, vol. 345, 2 (1994), 693–703. https://doi.org/10.1090/S0002-9947-1994-1270665-5

[26] X.–H. Hua, Ch.–Ch. Yang, *Dynamics of Transcendental Functions*, Gordon and Breach, New Delhi, 1998.

[27] M. Klimeš, Ch. Rousseau, *Generic* 2*–parameter perturbations of parabolic singular points of vector fields in* $\mathbb{C}$, Conform. Geom. Dyn., 22 (2018), 141–184. https://doi.org/10.1090/ecgd/325

[28] F. Klein, *On Riemann's Theory of Algebraic Functions and Their Integrals*, Dover Publications Inc., New York, 1963. http://www.gutenberg.org/ebooks/36959

[29] J. Jenkins, *Univalent Functions and Conformal Mapping*, Ergebnisse Der Mathematik Und Iher Grenzgebiete, Springer–Verlag, Berlin, 1958. https://doi.org/10.1007/978-3-642-88563-1

[30] S. K. Lando, A. K. Zvonkin, *Graphs on Surfaces and Their Applications*, EMS 141, Springer–Verlag, Berlin 2004. https://doi.org/10.1007/978-3-540-38361-1

[31] J. K. Langley, *Trajectories escaping to infinity in finite time*, Procc. Amer. Math. Soc. Vol. 145, Num. 5, May (2017), 2107–2117. https://dx.doi.org/10.1090/proc/13377

[32] J. L. López, J. Muciño–Raymundo, *On the problem of deciding whether a holomorphic vector field is complete*, in Operator Theory: Advances and Applications 114, E. Ramírez de Arellano *et al.* eds, (2000), 171–195. https://doi.org/10.1007/978-3-0348-8698-7_13

[33] J. C. Magaña–Cacéres, *Classification of 1–forms on the Riemann sphere up to* $PSL(2,\mathbb{C})$, Bull. Mexican Math. Soc., (3), 25, 3 (2019), 597–617. https://doi.org/10.1007/s40590-018-0217-7

[34] D. Masoero, *Painleve I, coverings of the sphere and Belyi functions*, Constr. Approx., 39, 1 (2014), 43–74. https://doi.org/10.1007/s00365-013-9185-3

[35] H. Masur, S. Tabachnikov, *Rational billiards and flat structures*, in Handbook of Dynamical Systems, Vol. 1A, B. Hasselblatt *et al.* Ed., North–Holland, Amsterdam, 2002, 1015–1089. https://doi.org/10.1016/S1874-575X(02)80015-7

[36] J. Muciño–Raymundo, *Complex structures adapted to smooth vector fields*, Math. Ann., 322 (2002), 229–265. https://doi.org/10.1007/s002080100206

[37] J. Muciño–Raymundo, C. Valero–Valdéz, *Bifurcations of meromorphic vector fields on the Riemann sphere*, Ergod. Th. & Dynam. Sys., 15 (1995), 1211–1222. https://doi.org/10.1017/S0143385700009883

[38] J. Mycielski, *Polynomials with preassigned values at their branching points*, Amer. Math. Montly 77, 8 (1970), 853–855. https://doi.org/10.1080/00029890.1970.11992599

[39] R. Nevanlinna, *Analytic Functions*, Springer–Verlag, Berlin, 1970. https://doi.org/10.1007/978-3-642-85590-0

[40] R. Nevanlinna, *Über Riemannsche Flächen mit endlich vielen Windungspunkten*, Acta Math., 58(1) (1932), 295–373. https://doi.org/10.1007/BF02547780

[41] F. Oberhettinger, *Hypergeometric Functions*, in Handbook of Mathematical Functions with Formulas, Graphs, and Mathematical Tables, M. Abramowitz *et al.* Ed., Ch. 15, 9th printing, Dover, New York (1972), 555–566.

[42] H. A. Schwarz, *Ueber diejenigen Fälle, inwelchen die Gaussische hypergeometrische Reihe eine algebraische Function ihres vierten Elementes darstellt*, J. Reine Angew. Math., 75 (1873), 292–335. https://doi.org/10.1515/crll.1873.75.292

[43] A. Speiser, *Über Riemannsche Flächen*, Comment. Math. Helv., 2 (1930) 284–293.

[44] K. Strebel, *Quadratic Differentials*, Springer–Verlag, Berlin, 1984. https://doi.org/10.1007/978-3-662-02414-0

[45] M. Taniguchi, *Explicit representations of structurally finite entire functions*, Proc. Japan Acad. Ser. A Math. Sci., Vol. 77 (2001), 68–70. https://projecteuclid.org/euclid.pja/1148393085

[46] M. Taniguchi, *Synthetic deformation space of an entire function*, Cont. Math., Vol. 303 (2002), 107–136. http://dx.doi.org/10.1090/conm/303/05238

[47] R. Thom, *L'équivalence de une function différentiable et d'un polynome*, Topology, 3, 2 (1965), 297–307. https://doi.org/10.1016/0040-9383(65)90079-0

[48] W. P. Thurston, *Three–Dimensional Geometry and Topology*, Vol. 1, Princeton University Press, USA, 1997.

Alvaro Alvarez–Parrilla, Grupo Alximia SA de CV, Ensenada, Baja California, CP 22800, México
Email address: alvaro.uabc@gmail.com

Jesús Muciño–Raymundo, Centro de Ciencias Matemáticas, Universidad Nacional Autónoma de México, Morelia, México
Email address: muciray@matmor.unam.mx